1979

The Skalkaho pyroxenite-synite complex east of Hamilton Montana and the role of magma immiscibility in its formation

Jeffrey J. Lelek
The University of Montana

THE SKALKAHO PYROXENITE-SYENITE COMPLEX EAST OF HAMILTON, MONTANA, AND THE ROLE OF MAGMA IMMISCIBILITY IN ITS FORMATION

by

Jeffrey J. Lelek

A.B., Dartmouth College, 1977

Presented in partial fulfillment of the requirements for the degree of

Master of Science

UNIVERSITY OF MONTANA

1979

Approved by

Chairman, Board of Examiners

Dean, Graduate School

6-7-79

Date

ProQuest LLC.
789 East Eisenhower Parkway
P.O. Box 1346
Ann Arbor, MI 48106 - 1346

ABSTRACT

Lelek, Jeffrey J., M.S., Spring, 1979 Geology

The Skalkaho Pyroxenite-Syenite Complex East of Hamilton, Montana, and the Role of Magma Immiscibility in its Formation (130 pp)

Director: Dr. Donald W. Hyndman

Various lines of evidence suggest that the bimodal rocks of the Skalkaho igneous complex east of Hamilton, Montana formed from co-existing immiscible magmas. Pyroxenites vary from nearly pure (>98%) salite, to biotite (vermiculite) pyroxenite, to amphibole pyroxenite rich in sphene, apatite, and magnetite. These pyroxenites are juxtaposed against syenites. Miarolitic cavities in an unusual pegmatite of anhydrous mineralogy attest to the shallow emplacement of the complex. Based on field relations, mineralogical similarities, and chemical considerations, the regionally uncommon pyroxenites and syenites appear both comagmatic and contemporaneously emplaced. Fractional crystallization as a differentiation mechanism may be ruled out on the basis of textural evidence such as the absence of cumulate-intercumulate phases, structural evidence such as the lack of layering, and elemental behavior. Differentiation of the two systems through the process of liquid immiscibility seems indicated. The bimodal, comagmatic, and contemporaneous nature of the rocks is compatible with such an origin. The complex is alkaline, as are many rock examples cited to illustrate immiscibility. Parameters seen to enhance experimental immiscibility are evidenced at Skalkaho. These include high Ti, P, and K, high K_2O/total alkalies, low pressure of emplacement, and probably moderate to high volatile contents. Partitioning of Ti, P, and REE into the mafic fraction is consistent with the operation of liquid immiscibility as opposed to fractional crystallization. Finally, the rocks plot near opposite ends of the determined immiscibility field on the join fayalite-leucite-silica (Roedder, 1951) with potential tielines paralleling those seen to exist between known immiscible factions.

ACKNOWLEDGMENTS

Special thanks go to Don Hyndman and Dave Alt, two believers whose excellent guidance was crucial to the evolution of this project. Discussions with Keith Osterheld, Bill Beyer, Gil Wiswall and Jim Harrington provided enlightening insights. I would also like to thank the Western Vermiculite Company for access rights and valuable information, and Lesa Anderson, whose undying patience and everpresent encouragement were invaluable to the completion of this effort.

TABLE OF CONTENTS

LIST OF FIGURES

LIST OF PLATES

LIST OF TABLES

CHAPTER I

INTRODUCTION

General Statement

Realizing the dangers of narrowed thinking, geologists along with professionals in all disciplines often look towards other areas for possible solutions to their own problems. Thus, as early as the late 1800's, geologists invoked the processes of liquid immiscibility so evident between oil and water to explain the common juxtaposition of magmatic rocks severely divergent in composition. This study deals with the petrology of an igneous complex which exhibits a bimodal character here interpreted to have resulted largely through magmatic immiscibility.

Early experimental work concerning silicate liquid immiscibility showed incomplete miscibility in binary systems of SiO_2 with CaO, MgO, FeO, Fe_2O_3, MnO, SrO, ZnO, NiO, and CoO. Greig (1927), however, demonstrated that these immiscibility fields occurred only at geologically unreasonable temperatures (about 1700°C) and compositions. Complete miscibility is attained with the addition of only a few percent common alkalies of alumina. Bowen (1928) discussed certain criteria for the recognition of rocks separated by immiscibility processes and stressed that no evidence of liquid immiscibility had ever been cited in naturally occurring rocks. He considered the mechanism geologically

insignificant, thereby squelching the idea of liquid immiscibility as a viable process in geology.

Roedder's (1951) discovery of a second type of immiscibility field, located entirely within the ternary system represented by the plane leucite-fayalite-silica and occurring at geologically reasonable conditions, resurrected consideration of liquid immiscibility (e.g. Holgate, 1954). Convincing examples of quenched immiscible silicate liquids have more recently been cited from lunar basalts (Roedder and Weiblen, 1970a, 1970b, 1972) as well as their terrestrial equivalents (Dé, 1974; Philpotts, 1976). As new rock examples of liquid immiscibility are proposed, experimental work reaches from refinements of immiscibility fields in phase diagrams, to the effects of common magmatic elements on immiscibility field dimensions, to elemental partitioning trends between immiscible silicate liquids. The topic of liquid immiscibility, or liquation in the Russian literature (Markov and others, 1974; Prokoptsev, 1977), has become popular in a surprisingly short time.

Alkaline rocks constitute a mere one percent or less of all exposed igneous rocks, their total worldwide outcrop being on the order of 5000 square kilometers (adapted from Heinrich, 1967, p. 205). Currie (1976) noted that the alkaline rocks are not so much rich in alkalies as poor in silica; desilicating the average granodiorite yields a rock compositionally very close to the average nepheline syenite, while average tholeiitic and alkaline olivine basalts show a similar relationship.

It is apparent that igneous complexes exist with rocks of all degrees of silica saturation.

Of the 35 major alkaline rock localities in the United States, 13 or 37 percent have associated carbonatites, defined by Verwoerd as "granular rocks consisting of primary calcite, dolomite, ankerite, or other rock-forming carbonates as principle constituents, with subordinate apatite, magnetite, silicates, and accessories, and the primary features of intrusive rocks (in Stanton, 1972, p. 353)." Carbonatites themselves, on the other hand, are almost invaribly associated with mafic to ultramafic undersaturated rocks, most commonly urtite, ijolite, melteigite (aegerine/diopside-nepheline rocks), pyroxenite, biotite or phlogopite pyroxenite, jacupirangite (magnetite-pyroxenite), and essexite (orthoclase nepheline gabbro). Normally occurring as zoned complexes, these iron-rich rocks are surrounded by nepheline syenite, syenite, or fenite, a sodium-ferric iron enrichment zone within country rock adjacent to the complex.

Carbonatites provide perhaps the most accepted example of magma immiscibility on a significant scale. Furthermore, the general category of alkaline rocks provides many of the examples believed to have arisen through the differentiation process of liquid immiscibility (Philpotts, 1978, 1976; Freestone, 1978).

Location of Skalkaho Igneous Complex

The Skalkaho complex lies approximately 20 air kilometers east of Hamilton, Montana in the southern Sapphire Mountains (Fig. 1).

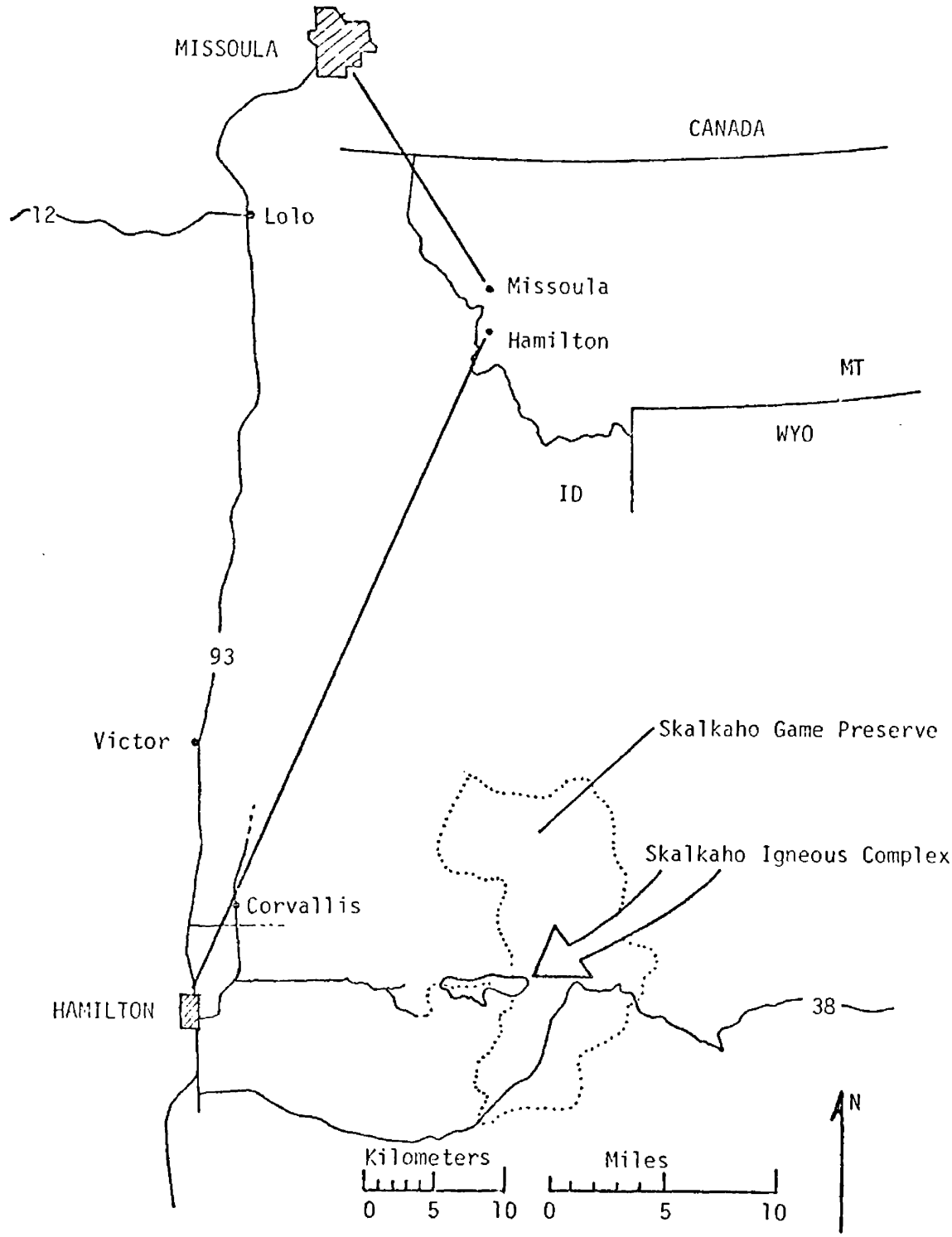

Figure 1. Location Map

Accessibility is excellent via a newly improved and graded dirt road serving a vermiculite mine situated in mica pyroxenite of the center of the complex. Abandoned logging roads provide limited peripheral access. The area, receiving 40-50 cm (15-20 inches) of precipitation yearly, is generally heavily forested and rugged, elevation ranging from near 1830 meters along St. Clair Creek to 2579 meters at Skalkaho Mountain. Numerous fallen trees hinder travel and generally poor outcrop restricts detailed mapping.

Previous Work, Mining History, and This Study

Heinrich (1966, p. 362) noted that a zone extending southeasterly from Missoula, Montana to Lemhi Pass in Idaho "displays many geological and mineralogical imprints characteristic of a major alkalic province in the uppermost stages of disinterment." Features represented in this belt include numerous tabular to lensoid rare-earth carbonates, thorite veins, barite veins, a pegmatitic fluorite deposit with rare-earth mineralization containing scandium in thortveitite, and the pyroxenite-syenite complex dealt with in this study.

Perry's (1948) brief report on vermiculite deposits near Hamilton is the only other reference to the complex, a two-page generalized capsule of the geography, mining history, geology, and economic prospects. He regarded the rocks as very similar to those of the Libby deposit (Rainy Creek Stock, see Boettcher, 1967) in all general characteristics.

Mining claims were initially staked on the vermiculite deposits in 1930. Numerous parties investigated the area by means of pits, trenches,

and short adits until 1976 when National Minerals Corporation obtained the property rights. Western Vermiculite Company of Victor, Montana is now actively exploiting the vermiculite deposits.

Field work for this study was conducted during the summer of 1978. The rocks were mapped on a scale of 1" = 600' using an enlarged U.S. Forest Service topographic sheet supplemented with U.S. Geological Survey 7 1/2 minute quadrangle maps. Magnetite, which is locally abundant makes Brunton compass measurements unreliable, and aerial photographs, surface features, and the altimeter were heavily relied upon to confirm locations.

CHAPTER II

GENERAL GEOLOGY

Regional Setting

Three major tectonic features, the Idaho batholith, the Dillon block, and the Overthrust Belt, dominate the geology of west-central Montana. The overthrust complexes which extend from near Las Vegas, Nevada northward into Canada are thought to be related to either crystalline basement block uplifts (Mudge, 1970; Price, 1971) or doming resultant from igneous intrusion (Armstrong, 1974; Burchfield and Davis, 1975; Hyndman and others, 1975). Horizontal movement of thrusted strata is believed to have occurred either through downslope gravity-induced sliding, or by lateral spreading responding to a gravity-related stress on an elevated or thickened section in the source area. This latter spreading process may be illustrated by certain modes of glacial movement such as that existing on Greenland.

Hyndman and others (1975) first recognized the Sapphire tectonic block, situated between the Idaho batholith and the Boulder batholith. The Sapphire block, some 100 km long and 75 km wide, consists of a 15-17 km thick slab of Precambrian Belt, Paleozoic, and Mesozoic sediments which slid approximately 60 kilometers eastward across a prominent mylonitic detachment zone, in response to emplacement of the Idaho batholith (Hyndman, 1979). This movement occurred about 75-80 MYBP and allowed isostatic rise of Idaho batholith granitic material

to form the present Bitterroot Range (Hyndman, 1979). Wiswall (1976) has reviewed the tectonics and structure of the region, emphasizing the southeastern edge of the Sapphire block. The Skalkaho igneous complex, which is the concern of this paper, is near the western or trailing edge of the Sapphire block.

The oldest rocks exposed in the Sapphire block belong to the Precambrian Belt Supergroup. From oldest to youngest, the main units are the Prichard Formation, Ravalli Group, Wallace Formation, and Missoula Group. Calc-silicate and quartzose rocks of the Wallace Formation surround the Skalkaho complex, and Ravalli Group argillitic quartzite is exposed within a few kilometers (Presley, 1970, LaTour, 1974).

Presley (1973) recognized two mappable units of the Wallace near the study area. Rocks of the calc-silicate unit are fine- to medium-grained and white to green, with layers varying from a few mm to 5 cm thick, generally grouped into zones up to 1 m thick. These calc-silicates are by far the most abundant rock type in the area and are the only meta-sediments in contact with the Skalkaho complex. West of Skalkaho Mountain they have undergone lower-amphibolite-grade metamorphism (Presley, 1970; LaTour, 1974). They contain diopside and in some cases scapolite crystals and white scapolite balls up to 5 mm in diameter. Interlayered with the calc-silicate rocks are very thin layers of fine-grained, biotite-quartz-rich rock. The upper part of the Wallace Formation, consisting of biotite and quartz with scapolite balls comprising up to 50 percent of the rock (Presley, 1973), does not abut the pyroxenite-syenite complex.

Godlewski (verbal communcation, 1979) noticed several types of breccia zones within the middle Belt, Wallace carbonate unit. He attributed these to soft-sediment deformation resulting from sliding on subaqueous slopes proximal to deep water basins. Such breccias, consisting of carbonate blocks in some cases larger than buildings, encased by a fine-grained carbonate, outcrop in several places near the northern and eastern edges of the Idaho batholith. A brecciated calc-silicate rock which occurs adjacent to the southwest portion of the Skalkaho pyroxenite-syenite complex probably is one of these syndepositional breccias. These breccias may serve as zones of weakness to help localize intrusives such as the Skalkaho complex or the Snowbird deposit, a pegmatitic rare-earth-rich quartz-carbonate body in the Wallace Formation west of Missoula, Montana (Metz, 1971).

Dioritic to granitic epizonal stocks, considered to be related to the Idaho and Boulder batholiths, constitute most of the igneous terrane within the Sapphire block (Wiswall, 1976). Structural evidence suggests emplacement during or just after movement of the block (Hyndman and others, 1975).

Additional igneous rocks in the area include diabase dikes and tabular carbonatite bodies (Crowley, 1960; Heinrich and Levisson, 1961; Heinrich, 1966, p. 362; LaTour, 1974). Calc-alkaline volcanic features occur to the south (Badley, 1977), and to the west in the Bitterroot Range outcrops a pre-mid Mesozoic metamorphosed mafic layered intrusive (Jens, 1974) and several small anorthosite bodies (Berg, 1964; Cheney, 1975).

Approximately 275 km to the north lies the Rainy Creek stock (Boettcher, 1966, 1967), which is similar to the Skalkaho complex. Both complexes may belong to the Canadian Cordilleran alkaline province delineated by Currie (1976). The Ice River complex of this belt, located about 320 km north and slightly west of the Rainy Creek stock, is another similar body composed dominantly of feldspar-free ultramafic rocks and syenites (Currie, 1976, p. 97-99). Beyond this conjecture, however, the tectonic significance of the Skalkaho complex remains as mysterious as that of the central Montana alkaline province.

General Geology of the Skalkaho Complex

The intrusive complex is elongate east-west for approximately 6-7 kilometers, and is about 1-1 1/2 kilometers across. Pyroxenite, about 36 percent of the complex in map view, is surrounded by two elongate horseshoe-shaped bodies of syenite (Fig. 2).

Three broadly defined varieties of pyroxenite are delineated: 1) anhydrous pyroxenite, a fine-grained, dark green, very hard rock composed almost entirely of salitic pyroxene; 2) mica pyroxenite, a coarse-grained to pegmatitic rock containing from <10 to >90 percent biotite, hydrobiotite, or vermiculite with salitic pyroxene; and 3) amphibole pyroxenite, a highly variable rock type composed largely of pyroxene and amphibole with abundant apatite, magnetite, and sphene. The latter rock type commonly exhibits a striking poikilitic texture, with patches of continuous mirror-like reflection up to 15 cm across visible when viewed on a sunny day.

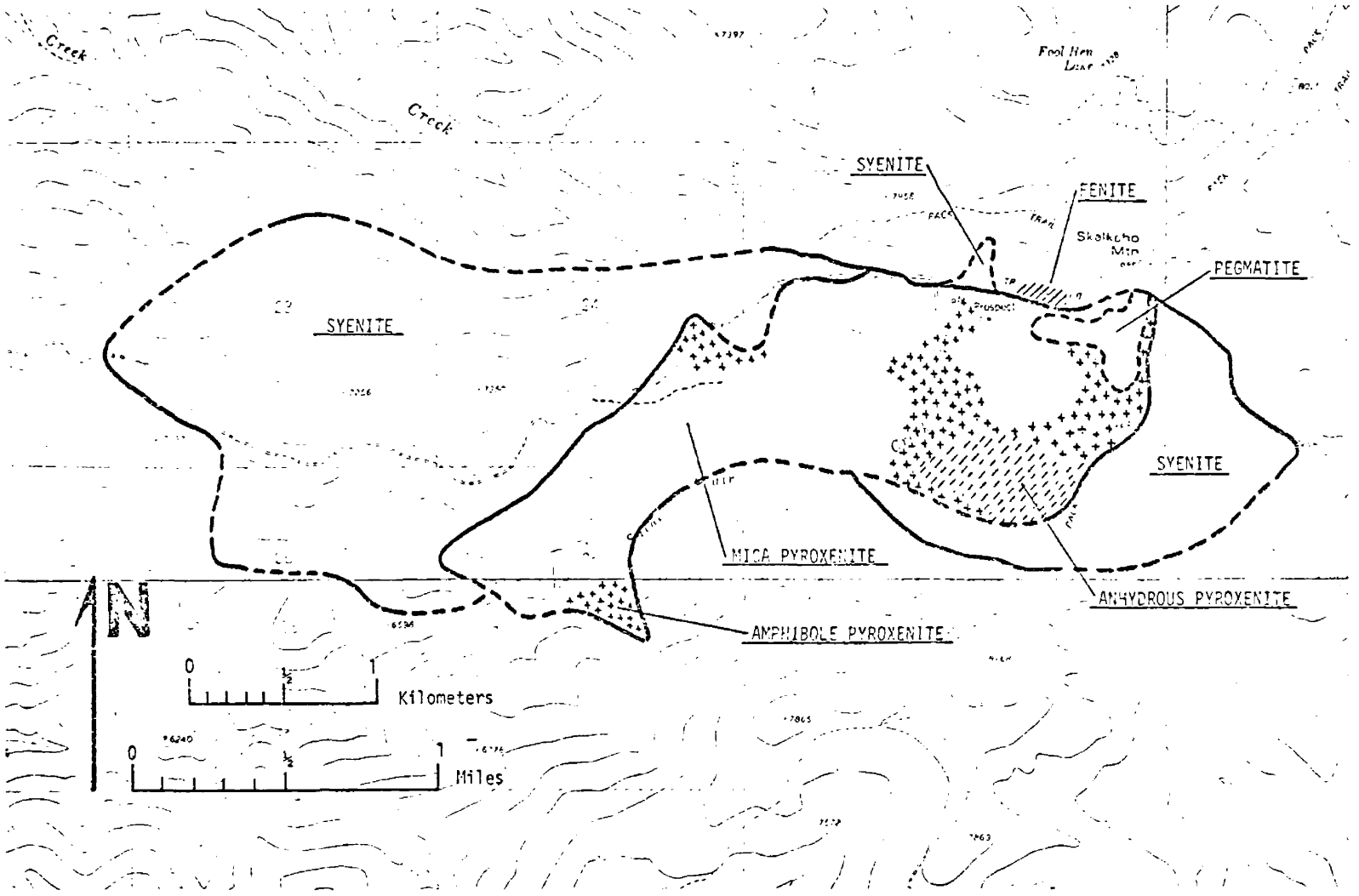

Figure 2. Geologic map of the Skalkaho complex.

Alkali-feldspar syenite, nearly all microperthite, varies to syenites which may contain up to 50 percent mafic minerals. Textures range from massive to trachytoid in the predominantly coarse-grained rocks.

An anhydrous, extremely coarse-grained pegmatite consisting of green pyroxene, white sodic feldspar, black garnet, honey-colored sphene, and miarolitic cavities, cuts the pyroxenites as does extremely fine-grained light-gray, vesicular, porphyitic trachyte. Linear and pod-like bodies of carbonate, in some cases intergrown with sodic amphibole also cut the pyroxenite, as do epithermal quartz-carbonate veins.

Minor shears run throughout the complex although post-crystallization deformation has been slight. A small zone of fenite exists in the country rock adjacent to pyroxenite. The main economic concern in the complex, vermiculite, is sporadically distributed, which will complicate mining.

The Skalkaho complex cuts the Belt Wallace Formation, indicating it is younger than these rocks, although the exact age is as yet undetermined. Furthermore, the presence of unfilled miarolitic cavities in the pegmatite and unfilled vesicles in the trachyte imply a much younger age. These data along with the presence of uneroded, epithermal-type veins and the undeformed nature of the rocks suggests emplacement after sliding of the Sapphire block. Interestingly, the

alkaline rocks of the Central Montana Province are Eocene in age. Biotite from the Rainy Creek stock to the north yielded a Sr-Rb age of 94 m.y.

Field Relations

Evidence of igneous activity abounds in the numerous cross-cutting relationships, inclusions, macro- and microscopic textures, and injection features which permeate the complex. Although poor exposure probably obscures many relations, the abundance of visible features indicates igneous activity was intense.

Many features point to active emplacement of the syenitic rocks ("syenitic" referring to all varieties of syenite and alkali-feldspar syenite according to the IUGS classification of igneous rocks--Streckeisen, 1976). Near the periphery of the complex, syenitic rocks contain numerous blocky inclusions of country rock in addition to rounded to angular chunks of mafic to intermediate igneous rock. Near the eastern extremity of the syenitic mass is a zone especially rich in such xenolithic material. Syenitic rocks record active stoping of the country rock and in places syenitic magma has injected itself between layers in the country rock. Dikes of syenitic material extend into the Belt meta-sediments.

Within the syenitic body, intrusive features reveal complex relations between various syenite types. Alkali feldspar syenites cut across and contain inclusions of more plagioclase-rich varieties, whereas

a leucocratic pegmatitic syenite transects alkali-feldspar syenite. Many syenitic rocks have a distinctive trachytoid texture, particularly along borders between intrusive phases or where the intrusive body is dike-like in form. Parallelism of grains in this texture is very strong except where it wraps around and is distorted by inclusions (see Fig. 13). No evidence of chill zones was seen anywhere except near the eastern syenite/country rock contact where grain size is generally smaller.

The pyroxenite body shows similar pervasive and complex intrusion patterns. Anhydrous pyroxenite, although existing as a very large discrete mass in the eastern part of the body, may be found throughout the complex as inclusions within amphibole pyroxenite and associated with mica pyroxenite. The relationships between mica pyroxenite and anhydrous pyroxenite is curious, nowhere showing a cross-cutting contact which would indicate a time relationship. This association is highly irregular, with stringers, pods, and patches (see Fig. 4) of mica-rich (in some areas over 90%) pyroxenite grading gradually or abruptly (within a few millimeters) to anhydrous pyroxenite. The two varieties in these cases appear texturally continuous; only the appearance of mica serves to distinguish two rock types. Near the western syenite/pyroxenite contact, a zone of foliation within the mica pyroxenite coincides with an area of associated mixed mica/anhydrous pyroxenite and the biotite concentrations appear to be intimately associated with or controlled by this trend, which may be a flow foliation.

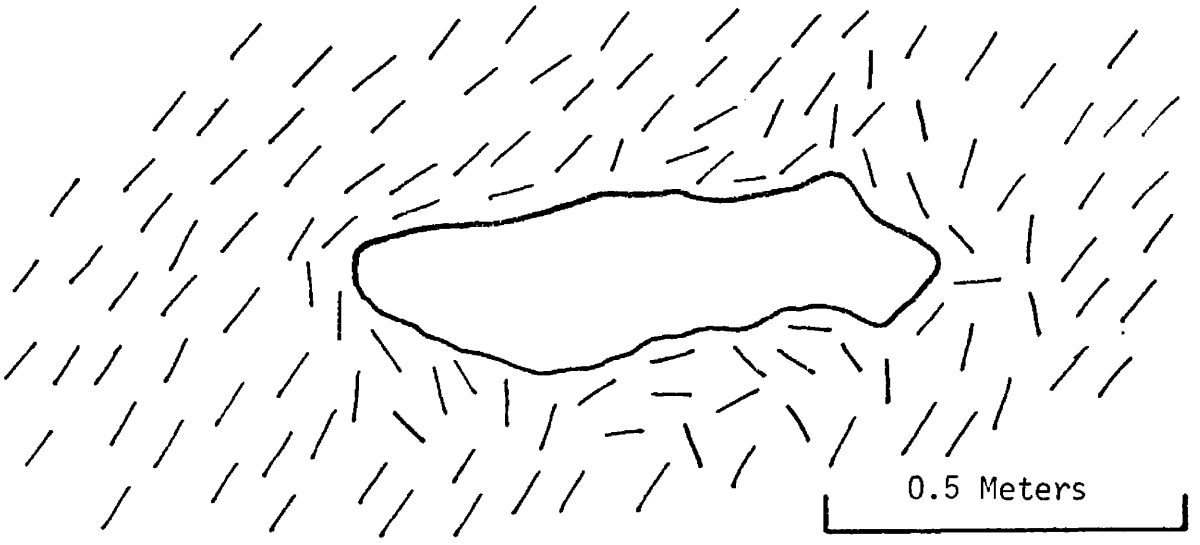

Figure 3. Sketch portraying trachytoid potassium feldspar crystals disoriented by an inclusion of Belt country rock.

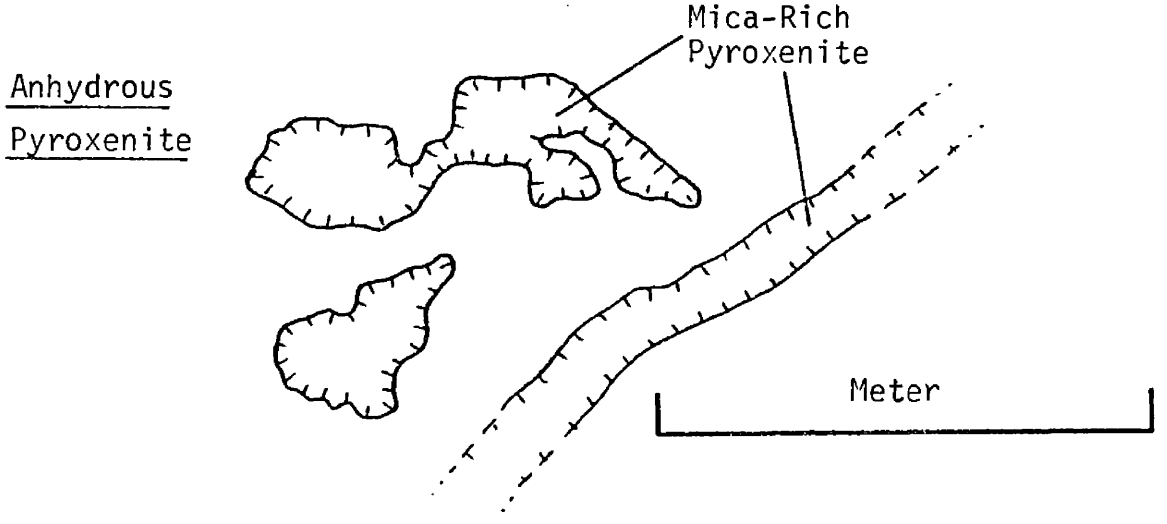

Figure 4. Sketch illustrating zones of mica-rich pyroxenite in outcrop of anhydrous pyroxenite.

Amphibole pyroxenite commonly transects mica pyroxenite and may cut anhydrous pyroxenite as well. In some cases, the percentage of amphibole approaches 90 percent and flow foliation or lineation is common. Inclusions of anhydrous pyroxenite are numerous, especially in the distinctive highly poikilitic variety. This coarse poikilitic amphibole pyroxenite, although ubiquitous, invariably forms the larger masses of amphibole pyroxenite generally situated at the outer edges of the pyroxenite body. In one case, this pyroxenite type was seen intruding fenitized Belt country rock.

Contact relations between syenitic rocks and the pyroxenite mass are nowhere visible, at least as sharp features. In some areas, as the hidden contact is approached, the syenite or alkali-feldspar syenite becomes enriched in mafics. This is clearly exposed at the last road fork before the vermiculite mine, and is evidenced where a patch of amphibole pyroxenite and hybrid rock is isolated in the western syenitic horseshoe. There, a small amount of hybrid rock (pyroxene-potassium feldspar in subequal amounts), swimming in a sea of mostly alkali-feldspar syenite, may indicate contemporaneity of syenite and pyroxenite as well as representing a produce of interaction between two highly diverse magma types.

Trachyte dikes cut pyroxenite with sharp contacts and show no wall-rock alteration. Two large dikes trending towards adjacent syenite apparently do not continue beyond the pyroxenite. The westernmost dike

lies in the zone of foliated biotite pyroxenite and is concordant with that foliation.

Anhydrous pegmatite forms the knob immediately south of Skalkaho Mountain in addition to cutting all varieties of pyroxenite. No evidence was seen of the pegmatite cutting either syenite or country rock. Where the pegmatite runs through mica pyroxenite, the pyroxenite adjacent to the pegmatite is commonly indurated for a distance of several decimeters. In rare cases, parallelism of pyroxene crystals in the wall immediately adjacent to an undeformed pegmatite dike suggests pre-injection shearing, possibly before total consolidation of the pyroxenite. Later, pegmatitic material may have been localized along the shear zone. Growth of pegmatite minerals within the dikes followed a prescribed paragenesis, resulting in comb-type structure with a central zone rich in feldspar and miarolitic cavities (Fig. 5). Dike forms are common as are pods, patches, and anastomozing zones of pegmatitic mineral. In rare cases, juxtaposition of fine-grained and extremely coarse-grained material of pegmatitic mineralogy is reminiscent of the aplite-pegmatite association in some granitic pegmatites (see Fig. 6).

In the pegmatite body forming the knob, inclusions of pyroxenite range from fist-sized to head-sized and probably beyond. They commonly serve as nucleation centers with initial crystallization of pegmatitic pyroxene resulting in a pattern radiating outward from the inclusion. Within this body, zones containing up to 50 percent apatite occur as very straight, sharply bounded dike-like features and as irregular to

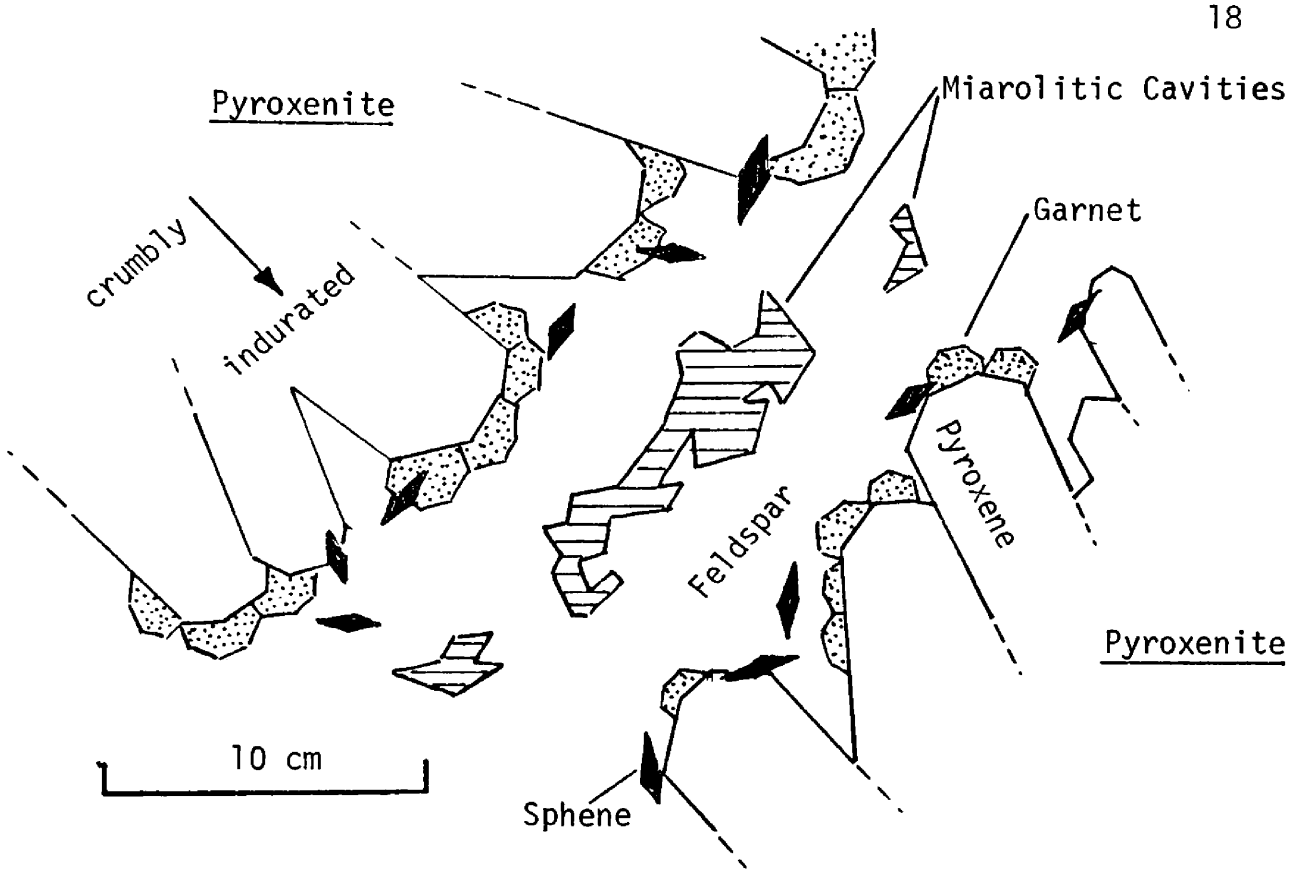

Figure 5. Idealized sketch showing comb structure of pegmatite dikes.

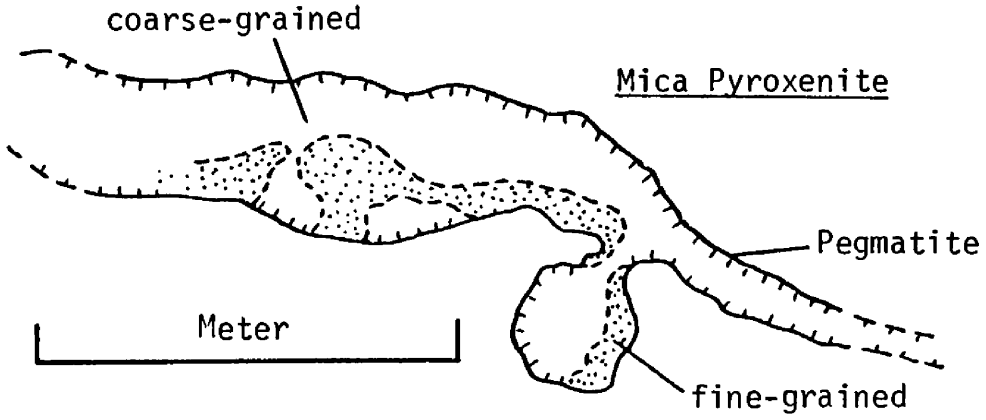

Figure 6. Field sketch of aplite-pegmatite type texture in pegmatite with anhydrous mineralogy.

amoeboid patches. The texture is unique, with such zones often running through only a portion of an individual crystal.

Linear and anastomozing carbonate bodies cut pyroxenite, and in several areas, small bodies of pure white calcite are associated with quartz. One linear form cutting vermiculite pyroxenite is composed of what appears to be ankeritic carbonate and quartz. This vein contains abundant cavities and weathers a bright orange ochre.

Belt metasediments comprising the country rocks are invariably the most resistant, forming almost all ridges and peaks surrounding the upper St. Clair Creek basin and the igneous complex. Changes in slope are common between country rock and intrusive rocks and talus piles are generally limited to the Belt rocks. Pyroxenite as expected is easily eroded resulting in poor exposure, exceptions being the vermiculite bearing ridges and areas where magma injection, particularly of pegmatite, has produced a more resistant structural framework. These vermiculite-bearing ridges may owe their existence to the abundant phases intruding them or possibly to rapid drainage through the generally permeable material. Syenite outcrops slightly better than pyroxenite whereas resistant pegmatite and trachyte are moderately good outcrop-formers.

CHAPTER III

PETROGRAPHY

Pyroxenite

As stated earlier, the rocks of the pyroxenite body may be grouped into three categories. Of these, the anhydrous pyroxenite is in all aspects of mineralogy and texture highly uniform, the mica pyroxenite varies widely in mica concentration and texture, and the amphibole pyroxenite comprises rock types which are still more varied, yet retain common characteristics. Modal compositions for all rocks estimated in thin section are listed in Table 1.

Anhydrous pyroxenite. The anhydrous pyroxenite variety occurs as a massive ridge-forming body in the southeast portion of the pyroxenite mass, as isolated outcrops within areas of other pyroxenite types, and as discrete fuzzy-bordered rounded inclusions within the amphibole pyroxenite. In handsample, this type is a hard, extremely fine-grained (less than 1mm), dark-green rock, generally showing complete lack of structure and forming rare bouldery outcrops. In isolated cases, a vague parallelism of pyroxene grains may be indicative of flow during crystallization.

Mineralogically, the anhydrous pyroxenite consists of at least 98 percent pyroxene grains which commonly show near 120° boundary configurations (Plate 1a). Grain size ranges from 0.1 mm to (rarely)

Table 1a. Modal Analyses of Pyroxenites

Sample #	Anhydrous Pyroxenites		Mica-Pyroxenites			Amphibole Pyroxenites																		Apatite-phase
	69	27B	20	134	167	5B	23	27A	32	35A	54	56A	56B	59A	60	60B	61	85	87	129	145	176	196	128
Augite	98	99	70	78	65/90	80	50	60	82	84	80	43	78	85	10	97/5	4	65	40	40	40	75	32	89
Biotite			26	10	30/5	1		1	2	7	1	2	1						T	1		T		
Amphibole						7	8	25	8	5	7	30	2	2.	82	0/84	84	12	50	42	50	8	10	
Apatite	1	1	T	T	T	3	2	4	2	T	4	3	5	1	3	2/3	5	3	4	3	1	2	2	10
Magnetite	T	T	T		T	3	1	4	.1	2	5	5	1	2	1	1/3	T	4	4	5	1	5	1	T
Sphene	1			T	T	2	2	4	3	1	2	15	2	1	2	0/4	2	2	1	3	3	5	3	T
Plagioclase			3	8	4	1	5	1	1	1			4	3	1			2	1	1	T	1		1
K-feldspar							30						5					10					45	
Epidote	T		T	T		4	2	1	1	T	T	2	2	5	1	1	5	2	1	3	4	1	2	
Calcite				3																				
Garnet	T													T									4	
Hematite	T		T	T	T		1	1	T	T	T				1		T	T		2	2	4	1	
Zircon																	T				T	T		
Chlorite																								

Table 1b. Modal Analyses of Syenites

Sample #	4c	18A	43A	46A
Perthite	88	89	40	50
Microcline			15	20
Plagioclase			25	30
Augite	3	6	7	
Biotite	T	T	T	T
Amphibole	5	2	9	
Apatite	1	1	1	
Magnetite	1	1	1	T
Sphene	2	1	1	
Epidote	T	T	T	4
Garnet	T			
Hematite	T		T	
Zircon			T	

Plate 1a: Photomicrograph showing 120° boundary configurations between pyroxene grains in the anhydrous pyroxenite.

1 mm

Plate 1b: Photomicrograph showing pyroxene grains embayed by biotite in mica pyroxenite. Note twinned, dismembered pyroxene grain. Crossed polars.

1 mm

Plate 1c: Photomicrograph showing interstitial nature of calcite in mica pyroxenite. Crossed polars.

1 mm

Plate 1d: Photomicrograph showing poikilitic nature of hornblende (at extinction) in amphibole pyroxenite. Enclosed, embayed grains are mostly pyroxene with some apatite and magnetite. Crossed polars.

1 mm

Plate 1a: Photomicrograph showing 120° boundary configurations between pyroxene grains in the anhydrous pyroxenite.

1 mm

Plate 1b: Photomicrograph showing pyroxene grains embayed by biotite in mica pyroxenite. Note twinned, dismembered pyroxene grain. Crossed polars.

1 mm

Plate 1c: Photomicrograph showing interstitial nature of calcite in mica pyroxenite. Crossed polars.

1 mm

Plate 1d: Photomicrograph showing poikilitic nature of hornblende (at extinction) in amphibole pyroxenite. Enclosed, embayed grains are mostly pyroxene with some apatite and magnetite. Crossed polars.

1 mm

Plate 1a: Photomicrograph showing 120° boundary configurations between pyroxene grains in the anhydrous pyroxenite.

1 mm

Plate 1b: Photomicrograph showing pyroxene grains embayed by biotite in mica pyroxenite. Note twinned, dismembered pyroxene grain. Crossed polars.

1 mm

Plate 1c: Photomicrograph showing interstitial nature of calcite in mica pyroxenite. Crossed polars.

1 mm

Plate 1d: Photomicrograph showing poikilitic nature of hornblende (at extinction) in amphibole pyroxenite. Enclosed, embayed grains are mostly pyroxene with some apatite and magnetite. Crossed polars.

1 mm

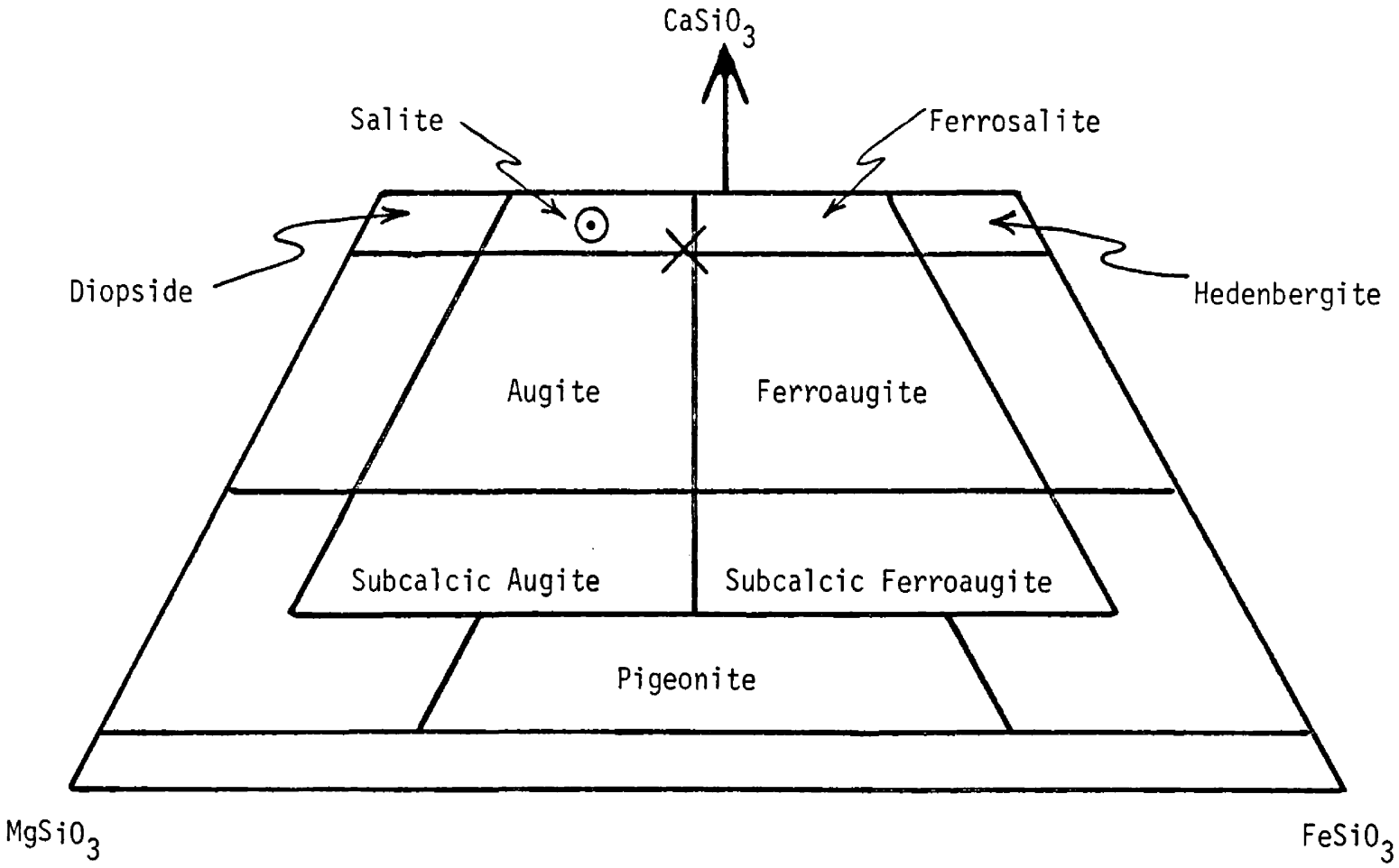

Figure 7. Composition of pyroxene composing the anhydrous pyroxenite. Circle represents chemical data. X is from optical data.

the appearance of hornblende, epidote, magnetite (?), $\pm$ sphene, $\pm$ garnet. These minerals appear both between and inside individual pyroxene grains, and are interpreted as an alteration or replacement assemblage.

Mica pyroxenite. The generally coarse- to very coarse-grained mica (biotite, hydrobiotite, or vermiculite) pyroxenite is the most abundant variety of pyroxenite, apparently making up most of the western portion of the pyroxenite body. In addition, a large mass outcrops along the roads immediately southwest of the pegmatite and numerous isolated patches are scattered throughout the remainder of the complex.

The mica proxenite outcrops as large rounded boulders similar to those common in semi-arid granitic areas, but is more commonly exposed as crumbly, decomposed, in situ material along roadcuts and trenches. Mica content is erratic, varying from 5 percent or so to over 75 percent, commonly within the space of a few centimeters. Segregations of mica-rich rock may occur as pods or small irregularly-shaped bodies. Although almost invariably massive in texture, near the western margin of the pyroxenite within 30-150 meters from the syenite, biotite pyroxenite outcrops appear "sheeted" due to the foliation defined by pyroxene and biotite grains. Biotite-rich zones, although still apparently pod-like, here lie subparallel to the foliation, which may have channeled late fluids.

The pyroxene in these mica pyroxenites appears identical to the salite of the anhydrous pyroxenite except that it contains extremely

thin opaque rods (ilmenite?) apparently exsolving within the grains along two crystallographic directions. Polysynthetic twinning is locally developed. The grains are generally stubby prisms 0.5 to 6 mm long often embayed by mica.

Mostly biotite, the mica is strongly pleochroic -- X = light brown, Y=Z = dark brown to dark olive brown -- and contains exsolved rods of clear rutile oriented along three crystallographic directions. Biotite grains are bent and broken, with deformation kinks developed. Poikilitic inclusions of pyroxene are commonly optically continuous and embayed (Plate 1b), suggesting replacement of pyroxene by biotite. Crystals range from 1 mm to more than 1 meter across and are generally in the 30 mm range. Minor amounts of green biotite occur as optically continuous patches on the edges of pyroxene grains and along fractures within them. This phase is probably a late-stage alteration. Increasing expandability in a flame, decreasing elasticity of the flakes, and a color change to golden-brown indicate that biotite has locally been altered to hydrobiotite or vermiculite.

Plagioclase forms continuous interstitial poikilitic patches which constitute 3-9 percent of the rock. It is normally zoned from An_{30} to An_{22}. Albite twinning is locally developed and pericline twins are rare.

Intergranular euhedral sphene, subhedral apatite, anhedral magnetite and epidote (X = colorless, Z = lime yellow) and hematite occur in trace amounts. Interstitial twinned calcite with $2V\alpha = 10°$ is present to a few percent. Its clearly interstitial occurrence (Plate 1c) and its

habit of enclosing plagioclase imply a late-stage product of crystallization. Paper-thin sheets of white material located between mica flakes were identified as α-quartz by means of x-ray diffraction. Similar interlamellar sheets occurring in biotite at the Rainy Creek Stock were identified as either quartz or tremolite (R. Kujawa, verbal comm., Sept., 1978).

Textural relations imply that initial crystallization of pyroxene preceeded later development of biotite. At least some and perhaps all of the biotite replaced earlier pyroxene. Interstitial plagioclase, epidote, and calcite crystallized later. Mild deformation of biotite flakes and a minor alteration to form green biotite are still later. Quartz interleaved in mica books probably attests to a late hydrothermal event.

Amphibole pyroxenite. Amphibole pyroxenite is by far the most variable and in fact may be viewed as an attempt to clump numerous rock species. Besides the diagnostic appearance of green amphibole, apatite, sphene, and magnetite are ubiquitous. Handspecimen textures vary widely from fine-grained (1-3 mm), to coarse-grained (25 mm), to poikilitic amphibole grains reaching 15 cm. Some units are massive whereas others show a weak to very pronounced foliation or lineation. In handsample the rocks vary from very dark green to light green with interstitial white patches, honey-colored sphene crystals, white apatite prisms, and/or magnetite or pyrite grains. All the varieties outcrop sporadically and occur as isolated pods, dike-like features, or small bodies which

complexely cut each other and the other pyroxenites. Field relations indicate that the amphibole pyroxenite postdates the other two pyroxenite types. Petrographic work corroborates this view.

The pyroxene of this group is also nearly identical to that of the anhydrous pyroxenite except for certain subtleties. Grain size varies from 0.1 mm to over 8 mm, with 1-3 mm being most common. Zoning was noted in a limited number of samples. The invariably light-green to nearly colorless centers and thin, darker-green rims suggests enrichment in sodium. $Z\wedge C$ varied from 43° in the core to 51° in the rim.

The percentage of amphibole, even within a single thin section, ranges from near zero to as high as 85. It is strongly pleochroic -- X = pale brown, Y = olive green, Z = dark green and rarely bluish-green on edges -- with weak to moderate dispersion. Slight zoning locally occurs with $Z\wedge C$ ranging from 16° in the core to 23° in the rim. The approximate average $2V\alpha$ is 55°. Some crystals showed exsolution of opaque rods causing the Schiller effect. Single grains ranging to 30 mm usually poikilitically contain all of the other minerals (Plate 1d), but in some cases optically continuous patches occur within larger pyroxene grains or interstitial to other grains. In several rocks, biotite with reaction rims of amphibole is enclosed in pyroxenite (Plate 2a). It thus appears the amphibole is later than pyroxene and biotite, and most amphibole pyroxenites may be metasomatic alterations of earlier anhydrous pyroxenites or biotite pyroxenites.

Invariably, the amphibole is associated with the distinctive assemblage apatite (1-5%), magnetite (1-8%), and sphene (1-15%). Sections of euhedral to rarely subhedral apatites range from 0.1 mm to 3 mm across. Its habit is very stumpy to extremely acicular. Crystals are locally enclosed in pyroxene and abundantly enclosed in amphibole or are intergranular. Apatite is inferred to have crystallized largely after pyroxene and before amphibole.

Magnetite, whose unusual abundance is roughly correlative with that of apatite, occurs both as anhedral to subhedral grains 0.1 to 5 mm across and as fine dusty patches within altering pyroxene grains. The grains are poikilitically enclosed by biotite, amphibole, and rarely pyroxene and interstitial sphene. The grains rarely enclose brown biotite. Magnetite is spatially associated with sphene, biotite, and epidote, and is commonly surrounded by a thin rim of sphene. In some cases it is rimmed by biotite, or more rarely by outward progressing rings of sphene and biotite. Although textural relations are inconclusive, apparent embayment by pyroxene and sphene ranging to definite interstitial habit suggests a long period of magnetite crystallization.

Another abundant mineral critical to the amphibole pyroxenites is sphene, which occurs in section as characteristic euhedral wedges from 0.1 mm to nearly 10 mm long, and locally as anhedral interstitial poikilitic patches up to 10 mm across. A $2V_{\gamma}$ of approximately 25-30°, and a green to yellow color, indicate a low Fe^{+3} and Al content, and corresponding high Ti (Tröger, 1979, p. 63; Deer and others, 1976, p. 18).

In most cases, dispersion is shown by incomplete extinction. Like magnetite, sphene appears to have had a long period of crystallization. Textures reveal a large percentage crystallized, like apatite, after pyroxene and before amphibole.

Plagioclase is normally either absent or constitutes up to 1 percent of the rock. In one case, however, a dike-like body contains about 4 percent of the mineral. The composition of plagioclase in this "dike" is An_{0-3}.

Perthitic potassium feldspar was detected in two samples of pyroxenite near the center of the complex. However in one case it occurs in a vein about 3 mm wide, and immediately adjacent to this vein in the interstices, possibly suggesting a late-stage injection. An alternate explanation is that the potassium feldspar liquid congregated and migrated away from its host pyroxenite along passageways.

Epidote is ubiquitous though subordinate (1-4%). Its distinctive pleochroism -- X = clear, Z = bright limey yellow -- and $2V\alpha$ close to 70° suggests it is an iron-rich variety (Tröger, 1979, p. 62). The high birefringence simplifies ready recognition of epidote as both a primary interstitial phase and as an alteration product within plagioclase and especially pyroxene. The only other minerals noted are local pyrite and rare, tiny, subhedral zircons which cause pleochroic haloes in amphibole.

As stated earlier, textures support field evidence for the later evolution of the amphibole pyroxenites. It appears clear that zones

of anhydrous pyroxenite and biotite pyroxenite are cut by various species of apatite-magnetite-sphene-bearing amphibole pyroxenites. It also seems clear that some units cross others as dike-like features. Most if not all formed by a deuteric or metasomatic alteration of earlier varieties of pyroxenite. Boundaries between rock types are in most cases gradational, and pods or segregation of one type in another are extremely common.

Paragenesis. Summarizing the interpretive paragenesis of the pyroxenites, it appears that an ultramafic magma crystallized anhydrous pyroxenite until changing conditions led to the formation of mica pyroxenite and finally amphibole pyroxenite. A generalized mineral paragenesis is shown in Figure 8. Volatiles and related elements not present in the early anhydrous pyroxenite emerge as important constituents during evolution of the pyroxenite body.

Water, possibly partly evolved from the primary magma but more likely derived from shallow crustal sediments, is essential to the development of mica. The low acmite content in pyroxene implies a low ferric iron concentration in the original magma. This in turn suggests low oxygen fugacity, or a low water content. Several factors suggest nearly all biotite formed by replacement of pyroxene, probably through the action of late-stage fluids. Mica concentrations are irregular and sporadic. They occur in patches and sometimes in layers roughly concordant with flow foliations of the pyroxenite. Borders with anhydrous pyroxenite are everywhere gradational. Biotite, normally brown in color (implying

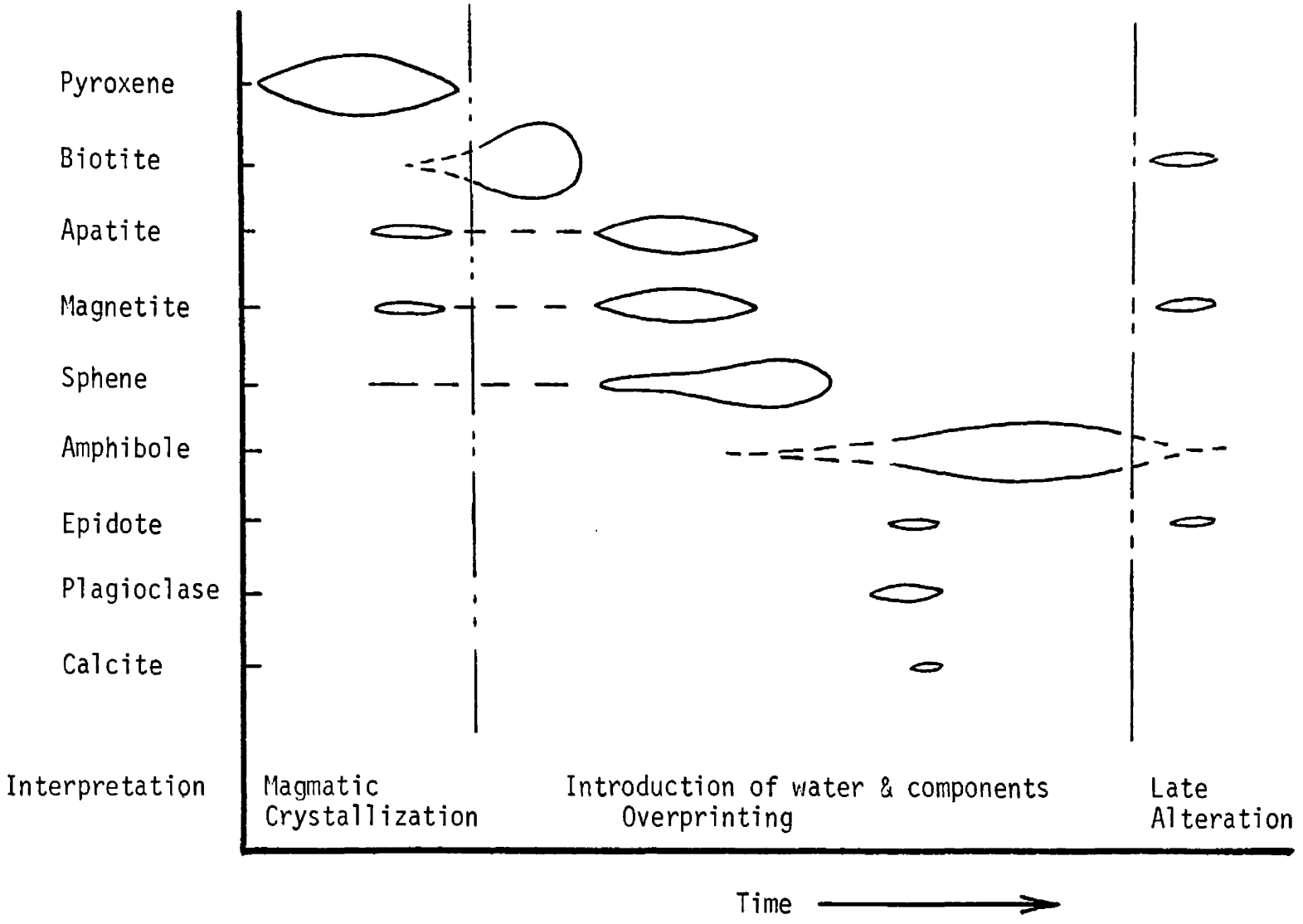

Figure 8. Idealized paragenesis of minerals of the pyroxenites.

higher temperature of formation relative to the later green alteration type), embays and dissects individual pyroxene crystals, implying direct replacement. It is also difficult to imagine mica books one meter across forming with fine-grained pyroxene crystals directly from a melt. The pegmatite, considered to be a residuum from the pyroxenite system, has an anhydrous mineralogy. This is perhaps due either to an elevated temperature of formation which restricted the mafic constituents to pyroxene and garnet, or more likely to the absence or low concentration of H_2O in the vapor phase. If so, this would place a further constraint on primary crystallization of biotite in the mica pyroxenite. The large amount of potassium necessary to form the biotite is believed to have come from the igneous system itself, specifically the potassium-rich syenite. At a much later time, leaching by groundwater and possibly some low temperature hydrothermal alteration transformed biotite to hydrobiotite and vermiculite. Boettcher (1966) dealt in depth with the formation of vermiculite and hydrobiotite from biotite at the Rainy Creek stock. The presence of quartz sheets between biotite plates also serves as evidence of late aqueous activity. In the mica pyroxenites, exsolution of rutile within biotite and of ilmenite (?) within pyroxene indicates a decreased capacity for these minerals to contain titanium, probably in response to a drop in temperature.

Later amphibole pyroxenites, also rich in water, contain more iron and greater amounts of "volatile-related elements" such as TiO_2, P_2O_5, and REE than either the anhydrous or mica pyroxenites. An increase in

alkali content with evolved pyroxenites is evidenced in the development of biotite followed by the appearance of sodic rims on pyroxenes, the appearance of perthitic potassium feldspar, and the highly albitic plagioclase seen in the amphibole pyroxenites. The mineral paragenesis pyroxene to biotite to amphibole would not normally be expected with increased evolved or concentrated water. Perhaps a large increase of potassium availability along with introduced water required biotite formation. Subsequent relative depletion in potassium may have fostered formation of amphibole-rich pyroxenite. Without high potassium activity, pressure-temperature conditions may have favored amphibole stability. Some amphibole pyroxenite appears magmatic, although most is probably replacement. Everpresent, significant amounts of apatite and magnetite attest to the ubiquitous introduction of at least phosphorus and iron in the amphibole pyroxenites.

The existence of a magma of such composition (alkali pyroxenite) to yield the pyroxenitic rocks of Skalkaho may seem unlikely, particularly with regards to liquidus relations and hypabyssal plutonic conditions. However, the pyroxenite suite as a whole is enriched in volatiles and elements such as P_2O_5 and TiO_2 which are known to reduce liquidus temperatures. As in the case of calcium carbonate which was shown to suffer a dramatic drop in crystallization temperature with addition of other constituents, pyroxenitic magmas may exist under reasonable geologic conditions when in solution with a sufficient amount of added constituents. The exixtence of pyroxenitic magma is a problem reminiscent

of that of the carbonatite magmas in the past and is herein considered plausible. Experimental work on alkalic ultramafic systems is warranted.

Syenitic Rocks

Alkali-feldspar syenite. Alkali-feldspar syenite comprises the bulk of the syenitic complex. Varieties differ mainly in percentage of mafic minerals which range from near zero to over 50 percent, and in texture which is commonly highly directional (trachytoid feldspar or lineation of mafics) but may range to massive. Stubby feldspar crystals generally about 10 mm long and smaller intergranular mafic minerals impart a blocky look to the rocks. Locally intense pyrolusite staining imparts a black sheen to the normally whitish-gray rock.

Potassium feldspar is the dominant felsic mineral in the rock. It is a microperthite or rarely perthite of the braid, patch, string, or band variety (Alling, 1938, p. 142). In some samples, the feldspar is microcline with characteristic tartan twinning. Up to 15 percent twinned plagioclase of composition An_{6-8} in some cases exsolves along grain boundaries or within grains as discrete blocks up to 0.25 mm across. Characteristically about 10 mm long, crystals may be as small as a few mm or as large as 20 mm. Locally present is minor primary plagioclase of composition near An_{3-5}.

The mafic and accessory minerals generally occupy spaces between the feldspars (Plate 2b). Pyroxene grains averaging 0.5 mm across show moderate pleochroism -- X = green, Y = light green, Z = light yellow-green. A $2V_Y$ of 70° $\pm$ 1°, and $X\wedge C$ between 34°-39° determined on the

universal stage, indicate the pyroxene is enriched in alkalies, and is probably a salite containing about 15 percent acmite molecule (Tröger, 1979, p. 83). Amphibole with strong pleochroism -- X = light brown, Y = light green, Z = dark green to rarely bluish green -- and $2V\alpha$ close to 55° is probably a hornblende. Rare pale bluish-green rims may be actinolite or may indicate late sodium enrichment. The ratio between pyroxene and amphibole is highly variable, and textural relations indicate that at least some amphibole replaces pyroxene. Traces of biotite with X = light brown, Y = Z = dark olive green mixed with orange-brown occur within amphibole grains and as anhedral books surrounded by feldspar grains.

Twinned acicular crystals of sphene about 2 mm long are a characteristic accessary in the alkali-feldspar syenites, and in that habit invariably differ from the abundant sphene of the pyroxenite and pegmatite (Plate 2c). Sphenes sometimes enclose opaque minerals and are commonly associated with them as well as pyroxenes. Euhedral to subhedral stubby apatites are commonly about 1 mm across. Anhedral magnetite and pleochroic epidote with X = colorless, Z = bright yellow, are also major accessories. Tiny zircons surrounded by pleochroic haloes in biotite were noted.

Syenite. Several varieties of syenite containing 25-30 percent plagioclase occur as minor phases throughout the outer part of the complex and as apophyses within the Belt country rocks. Except for a leucrocratic pegmatitic variety with potassium feldspar megacrysts commonly 15 cm long, the syenites are relatively fine-grained

(average 1-5 mm) compared with the alkali feldspar syenites. Mafic minerals may be nearly absent or may constitute up to 25 percent of the rock.

Microperthite grains are most abundant and appear to be forming from generally smaller microcline crystals which show well-formed tartan twinning. Braid, string, and ribbon perthites are most common. Perthite megacrysts commonly show Carlsbad twinning.

Plagioclase grains show albite, pericline, and Carlsbad twinning, and normal zoning. Compositions measured vary between An_5 and An_{15}. Slight deformation is evidenced by minor bending of twinned crystals.

The mafics and accessories of the syenite are nearly identical to those in the alkali feldspar syenite. Pyroxene grains show a lighter color with the same pleochroic scheme, and biotite grains are uniformly green. In a single sample of float collected on a syenitic hilltop, coarse muscovite flakes 15 mm or more across are bent and highly embayed by deformed plagioclase grains and potassium feldspar grains and megacrysts. This may represent an equilibrating inclusion, possibly related to the nearby Willow Creek stock, comprised in part of muscovite granites.

Two outcrops of quartz monzonite were found; one outside the northern boundary of the complex, and the other at its western margin. Although mafic and accessory minerals resemble those of the syenitic rocks, higher anorthite content of the plagioclase, the presence of quartz with abundant myrmekite, and field relations, suggest this rock is not directly connected to the syenite-pyroxenite event. Quartz monzonite occurs elsewhere in the region.

Paragenesis. Inclusions of mafic minerals and accessories in feldspar grains of the syenites are sparse except near the edges of the grains. Relations between mafic minerals and accessories suggest nearly simultaneous periods of crystallization for these minerals, with the possible exception of the early appearance of pyroxene and biotite. Thus, crystallization in the syenites began with the formation of feldspar and ended with crystallization of all minerals.

Slight deformation of the syenitic rocks is indicated by some bending of micas and plagioclase, and minor mortar texture in some samples. Cross-cutting relationships are common and complicated. Preferred orientations in feldspar and mafic grains are interpreted as flow lineations since they normally occur where dikes or border zones are discernable. Numerous inclusions of Belt country rock and various igneous granitics, along with evidence for frozen piecemeal stoping and injection of syenitic material between layers of the country rock, illustrate the magmatic nature of the syenitic rocks. No evidence suggesting this is fenite was detected.

In conclusion, the varieties of syenitic rocks are interpreted to have resulted from progressive differentiation of an original alkali-rich syenitic magma. Early syenites formed along the cooler borders of the complex while alkali-feldspar differentiates generally occupy more central locations. Feldspars crystallized early with later crystallization of feldspar, mafics, and accessories.

Hybrid Rocks

In two places, both associated with poikilitic amphibole pyroxenite and both lying very close to syenite, a characteristic pyroxene-potassium feldspar rock was encountered. In handspecimen, stubby dark-green crystals up to 3 cm long together with smaller greenish crystals appear suspended in a white matrix. In some instances, intense weathering of mafic minerals has left a boxwork-type structure of white feldspar. One occurrence is located on the northern edge of the pyroxenite body less than 40 meters from a syenite outcrop to the north, in a zone rich in amphibole pyroxenite and pegmatite. The other locale lies within the western lobe of syenite, over 100 meters from the pyroxenite body. There, an isolated patch of amphibole pyroxenite occurs with some pyroxene-potassium feldspar rock.

Mineralogically, the rock consists of about half microperthite forming extensive continuous poikilitic patches. Pyroxene, with some amphibole and minor garnet, sphene, apatite, magnetite, and epidote, appears randomly distributed within the feldspar. A slab stained for potassium feldspar shows a striking bright yellow and green pattern.

The pyroxene is moderately zoned from light green to rarely clear cores to darker rims with X = green, Z = yellowish green. The zoning is complex with irregular-shaped cores, suggesting either early resorption with later overgrowth or possibly non-uniform peripheral replacement of one pyroxene by another. In some instances, pyroxene is altering to amphibole, garnet, epidote, and magnetite. Amphibole

with X = light brown, Z = dark green forms optically continuous patches with included remnant pyroxene grains. Garnet is isotropic and light orange-brown. Epidote is iron-rich (X = clear, Z = yellow), and sphene forms long, acicular, twinned crystals.

Possibly related to these hybrid rocks are the very mafic-rich syenites or alkali-feldspar syenites which appear concentrated near the pyroxenite-syenite border. The dominant mafic mineral is generally amphibole, which in some areas shows a very strong flow lineation. With extreme weathering, a light black soil develops which is easily confused with the soils developed on rocks of the pyroxenite clan. The possible origin and significance of this rock type is discussed below.

Pegmatite

The relatively resistant pegmatite outcrops as blocks sporadically poking out of the ground or as linear zones and isolated, locally anastomozing patches within pyroxenite. It appears to be limited to the northern and northeastern parts of the pyroxenite body with the bulk forming the knob immediately south of Skalkaho Mountain. Mineralogically simple, the rock is chemically unusual and, together with the similar pegmatite at Rainy Creek, is possibly unique. A literature search failed to locate any description of a similar occurrence. Feldspar and pyroxene are invariably present in subequal amounts, with varying percentages (0-20%) of garnet and sphene. Less than one percent magnetite occurs locally. Apatite concentration is variable. Point counting was conducted on outcrops using a 1/4" mesh wire screen. The results of

counts on eight outcrops along with total counts to approximate an "average" sample are shown in Table 2.

Table 2. Pegmatite Point Counts

Sample	#1	#2	#3	#4	#5	#6	#7	#8	#	%
feldspar	274	442	218	369	462	354	412	262	2793	38.6
pyroxene	384	288	254	310	301	371	360	239	2507	34.6
garnet	2	8	98	270	126	102	130	87	823	11.4
sphene	67	40	81	82	102	74	69	56	581	8.0
cavities	--	8	--	--	14	2	4	--	28	0.4
pyroxenite	--	265	--	--	--	79	160	--	504	7.0
total	727	1061	651	1031	1005	982	1135	644	7236	100.0

Albitic plagioclase is the most common feldspar, commonly An_0 but ranging to An_{11}. Normal zoning is pronounced enough to see in handsample. Albite twins, locally taking on a checkerboard character, are slightly bent indicating minor post-crystallization stress. Antiperthite is also widespread, but generally makes up less than about 25 percent of the rock. This mineral stains poorly with sodium cobaltinitrite. Perthitic orthoclase occurs only sporadically. In both these bimineralic feldspars, the ratio of sodic plagioclase to potassium feldspar is generally near unity. Trace amounts of magnetite,

sphene, and epidote are the only inclusions. All feldspars occupy interstitial spaces or are enclosed in garnet or pyroxene.

Pyroxene crystals generally a few centimeters long may exceed lengths of 20 or more centimeters. In handsample, some have darker cores which are seen in thin section to be relatively unaltered and pure, slightly pleochroic pyroxene with X = dark green, Z = light slighly yellow green, $2V_{\gamma}$- 64°, and XΛC around 32°. The rims on these grains are lighter-colored due to abundant included feldspars and epidote, with magnetite and some sphene. The epidote-magnetite-sphene assemblage is particularly common where garnet abuts the pyroxene. Pyroxene-feldspar grain boundaries are ragged with feldspar embaying pyroxene. This suggests either disequilibrium conditions or simultaneous crystallization of feldspar and pyroxene in the later stages of pyroxene formation.

Black, euhedral garnets up to 6 cm across commonly nucleated on pyroxene crystals (see Fig. 5). Dark reddish-brown in thin section, these garnets invariably have growth rings defined by changes in color intensity and oriented inclusions of feldspars. A specific gravity of 3.77 and a unit cell edge of 12.006 $\mathring{A}$ indicates the garnet is andradite 73 percent, grossularite 27 percent (J. P. Wehrenberg, 1979). Titanium content is low.

Euhedral sphene crystals attaining diameters of 2 cm are either honey-colored or yellowish-green and have a resinous luster. Sections through crystals are characteristically wedge-shaped.

Iron-rich epidote, pleochroic X = colorless, Z = yellow, occurs within pyroxene and feldspar grains and as interstitial crystals. Within pyroxenes, it is commonly associated with euhedral magnetite. Traces of biotite with X = light brown and Y = Z = dark orange-brown occur with feldspar patches. Traces of amphibole (X = light brown, Z = dark green to blue-green) appears as opitcally continuous patches in large pyroxene grains. Apatite crystals averaging 1.5 mm across normally account for less than a percent of the rock.

Miarolitic cavities up to 4 cm across are extremely common in the pegmatite. Although the cavity walls are commonly bounded by feldspar faces, garnet, pyroxene, and sphene crystals locally jut into the spaces. In one instance, euhedral emerald-green epidote tablets grew in a cavity. The low ferric iron content of pyroxene within the pegmatite as well as the pyroxenite implies a low water content (low f_{O_2}) in the system. These miarolitic cavities are therefore interpreted to reflect a CO_2-rich volatile phase. Two-phase fluid inclusions are common.

Inclusions of all three types of pyroxenite were seen within pegmatite masses. These served as nucleation sites for pegmatitic pyroxene crystals which radiate outward from the pyroxenite. In a similar fashion, where pegmatite transects pyroxenite, the earlier pegmatitic pyroxene is oriented perpendicular to the country rock contact. This gives a comb structure to narrow pegmatitic dikes. The dikes are zoned inward from pyroxenite country rock (often a crumbly soil), to indurated pyroxenite, to a zone rich in pegmatite pyroxene,

to a garnet-sphene zone, to a feldspar core containing miarolitic cavities (see Fig. 5). In one case, foliation of wallrock pyroxenes suggests shearing along a zone which then acted as a passageway for pegmatitic fluids. Mineral paragenesis in the dikes parallels that in the pegmatite proper: early pyroxene yielding to garnet and finally interstitial feldspars and epidote. Moderate overlap is apparent, and minor sphene correlates roughly with garnet crystallization.

Apatite phase. An apatite-rich variety of pegmatite is abundant enough to be obvious in the field. In handsample or thin section, the percentage of apatite is easily estimated at 30-50 percent. It occurs as white crystals 1-3 mm across and 5-20 mm long which appear poikilitically included in virtually all minerals of the normal pegmatite (Plate 2d). The long crystals are commonly skeletal (Plate 3a), enclosing the same major minerals of the pegmatite. The apatite is biaxial with 2V approximately 10°. It is euhedral to nearly euhedral.

The apatite phase occurs in two forms. The first is as isolated amoeboidal patches within the pegmatite; the second as distinct dike-like features running through the pegmatite and cutting individual mineral crystals within it. Large single euhedral garnets, for instance, may contain up to 50 percent apatite crystals poikilitically enclosed in one half whereas the other side of the garnet, outside of the "dike" trend, may be nearly pure (Plate 3b).

A pyroxenite inclusion from a zone of apatite-rich pegmatite was seen in thin section to contain about 15 percent or more acicular apatite

Plate 3a: Photomicrograph showing skeletal nature (here in cross-section) of apatite in apatite-phase of pegmatite. Dark areas are garnet.

1 mm

Plate 3b: Photograph showing apatite phase cutting individual garnet crystal of pegmatite. Apatite phase constitutes the upper half of the photograph. Penny for scale.

Plate 3c: Photomicrograph showing inter-growth of calcite and magnesiohastingsite. Crossed polars.

1 mm

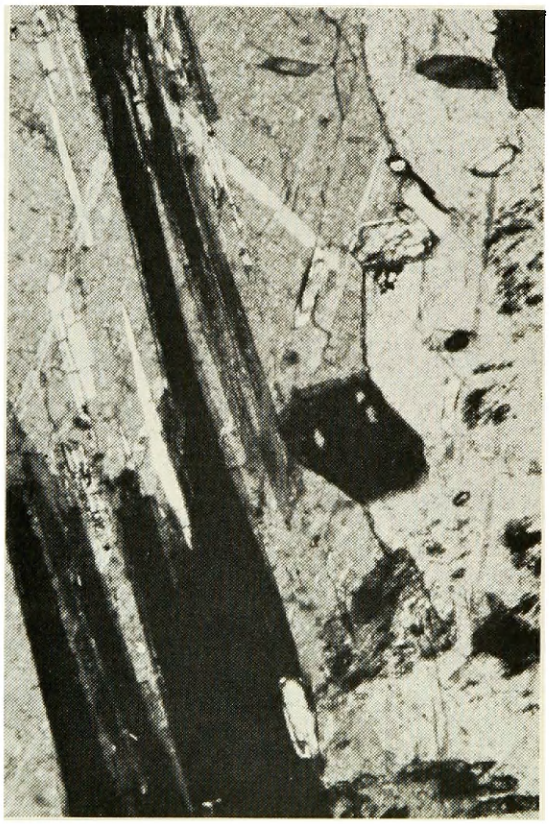

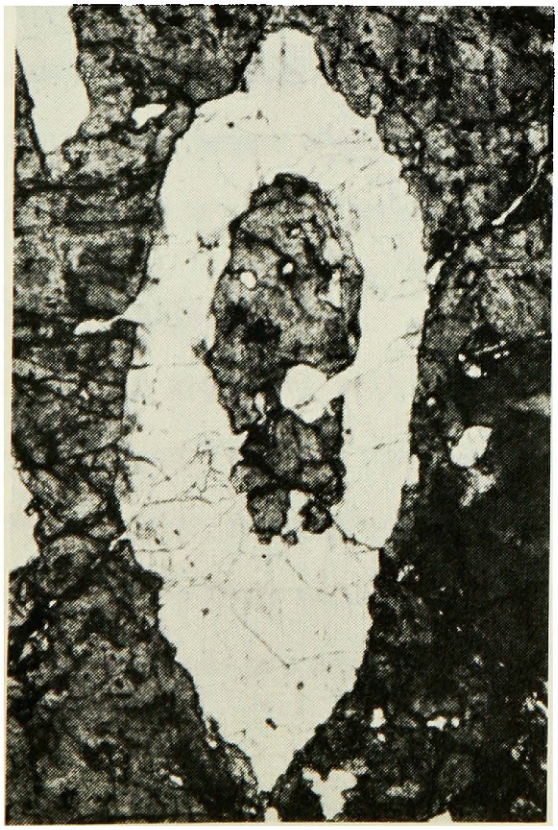

crystals. Except for a percent of interstitial plagioclase and one large interstitial patch of sphene, this rock is composed wholely of apatite and pyroxene. The pyroxene cores are identical to the pyroxene of the anhydrous pyroxenite. The rims are much darker green and have a higher ZΛC angle.

The genesis of this texture is unclear. Skeletal habit suggests rapid crystallization from a melt (Wyllie and others, 1962; Watkinson, 1970). Skeletal, acicular apatite crystals have been reported from a number of carbonatite complexes such as at Oka, Quebec (Watkinson, 1970), Chishanya, Southern Rhodesia (Heinrich, 1966, p. 177), Kaiserstuhl, West Germany (Heinrich, 1966, p. 433), and Oldoinyo Lengai in Africa (Donaldson and Dawson, 1978). The skeletal nature of the apatite and its unique inclusion nature suggest perhaps a replacement origin for some of the pegmatite or possibly initial rapid crystallization of an apatite skeleton within the pegmatitic liquid with subsequent crystallization of other minerals around this framework. Clearly, more work is needed to assign a genesis to this rock variety.

Carbonatite (?)

Two types of veinlike carbonate cut pyroxenite. The first is associated with silica either as boxwork opal or chalcedony-type material or as clear to whitish quartz which commonly forms well-terminated crystals within vugs. The carbonate material is characteristically pure, snow-white, coarse-grained calcite, although in one locale it was

an orange-brown ankeritic carbonate. These quartz-carbonate bodies contain essentially no accessory minerals except for quartz and feldspar, and they form sharp contacts with non-altered mica pyroxenite. In some cases, an ochre-colored alteration is pronounced. These vein-like bodies are interpreted to be typical hydrothermal deposits, probably indicative of post-intrusive hot spring type activity.

The other variety of carbonate poses a more perplexing problem. Mostly medium-grained calcite intergrown with a blue pleochroic amphibole (Plate 3c), these dike- or vein-like forms nowhere show sharp contacts with pyroxenitic wallrock. Instead, the amount of amphibole commonly increases into the outward grading to the encasing rock. The carbonate is calcite, containing no detectable Sr, Ba, or Mn, when analyzed with a carbon-arc spectroscope. It is in most cases medium-grained throughout, but one body contains subangular fragments of an extremely fine-grained, banded variety.

The amphibole is strongly pleochroic, X = colorless to pale green, Y = pale blue-green, Z = blue-green, with a fibrous radiating habit. Universal stage measurements revealed a $2V\alpha = 72°$ and a $Z\wedge C$ between 30° and 32°. It is length-slow, shows moderate dispersion, and has an optic plane oriented parallel to (010). The α-axis has a refractive index of $1.627° \pm 0.001°C$. Based on these data, the amphibole is probably magnesiohastingsite (Troger, 1979, p. 96). X-ray diffraction data corroborate this identification. Quartz, feldspar, pyrite, and a low briefingent mineral forming fibrous aggregates are rare. These

accessories were concentrated with the blue amphibole by dissolving a chunk of the rock in hydrochloric acid. The non-soluble residue constituted about 6 percent by volume of the original rock, with amphibole constituting about 90 percent of this.

Magneseohastingsite is common in alkalic igneous rocks including diorite, gabbro, and pyroxenite, and is less common in nepheline syenite, alkali syenite, nordmarkite, and alkali granite (Heinrich, 1965, p. 269). Its relative hastingsite occurs in carbonatite (Heinrich, 1966, p. 159). Although the available data are insufficient to state conclusively the genesis of this carbonate type, the gradual contacts, the lack of vugs, opaline quartz, adularia, or other hydrothermal indicators, and the presence of hastingsite argue against a hydrothermal origin. The form of the bodies precludes their being interpreted as inclusions, and the massive texture does not favor rheomorphosed carbonate. It is concluded that these bodies may be carbonatite intrusions. The abundance of apatite and magnetite in the complex and its alkalic nature is compatible with, if not suggestive of, the carbonatite association. It is odd that these minerals are not abundant in the carbonate, but perhaps the conditions during crystallization at this level did not favor their formation, or perhaps they had crystallized much earlier.

Trachyte

Alkali-rich trachyte dikes exist as two ridge-forming bodies 25 meters wide and 40 meters wide and as a few smaller dikes. All bodies are nearly vertical and transect pyroxenite in a general north-south direction. The light gray rock where fresh forms piles of blocky talus downslope from dikes. In handsample, a few phenocrysts of feldspar and amphibole less than 3 mm long may be seen in the aphanitic groundmass along with up to 10 percent vesicles reaching to 10 mm long. In the 25 meter-wide dike these vesicles are flattened, defining a flow foliation parallel to the trend of the dike. The country rock adjacent to this dike is the foliated biotite pyroxenite mentioned earlier; its foliation parallels that of the trachyte.

The major phenocryst in the dikes is euhedral sanidine, which together with xenocrystic plagioclase constitutes about 5 percent of the rock. Phenocrysts are a few mm across and form glomeroporphyritic clusters. Sanidine has $2V\alpha = 12°$ and the optic plane parallel to (010). This indicates a structure with 36 percent albite (Tröger, 1979, p. 123). Xenocrystic plagioclase, which shows albite and minor Carlsbad twinning and is slightly normal zoned, locally in oscillatory fashion, averages An_{40}. Crystals are normally slightly embayed, appearing out of equilibrium with the groundmass.

Minor phenocrysts include pleochroic amphibole with X = light brown and Z = dark olive green, and biotite with X = medium brown and Y = Z =

very dark brown. The amphibole occurs solely as phenocrysts in the rock whereas biotite is enclosed in amphibole and sanidine phenocrysts in addition to forming isolated phenocrysts.

Zoned potassium feldspar laths about 0.1 mm long, locally showing skeletal form, constitute the bulk of the groundmass. Up to 10 percent plagioclase of undetermined composition and low relief is present. A few percent magnetite and partially devitrified glass form the remainder of the rock. Vesicles are locally filled by secondary quartz or radiating clumps of a probable zeolite. Around some vesicles is a bleached zone about 0.5 mm wide.

The trachyte dikes appear to have a mineralogy very similar to that of the alkali syenite. Such extremely potassium-rich rocks are uncommon in the region. These facts, together with the limitation of the trachyte to areas of pyroxenite, suggests the dikes are magmatically related to the complex. They may represent a venting of the syenite following at least partial consolidation of the pyroxenite. If so, the dike contact represents the only definite contact between syenitic material and the pyroxenite body.

Fenite

Fenitization is typically an alkali (generally sodic)- ferric iron metasomatism of country rock wherein alkali feldspars replace original quartz, potash feldspar is clouded, albitization of plagioclase occurs, and mafics are altered to aegerine or alkali amphiboles (Joplin, 1968). Fenitization as a type of wallrock alteration is "so

characteristic that its recognition always constitutes prerecognition of the presence of an adjacent alkalic intrusive" (Stanton, 1972). Zones of fenitization normally extend within a few hundred meters of the intrusive although this distance varies greatly, probably as a function of CO_2 content and degree of alkalinity.

The Belt metasediments surrounding the Skalkaho complex were examined closely in the field for any signs of contact effects. Several thin sections of country rock adjacent to the intrusive rocks were also examined. No evidence of fenitization may be seen associated with the syenitic intrusives, however one interesting texture was noticed. Scapolite, which is common in the regional metamorphosed Wallace Formation, in some cases forms poikilitic white balls measuring up to 5 mm in diameter (Presley, 1970, p. 56). A sample of country rock taken from within 100 meters of the syenite contact showed white clots from 5-10 mm across lying in a light green groundmass. Microscopic examination revealed the white clots to be not scapolite but fine-grained aggregates of quartz and potassium feldspar with minor plagioclase and myrmekite. The matrix was composed of similar-sized grains of pyroxene with subordinate biotite, poikilitic scapolite, plagioclase, potassium feldspar, quartz, and epidote. There is no evidence of fenitization. The rock may be a variety of spotted hornfels with reversal of the common pattern which invariably shows mafic spots in a lighter-colored matrix.

In one roadcut immediately south from Skalkaho Mountain, near the inferred pyroxenite-country rock contact, a dike of amphibole pyroxenite

intrudes a dark-green rock interpreted to be fenite. Very near the pyroxenite intrusive, the rock is a hard, medium-green species with discrete concentrations about 10-30 mm across, composed mostly of feldspar with coarse crystals of dark reddish-brown garnet and emerald-greenish pyroxene extending into it from the surrounding matrix. Progressing outward from the inferred contact is a gradual increase in compositional layering and textures typical of the country rock. Approximately 100 meters from the contact is unaffected Wallace calc-silicate rock.

The pyroxene of the fenite, varying from 0.1 to 0.2 mm across, is a colorless to slightly green diopside with a ZΛC of 41°. This is typical of the calc-silicate metasediments in the area which have reached the amphibolite facies (LaTour, 1974; Presley, 1970). Uncommon, yet indicative of metasomatism, is the development of rims showing slight pleochroism in limey-yellow-greens. The garnet of the fenite is an anhedral isotropic mineral generally nearly colorless to a very pale yellow-brown in thin section. Calcite constitutes about 10 percent of the rock as does garnet, and the two seem to be concentrated within certain layers. A few percent of perthitic potassium feldspar and 10 percent or so albite form large (up to 30 mm) poikilitic patches containing the other minerals. Some patches of slightly checkerboard-twinned albite appear to have cores of perthite characterized by patch-type twins. This texture may reflect widespread albitization. Accessory minerals include 1-2 percent sphene and traces of magnetite.

The compositional layering, the parallelism of layering with adjacent country rock layering, an appearance different from that of any pyroxenite, and mineralogic similarity to Wallace calc-silicate rock establishes that this unit is indeed country rock. Amphibole pyroxenite clearly cross-cuts the compositional layering, which probably reflects original bedding. The rock is, however, not simple Wallace Formation. Plagioclase is albite as opposed to the common plagioclase (An_{30-70}) of the metasediments, and the pyroxene has local development of yellow-green rims. Both features appear a result of sodium-ferric iron metasomatism of the country rock associated with the adjacent pyroxenite intrusion. The degree of fenitization, however, is slight.

CHAPTER IV

CHEMISTRY

Sørensen (1974) illustrated the confusion surrounding the term "alkaline" through a five page survey of historical definitions. Various of these definitions may be used to apply this unfortunately ambiguous term to the igneous rocks of the Skalkaho complex. The most evident path is a mineralogical one. The pyroxenites are composed chiefly of pyroxene, a generally silica-saturated mineral, and biotite, an alkali-rich silicate. The syenitic rocks are enriched in potassium feldspar. No quartz or feldspathoidal minerals were apparent. The alkaline rocks at Skalkaho are, perhaps atypically, more enriched in alkalies than depleted in silica.

Five pyroxenites and four syenitic rocks were chemically analyzed by the Los Alamos Scientific Laboratory (Table 3). The reported cation weight parts per million (ppm) are shown calculated to major-oxide percents in Table 4a. Silica, not analyzed, is assigned an approximate value equivalent to the difference between 100 percent and the sum of the other oxide percents shown. Also shown in Table 3 are analyses for a trachyte dike, a "vermiculite" from the mine area in mica pyroxenite on ABM ridge, and a sphene separate from the pegmatite.

The eight major rock analyses converted to oxide percents appear as CIPW normative analyses in Table 4b. From these, it is evident

Table 3. Chemical Analyses (weight parts per million) Negative sign indicates maximum value.

I. Analytical Method -- Neutron Activation Analysis
Accuracy -- At concentration values one order of magnitude above lower detection limit, errors are generally <10%.
Note -- Because of elemental interference, the detection limits for those elements determined by NAA will shift as a function of the composition of the sample. Idealized values are shown.

Element	Minimum Detection	#27B	#134	#20	#56A	#95	#4c	#32	#14B	#14	#V	#sph
Al	200	17160	34560	27211	20840	100300	90340	102500	71230	79190	79420	8156
Au	0.01	-0.11	-0.19	-0.26	0.22	-0.05	-0.06	-0.04	-0.11	-0.10	-0.16	1.49
Ba	300	-221	1293	742	-258	9608	16510	5305	10960	926	2656	-191
Ca	4000	135800	111400	116500	103100	3544	15350	3137	25930	5706	21390	172500
Ce	10	24	19	23	200	20	49	3	195	88	-6	1752
Cl	200	-139	230	301	-169	192	-107	377	125	226	132	1752
Co	2	16.0	29.5	32.3	58.9	2.9	3.8	2.0	7.3	2.8	66.2	3.5
Cr	20	53	122	-23	-12	-5	-7	-4	-11	-9	-14	43
Cs	2	-1.5	-2.6	-3.6	-2.0	-0.5	-0.8	-0.4	-1.5	6.0	-2.3	-1.8
Dy	2	3	2	-1	11	1	5	-1	5	2	-1	123
Eu	0.8	1.4	1.3	1.4	7.3	0.7	1.5	.03	3.0	1.1	1.6	41.2
Fe	2000	51910	30740	56080	113400	5199	12260	1534	34190	9781	55000	8516
Hf	1	2.9	-1.6	-2.2	6.0	1.3	3.4	1.2	4.4	7.1	-1.4	41.7
K	2000	-5572	19200	11170	-6663	79960	56190	76600	52640	35470	17660	-2039
La	6	-7	-12	-17	70	17	31	-4	125	51	-12	707
Lu	0.3	0.3	-0.2	-0.3	0.6	-0.1	0.5	-0.1	0.6	0.4	-0.2	2.7
Mg	3000	84260	128300	101300	38550	3379	-4256	-3673	-5265	-4440	53590	-3393
Mn	10	2449	1049	1226	2943	114	694	42	1236	104	848	657
Na	150	4560	5928	7595	4753	30130	19270	26320	15620	24620	917	1092
Rb	30	-23	-32	-53	-32	55	45	68	66	84	-39	-32
Sb	1	-3	-6	-9	-5	-1	-2	-1	-3	-3	-5	9
Sc	0.1	22.8	45.0	69.0	30.5	1.1	1.7	0.3	8.3	5.0	14.9	1.2
Sm	0.5	6.1	1.7	4.4	45.4	2.1	5.3	-0.4	10.2	6.3	-1.0	255.5
Sr	300	-564	-439	-557	-645	6451	6745	8088	5111	-272	-423	1510
Ta	1	-1	-1	-2	4		-1		-1	-1	-1	61
Tb	1	-1	-1	-2	4		1		-1	-1	-1	19
Th	0.8	-1.2	-1.9	-2.7	5.8	1.5	2.2	-0.5	15.9	19.8	-1.7	68.4
Ti	200	5203	5920	4647	17670	825	2357	-526	4061	1322	11250	98993
V	5	252	168	259	548	47	106	-6	237	-7	201	670
Yb	3	2.0	-3.5	-4.9	6.2	-0.9	4.4	-0.7	4.5	-1.7	-3.0	33.7
Zn	20	54	-48	-86	-43	-12	44	-18	-36	86	111	

II. Analytical Method -- X-Ray Fluorescence
Accuracy -- Standard deviation $\simeq$ 10% at 100-ppm level and $\simeq$ 20% at 20-ppm level

Element	Minimum Detection (ppm)	#27B	#134	#20	#56A	#95	#4a	#32	#14B	#14	#V	#sph
Ag	5	-5	-5	-5	-5	-5	-5	-5	-5	-5	-5	-5
Bi	5	-5	-5	-5	-5	-5	6	-5	-5	6	6	8
Cd	5	-5	5	-5	-5	-5	-5	-5	-5	-5	-5	-5
Cw	10	117	153	125	310	18	58	48	44	16	21	-10
Nb	20	-20	-20	-20	66	21	-20	-20	32	-20	-20	60
Ni	15	-15	45	-15	-15	-15	-15	-15	-15	-15	18	-15
Pb	5	-5	-5	-5	-5	-5	-5	6	-5	6	-5	-5
Sn	10	-10	-10	-10	13	-10	-10	-10	-10	-10	-10	54
W	15	-15	-15	-15	-15	-15	-15	-15	-15	-15	-15	-15

III. Analytical Method -- Arc-Source Emission Spectrography
Accuracy -- Precision is ~50% at lower detection limit and 25% at one order of magnitude above it.

Element	Minimum Detection (ppm)	#27B	#134	#20	#56A	#95	#4a	#32	#14B	#14	#V	#sph
Be		1	-1	-1	-1	-1	-1	-1	-1	2	-1	6
Li		2	48	53	-1	-1	-1	2	5	67	-1	-1

#27B---Anhydrous Pyroxenite
#34, #20---Mica Pyroxenite
#56A---Amphibole Pyroxenite
#95, #4c, #32---Syenitic Rocks
#14B---Syenite Dike in Pyroxenite
#14---Trachyte
#V---Vermiculite
#Sph---Sphene from Pegmatite

Table 4a. Whole Rock Oxide Analyses

Sample #	27B	134	20	56A	95	4C	32	14B
SiO_2	54.64	48.42	51.14	56.42	66.85	68.61	66.52	68.37
TiO_2	.87	.99	.78	2.95	.14	.39	.09	.83
Al_2O_3	32.4	6.53	5.14	3.94	18.95	17.07	19.37	13.46
FeO	6.68	3.96	7.22	14.59	.67	1.58	.20	4.40
CaO	19.00	15.59	16.32	14.01	.50	2.15	.44	3.63
MgO	13.97	21.27	16.80	6.39	.56	.71	.61	.87
MnO	.32	.14	.22	.26	.02	.09	.01	.16
Na_2O	.62	.80	1.02	.64	2.71	2.60	3.55	2.11
K_2O	.67	2.31	1.35	.80	9.63	6.81	9.23	6.34

Table 4b. CIPW Normative Calculations (Johannsen, 1939)

Pyroxenites

#27B			#134			#20			#56A		
	Q	1.26		or	7.23		or	7.78		Q	14.76
	or	3.89		ab	10.90		ab	4.19		or	5.00
	ab	5.24		an	3.69		an	5.56		ab	5.24
	an	4.17		di	46.80		ne	2.27		an	2.78
	di	71.96		ol	26.27		di	60.48		di	55.78
	ol	11.74		il	1.82		ol	18.12		ol	10.37
	il	1.67		cs	3.27		il	1.52		il	5.62

Syenitic Rocks

#95			#4C			#32		
	Q	11.88		Q	18.90		Q	9.18
	or	56.71		or	40.03		or	54.49
	ab	23.06		ab	22.01		ab	29.87
	C	3.16		an	14.07		C	2.75
	hy	2.46		di	0.92		hy	1.06
	il	0.30		hy	4.15		il	0.15
				il	0.76			

that within the pyroxenite body, the anhydrous pyroxenite is nearly silica saturated, the mica pyroxenites are moderately to highly undersaturated, and the amphibole pyroxenite analyzed is oversaturated. The syenitic rocks are all oversaturated. Because the percentages used for these calculations involved the silica maxima derived through difference, the normative values probably represent a maximum quartz-normative analysis. Nevertheless, the bulk of the pyroxenites are truly undersaturated and the syenitic rocks are probably oversaturated.

CHAPTER V

PETROGENESIS OF THE COMPLEX

Comagmatism and Contemporaneity

As established above in a discussion of field relations, the Skalkaho complex was clearly intruded as a magma. Any hypothesis concerning its origin must accommodate the consanguineous and contemporaneous relationship which exists between the pyroxenite and syenite masses.

Evidence for comagmatism follows several lines of reasoning. Chemically, both rock types exhibit an alkaline composition, being enriched in potassium. Neither quartz nor feldspathoidal minerals occur in either mass. Similar rocks do not occur elsewhere in the immediate region.

Mineralogical similarities abound, particularly in the mutual occurrence of sphene, apatite, magnetite, and primary (?) epidote. Percentages of all minerals vary between syenitic and pyroxenitic fractions, which reflects elemental partitioning by some method. Mafic minerals in the syenites bear strong resemblance to those of the pyroxenites, except for the slightly more acmitic nature of the pyroxene, which is surely due to equilibration with the increased alkali content of the syenite. Plagioclase within the pyroxenite is unusually low in calcium and in some cases attains a nearly pure, albitic nature. Rare

perthitic potassium feldspar in the pyroxenite is also similar to that of the syenite.

Finally, the remarkable juxtaposition of the syenite and pyroxenite requires some special considerations for emplacement. The ringing dual horseshoe character of the syenite around the pyroxenite in a region where such alkaline rocks are not common strongly suggests firm controls on injection of the magmas and some genetic relationship. Coupled with evidence cited above, this suggests the syenite and pyroxenite must be comagmatic.

Contemporaneity of plutonic rocks is difficult to illustrate. Unlike cases of extruded basalt and rhyolite magmas which show such features as mixed welded tuffs, banded pumice, and composite dikes and flows, a negative sort of evidence must be utilized. If immiscibility played a major role in liquid separation, time has been sufficient to allow consolidation of the divergent fractions. This would obliterate evidence such as globules or ocelli common in some dikes and flows in other alkaline occurrences. At Skalkaho, no cross-cutting relations are seen between the syenite and pyroxenite which would indicate disparate temporal relations. No apophyses of one in the other occur except for several trachyte dikes which cut only the pyroxenite. These dikes, which are chemically and mineralogically similar to the syenite, are interpreted as features which represent venting of the syenite through more consolidated, overlying pyroxenite. Nowhere do sharp borders separate the syenite and pyroxenite nor do chill zones. A fining in

grain size is evident, however, in the syenite near the country rock contact. Instead of sharp contacts, either increases in mafic content of the syenite or the unusual hybrid rock appear to separate syenite and pyroxenite masses. A contemporaneous relationship for the two main rock masses thus appearslikely.

Several types of events may lead to the juxtaposition of magmas as compositionally divergent as syenite and pyroxenite. Because of the comagmatic nature of these rock bodies at Skalkaho, several of these events may be ruled out, namely the chance convergence of two completely unrelated magmas and the derivation of a discrete syenitic magma through crustal melting by a rising pyroxenitic liquid. This latter method poses problems in the derivation of a primary pyroxenitic magma as well as in the necessarily chance chemical and mineralogical similarities which now exist between the resultant rocks. Much more reasonable within the present constraints is the differentiation of a primary alkaline mafic magma to yield the two polar rock types now exposed.

Magmatic Differentiation

Assuming an initially homogeneous parent magma, several methods are available for subsequent differentiation.

Fractional crystallization. Fractional crystallization encompasses four possibilities whereby changes in magma result from crystallization. A process highly respected, and accepted to operate in the case of large,

slow-cooling, mafic layered intrusives (Wager and Brown, 1968) is that of crystal settling. Early-formed crystals, possibly olivine, plagioclase, or pyroxene, may differ greatly in density from the liquid in which they form. Gravity may force such crystals to the floor or ceiling of a magma chamber. The resultant crystal mush may in effect isolate these minerals from the bulk of the liquid system, pushing the remaining melt along a liquidus surface or cotectic through changing compositions. Crystal settling, which may not operate in small bodies having relatively rapid cooling and crystallization, commonly results in repetitive mineralogical layering and general chemical variation upwards in a near-horizontally-stratified rock body. Cumulus, or primary-settled crystals, in most cases are enveloped in an intercumulus phase representing residual interstitial trapped magma.

The complex at Skalkaho is nowhere extensively layered, either rhythmically or cryptically, but rather reflects moderately violent intrusive activity, with multiple intrusions of magma and metasomatic fluids and the resultant irregular-shaped stringers and bodies of rock. No evidence is exposed to suggest cumulate textures; even the anhydrous pyroxenite lacks an intercumulus phase unless such a phase was a pure pyroxene liquid leading to total adcumulus growth. Moderate zoning indicates growth of pyroxene with changing composition typical of solid solution series minerals, however classic adcumulus growth textures are missing. The density difference between pyroxene crystals and a pyroxenitic magma might not be great enough to induce ideal crystal settling.

During logical crystallization trends of most mafic-rich magmas, more mafic constituents crystallize early, resulting in a more felsic differentiate. Such a liquid will generally concentrate the volatile constituents and elements which do not fit easily into the common rock-forming silicate minerals. This enrichment in incompatible elements is often very different from the elemental partitioning which proceeds during differentiation by other methods such as liquid immiscibility. This criterion will be applied to the Skalkaho complex in a later section. Elemental distribution notwithstanding, on textural and field relation data, it is concluded that the major portion of the Skalkaho complex did not differentiate through means of crystal settling.

Filter-press action is another fractional-crystallization process sometimes invoked to explain magmatic differentiation. As a result of tectonic stresses, interstitial fluid may be squeezed out of a crystal mush representing a magma in the later stages of crystallization. This would result in a closer-packed arrangement of crystals of a certain total composition and presumably a separated body of liquid of differing composition. Similar to this is filter differentiation whereby a mixture of crystals and liquid flowing through small spaces leaves behind crystals which are larger than the passageways. This process also results in separated bodies of differing composition.

The size of the Skalkaho body rules out filter differentiation. Filter-press action may be disregarded as a viable alternative for two reasons. Bimodal complexes similar to the Skalkaho body exist in varied

tectonic settings, some in stable areas almost certainly free of the stress required for squeezing. Although some complexes may have differentiated through filter-press action, others could not have. A more universal differentiation method would be favored. Also the common juxtaposition of the rock types is incompatible with the squeezing out and subsequent voyage and isolation of residual material. At Skalkaho, the syenite and pyroxenite are adjacent to one another and the pyroxenite shows little textural evidence of being a squashed framework. Although filter-press action may be important elsewhere, it was not responsible for the major differentiation in this igneous body.

Flowage differentiation, which operates in intrusions less than about 100 meters across (Bhattacharji and Smith, 1964), results in a concentration of solid crystals within the central rapid flow region, away from the walls in a moving fluid. Finally, crystallization without continuing equilibrium may remove cores of zoned crystals from further reaction with the melt. This would leave a differentiated liquid to crystallize in the interstices of early crystals. Neither of these last two processes could have been responsible for the extreme differentiation at Skalkaho.

Movement of volatiles. A second process leading to differentiation of magma which has not been as well documented as fractional crystallization involves movement of volatiles. One form of this method, gaseous transfer, involves evolution of a gas phase during second boiling due to an increased gas pressure which overcomes the load pressure. This

may result from progressive crystallization which reduces the amount of liquid called upon to dissolve the volatiles of the system, or by decreasing pressures brought about by a rise of the magma. In either case, rising gas bubbles may preferentially remove and segregate pneumatolytic constituents such as Na, Fe, Mn, Ti, P, Rb, La, Ce, Y, Zr, Nb, and U (Hyndman, in prep.), or might even push residual interstitial liquids upwards in the latter stages of crystallization. A second process, volatile streaming, presumably accomplishes the same task, but moves volatiles and related constituents to areas of lower pressure without the development of a gas phase.

Differentiation by movement of volatiles is hard to recognize in rock systems since very little experimental work exists. At Skalkaho, a high volatile content is evidenced and volatile movement probably played a minor role. However, element partitioning between the syenite and pyroxenite is not consistent with experimentation cited above. The great masses of syenite and lack of a similar material in the interstices of the pyroxenite are also inconsistent with this method.

Compositional differentiation of magmas may also take place by means of liquid immiscibility. Attention is now turned to this recently revived concept.

Current Status of Liquid Immiscibility

Non-silicate - silicate systems. Although immiscibility between silicate liquids clearly is of paramount importance in geologic systems,

vivid examples of non-silicate - silicate immiscibility seem to have been better received and accepted; some of these latter cases are now reviewed. Perhaps due to economic incentive, immiscibility between sulfide liquids and silicate liquids was recognized early, particularly in basaltic rocks such as at Kilaueau, Hawaii (Skinner and Peck, 1969). Moore and Calk (1971) noticed micron-sized spherules of iron, copper and nickel sulfides in the glassy margins of virtually all dredged ocean-floor pillow basalts they examined. Although they invoke ionic diffusion of cations from basaltic liquid to pre-existing visicles, they feel processes of immiscibility preserved the resultant liquid sulfide globules. Similar sulfide globules occur in some drastically quenched subaerial lavas.

Rocks composed of a fairly consistent ratio of iron-titanium oxides (magnetite) and apatite were early deduced to represent a eutectic relationship (Philpotts, 1967). Experiments showed that such a melt composition is immiscibile at elevated temperatures with a liquid of dioritic composition. In fact, in this system three immiscible phases form. The apatite-magnetite association is recognized as being related to an end-member type of carbonatite, the polar variety being enriched in rare earth elements (Hyndman, 1972, p. 214). The process of liquid immiscibility has strong ramifications relating to the genesis of carbonatites in general.

Wyllie (1966) noted four hypotheses on the origin of carbonatites. Although experimental work provides permissive evidence for each, data

supporting a genesis through immiscibility is becoming overwhelming. Koster van Groos and Wyllie (1973, 1968, 1966) have shown experimental immiscibility between silicate and carbonate melts, particularly in the join $NaAlSi_3O_8$ - $CaAl_2Si_2O_8$ - Na_2CO_3 - H_2O. At certain compositions, under one kilobar pressure with 10 percent H_2O, a carbonate-poor peralkaline silicate liquid coexists with a silica-poor calcium-enriched carbonate liquid and an aqueous vapor phase enriched with sodium silicate and CO_2. Koster van Groos concludes that these three fluid phases correlate well with the undersaturated alkaline urtite-ijolite melt series, the carbonatites, and the metasomatic fenites which generally constitute carbonatite complexes (Koster van Groos, 1973). Research has advanced to such areas as the effect of high CO_2 pressures and temperature on these alkalic systems (Koster van Groos, 1975a) and partitioning of elements such as strontium between coexisting silicate and carbonate liquids (Koster van Gross, 1975b).

Natural examples suggesting immiscibility between carbonate and silicate liquids abound. Rankin and LeBas (1974) report carbonate-rich and silicate-rich inclusions within apatite from some East African carbonatites and ijolites. These inclusions reflect conditions prevailing during crystallization, and imply the presence of two immiscible fractions. Such inclusions may yield critical data on the character of carbonatite magmas (LeBas and others, 1977). At Epembe, Southwest Africa (Ferguson and others, 1975), identical styles of metasomatism associated with carbonatite and nepheline syenite intrusives suggest the two magmas

existed in equilibrium as an immiscible pair of liquids. Furthermore, at Epembe as well as elsewhere (eg. Ferguson and Currie, 1971) are found carbonated lamprophyric and syenitic dikes containing carbonate ocelli. And certainly, the common association of carbonatite with alkaline rocks is consistent with an immiscibility relationship.

Koster van Groos and Wyllie (1969) showed limited solubility of NaCl melt in a water-saturated $NaAlSi_3O_8$ system at one kilobar, suggesting that drops of NaCl liquid might exist in feldspathic silicate melts. Roedder and Coombs (1967), in their study of fluid inclusions within quartz and feldspar of ejected granitic blocks from Ascension Island, deduced that three immiscible phases probably existed in the original magma. One of these was a hydrous fluid, which coexisted with silicate liquid and molten NaCl. Undoubtedly, even more exotic examples occur of naturally occurring systems utilizing processes of liquid immiscibility. But it is with silicate systems geologists must ultimately deal.

Silicate - Silicate Experimental Work

The system K_2O-FeO-Al_2O_3-SiO_2. As related in the introduction, early work by Greig (1972) lent credence to Bowen's (1928) denunciation of widescale silicate liquid immiscibility and it was not until much later (Roedder, 1951) that a "low temperature field of immiscibility" was discovered. This two-liquid field was delineated along the tridymite-fayalite cotectic in the join $KAlSi_2O_6$-Fe_2SiO_4-SiO_2 at temperatures between about 1270° and 1100°C.

Later studies were undertaken to verify and refine this field but variable experimental conditions make exact comparisons impossible. Watson (1976), for example, constructed the two-liquid field at the 1180°C isotherm in order to study elemental partitioning. Because they failed to differentiate between stable immiscibility and metastable immiscibility which caused quench exsolution, Visser and Koster van Groos (1976) showed an immiscibility field with a vastly different shape and configuration from that of Roedder. Later (Visser and Koster van Groos, 1979), they determined phase relations in the same system, K_2O-FeO-Al_2O_3-SiO_2, at one atmosphere, emphasizing the field of low temperature stable immiscibility (Fig. 9). Choosing molybdenum foil as a container material, oxygen fugacity was controlled by the Mo-MoO_2 buffer which lies within the wustite stability field. A stable immiscibility field occurring between 1235° $\pm$ 5°C and 1110° $\pm$ 5°C separates a SiO_2-rich liquid from an FeO-rich liquid. All data were projected onto the join (K_2O/Al_2O_3)-FeO-SiO_2 with molar K_2O/Al_2O_3 = 1 even though a quaternary system is needed to show aluminum and potassium partitioning between coexisting fractions. The enrichment of both aluminum and potassium in the silica-rich immiscibile liquid may be seen in Figure 10, this enrichment being more extreme for K_2O. Metastable immiscibility produced bluish irridescent or dull brownish-gray glasses which show submicroscopic unmixing features in the range of 0.1 micron. This metastable extension of the immiscibility field was determined as far as it is kinetically relevant and then projected on the join fayalite-

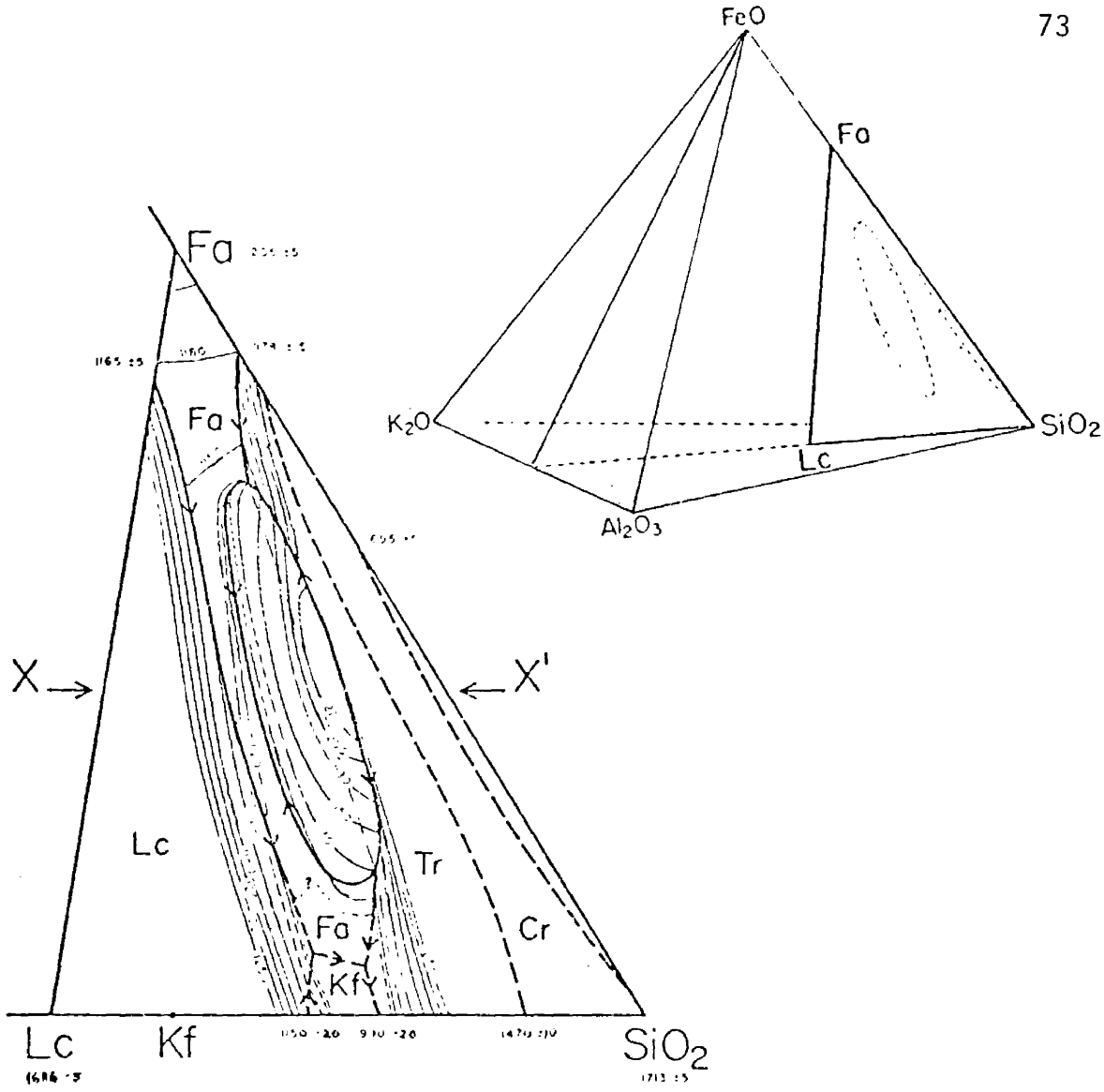

Figure 9. above: The join Fa-Lc-SiO_2 in the system K_2O-FeO-Al_2O_3-SiO_2. The immiscibility field shown was determined by Roedder (1951). Diagram is in weight percent.
below: Liquidus relations in the join Fa-Lc-SiO_2 as depicted by Visser and Koster van Groos (1979). Compositions in weight percent.
Fa=fayalite; Lc=leucite; Kf=K-feldspar; Tr=tridymite; Cr=cristobalite (From Visser and Koster van Groos, (1979)

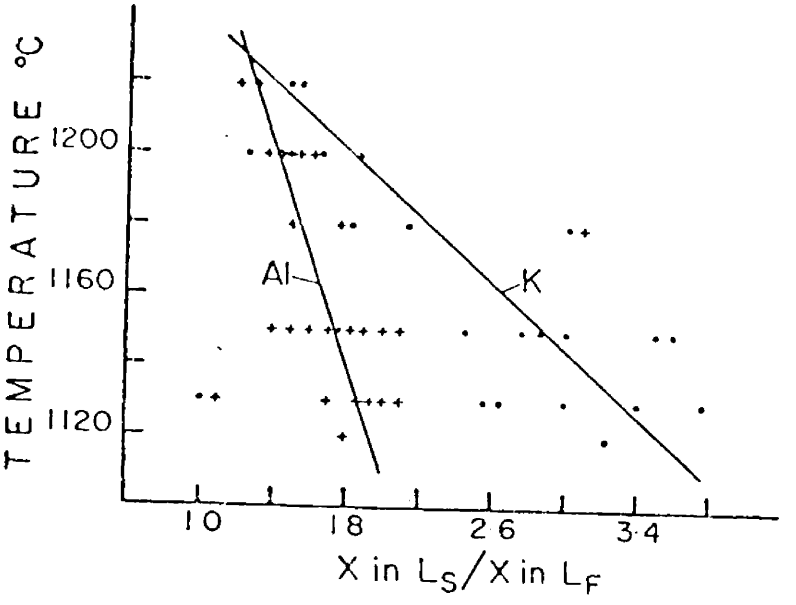

Figure 10. Distribution coefficients for Al_2O_3 and K_2O between two coexisting liquids as a function of temperature. L_S=silica-rich liquid; L_F=iron-rich liquid. (From Visser and Koster van Groos, 1979)

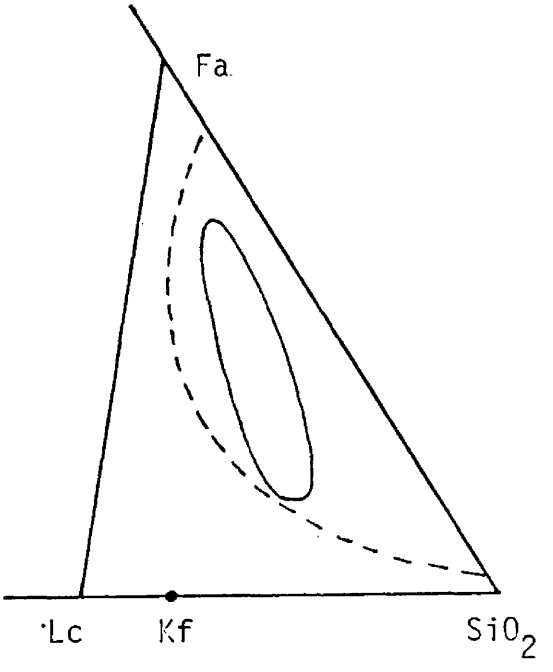

Figure 11. The metastable extension of the stable immiscibility field projected on the join Fa-Lc-SiO_2, bounded by the dashed lines. (After Visser and Koster van Groos, 1979)

leucite-SiO_2 (Fig. 11). In a temperature-composition section along the 30 percent FeO isopleth (X-X' in Fig. 9) of this join, the relation between the high- and low-temperature stable immiscibility fields is illustrated, being connected by the metastable subliquidus field of immiscibility near the stable liquidus (Fig. 12).

Since the low-temperature immiscibility field seen in the join leucite-fayalite-SiO_2 was only a slice through a three-dimensional immiscibility volume in the system K_2O-FeO-Al_2O_3-SiO_2, extrapolation to real systems is difficult. Roedder (1978) reported results from unfinished experiments designed to attack this problem of volumetric dimensionality.

Working with fourteen planes defined by FeO, SiO_2, and various ratios of K_2O/Al_2O_3, he determined phase relations for the high-silica part of the tetrahedron for planes of 0, 10, 30, and 50 weight percent FeO. The low-temperature stable immiscibility field, essentially straddling the 1:1 (molar) K_2O:Al_2O_3 plane, appears at 10 percent FeO, expands upon addition of FeO, and subsequently contracts and disappears at about 43 percent FeO (Roedder, 1978). Roedder notes that isothermal surfaces in the fayalite field are severely warped in the vicinity of the immiscibility field, causing somewhat unusual crystallization behavior. Furthermore, the geometry of the immiscible volume, the temperatures involved, and the placement of tielines are such that extremely large changes in amounts of phases occur with very small changes in temperature.

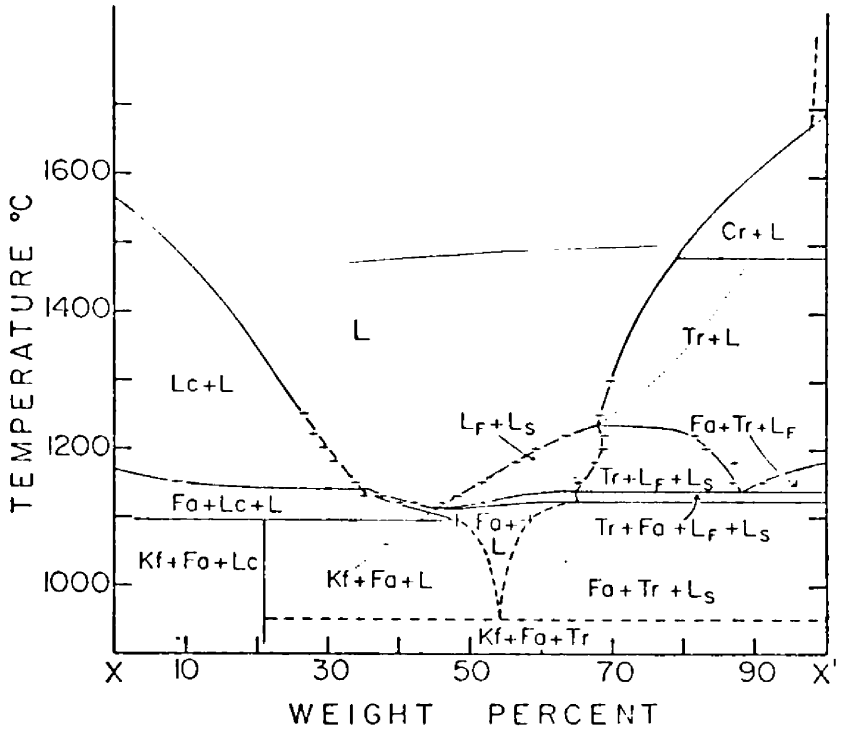

Figure 12. Binary phase diagram to illustrate the relation between stable and metastable immiscibility. A temperature-composition section along the 30 percent isopleth in the join Fa-Lc-SiO_2 (see Fig. 9). The dotted line represents the metastable extension of the two-liquid field. L=one homogeneous liquid, disregarding metastable phase separation. (After Visser and Koster van Groos, 1979)

The immiscibility volume determined by Roedder is associated with large areas of metastable immiscibility. As Holgate (1954) noted, metastable immiscibility nears the liquidus surface in those systems having sigmoidal liquidus surfaces, and may be present in many other cases as well. These subliquidus fields, which some feel exist in most silicate systems (Roedder, 1978), may break the liquidus surface whenever other constituents or factors cause a more rapid drop in the liquidus than in the solvus.

Effects of added components. To determine the effect of calcium on the system used by Roedder and others, Naslund (1977) investigated the system K_2O-CaO-FeO-Fe_2O-Al_2O_3-SiO_2 and determined the immiscibility field on the plane $An_{50}Or_{50}$-FeO-SiO_2. A two-liquid stable immiscibility field in the join Or-FeO-SiO_2 extends into the field of anorthite, and was seen to exist in the system $An_{50}Or_{50}$-FeO-SiO_2 from FeO-SiO_2 rich compositions to compositions having 50 percent feldspar. Addition of either CaO or Al_2O_3, however, causes a decrease in the divergence of the two liquids and with increasing Al_2O_3 content of coexisting liquids, Ca^{++} increases in the silica-rich liquid relative to the iron-rich fraction. Partitioning of some other elements was also studied.

Working in the system $KAlSi_3O_8$-$NaAlSi_3O_8$-FeO-Fe_2O_3-SiO_2, Naslund (1976) found fields of immiscibility very similar to those in the leucite-fayalite-silica system, and it appears that in terms of melt structure K_2O may proxy for Na_2O as does FeO for CaO and MgO (Freestone, 1978). Naslund concludes that although immiscibility is

best developed in the potassium-rich part of the system, a high K_2O/total alkali is not crucial to the appearance of two immiscible liquids. This is also consistent with the data of Massion and Koster van Groos (1973).

Irvine (1976) found large regions of metastable immiscibility in the system Mg_2SiO_4-Fe_2SiO_4-$CaAl_2Si_2O_8$-$KAlSi_3O_8$-SiO_2 beneath the pyroxene and olivine liquidus fields. He feels there is a strong possibility that other factors, such as the addition of components like P_2O_5 and TiO_2 in apatite and sphene, may induce stable immiscibility. Also, the effects of the metastable field on the liquidus relations of magmas and the crystallization and fractionation trends of these magmas may be profound.

Kushiro (1974) noticed regularities in the effects of various oxides on shifts in liquidus boundaries between olivine, pyroxene, and silica. These shifts, which also respond to changing pressure, can be explained in terms of silicate melt structures relating to addition of cations with different valences. In addition to ramifications concerning partial melting of mantle materials, addition of these oxides, which causes melting-point depression, affects the dimensions of the miscibility gap (Kushiro, 1975). Oxides of polyvalent (≥ 3) cations such as Cr_2O_3, TiO_2, and P_2O_5 promote polymerization of SiO_4^{-4} tetrahedra and very strongly affect expansion of the two-liquid regions of immiscibility. Monovalent cations, on the other hand, inhibit polymerization and have much more subtle effects on the immiscibility field. At higher pressures, polymerization is enhanced.

Many of the rocks serving as proposed products of liquid immiscibility (Philpotts, 1976; Freestone, 1978) are enriched in TiO_2 and/or P_2O_5, polyvant cation oxides which Kushiro (1975) felt would expand the immiscibility field. Freestone (1978) studied the effect of adding 1 mole percent P_2O_5 and 3 mole percent TiO_2 to melts in the familiar system K_2O-FeO-Al_2O_3-SiO_2. These percentages, construed to model certain gabbroic rocks in the Montergion Hills (Philpotts, 1976), caused a marked expansion of the two-liquid field towards potassium-rich compositions (Fig. 13). Such an expansion of the field may be accounted for in terms of melt structure, as in the following model (Freestone, 1978). Trivalent aluminum enters tetrahedral sites in the silicate polymers of the silica-rich fraction while K^+ cations compensate for the resultant negative charge. The cations P^{5+} and Ti^{4+} have high field strengths but cannot enter a tectosilicate network. These two cations concentrate in the iron-rich melt and serve as an oxygen sink, increasing non-bridging oxygens and thereby expanding the two-liquid field.

To more realistically represent natural systems, the immiscibility field may be plotted on a ternary diagram with the corners SiO_2, MgO + CaO + FeO + TiO_2 (+ P_2O_5), and Al_2O_3 + K_2O + Na_2O. Such diagrams are currently in vogue among immiscibility researchers (eg. Gelinas and others, 1976; McBirney and Nakamura, 1974; Freestone, 1978) and are used extensively to plot immiscibility fields and relate them to naturally occurring rocks. This diagram appears repeatedly in the next chapters.

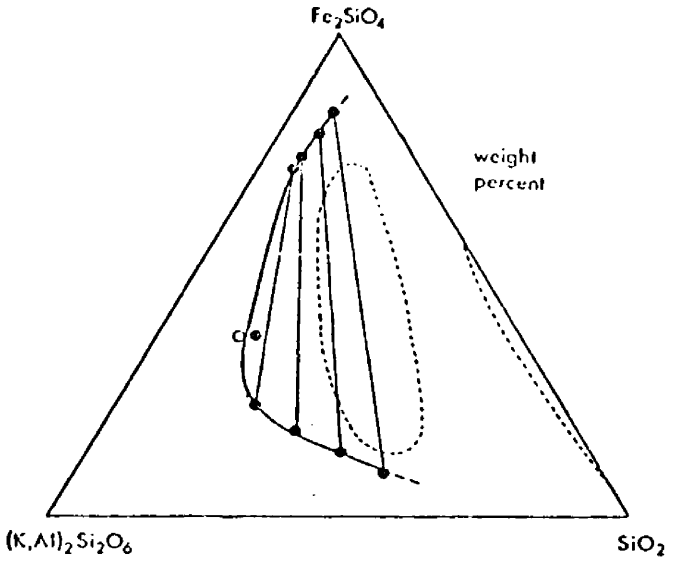

Figure 13. Effect of adding 1 mole % P_2O_5 plus 3 mole % TiO_2 on the immiscibility field. Dashed lines outline the two-liquid fields outlined by Roedder (1951) in the TiO_2, P_2O_5-free system. Solid line represents the extended field. (After Freestone, 1978)

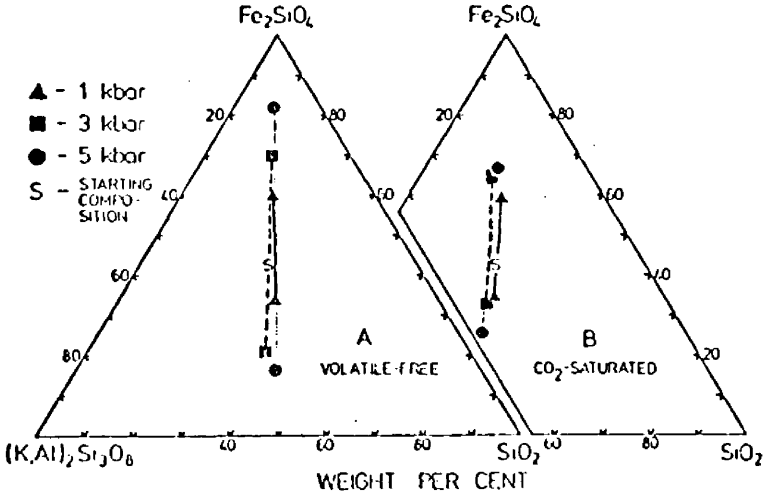

Figure 14. Coexisting melt compositions in the system K_2O-FeO-Al_2O_3-SiO_2 at 1, 3, and 5 kilobars, 1160° C. (A) Volatile-free; (B) CO_2-saturated. (From Watson and Naslund, 1977)

Two other factors relevant to changes in the extent of silicate immiscibility have been examined. Naslunc (1976) noted that except for a brief respite reflecting a rapid change in the magnetite liquidus, liquid immiscibility fields expand with increasing oxygen fugacity in the system $KAlSi_3O_8$-FeO-SiO_2. Thus, although Freestone's (1978) work was conducted at oxygen fugacities lower than those appropriate for terrestrial magmas, the results are viable and in fact should represent minimum immiscibility field dimensions, at least in terms of common f_{O_2} values.

With regards to pressure, Nakamura (1974) showed that the immiscibility field in the system leucite-fayalite-silica is nearly obliterated at 15 kb. Watson and Naslund (1977), however, arrived at seemingly opposing results under both volatile-free and CO_2-saturated conditions. Runs conducted at 1, 3, and 5 kb and 1160°C on a starting composition of $Or_{31.0}Fa_{42.5}QT_{26.5}$ formed two coexisting liquids whose compositions diverged as the pressure rose. The effects were much smaller on the CO_2-saturated liquids (Fig. 14). Markov and others (1974) arrived at similar results regarding pressure effects on melt derived from a melanocratic olivine nephelinite. It may yet be determined that in the low-pressure range (<5 or 10 kb), an increase in pressure favors expansion of the immiscibility field whereas higher pressures eventually cause the field to contract and disappear.

In summary, a low temperature, low pressure region of liquid immiscibility occurs within experimental systems correlable to natural

magmas. The system K_2O-FeO-Al_2O_3-SiO_2 may be used to represent real magmas, with K_2O proxying for Na_2O and FeO for CaO and MgO. It appears that a high K_2O/total alkali is not essential to unmixing but that immiscibility may be more pronounced under such conditions. Addition of P, Ti, and possibly other polyvalent cations such as Cr or even C, increases the extent of the immiscibility field, whereas increasing Ca, Mg, and Al causes a lesser degree of shrinking. These effects are explicable in terms of melt structure.

Increased oxygen fugacity expands the field as do increased volatile components in general (Irvine, 1975) by depressing the liquidus. The role of pressure is uncertain, since preliminary data are somewhat inconsistent and hard to correlate. It may develop that lower pressures (<10 kb) may be necessary for significant unmixing. Metastable immiscibility regions continue from stable zones beneath adjacent liquidii and it seems likely that such regions are widespread in most silicate systems. Liquidus surfaces are commonly disrupted or sigmoidal in these cases, and crystallization behavior probably will be altered. Clearly, from experimental work, it appears that liquid immiscibility should function in certain igneous systems.

Elemental partitioning. A direct result of the difference in polymerization between coexisting immiscible silicate liquids is a distinct elemental partitioning between the two immiscible fractions. This partitioning is dependent upon the structures of the melts and in theory resembles the partitioning noted between coexisting crystals and

melt (eg. Banno and Matsui, 1973). Although elemental partitioning will certainly depend to some extent on the compositions of experimental systems and magmatic bodies involved in liquid immiscibility, it appears from the preliminary work accomplished that the behavior of certain elements differs during the differentiation processes of fractional crystallization and liquid immiscibility.

Various researchers (Naslund, 1977; Wood and Hess, 1977; Ryerson and Hess, 1978) have noted partitioning patterns in immiscible silicate melts similar to those reported after systematic work by Watson (1976). He conducted a series of doping experiments to illuminate the partitioning behavior of elements in a system created by mixing leucite, fayalite, and silica to yield a starting composition in the center of the immiscibility field in the experimental system K_2O-Al_2O_3-FeO-SiO_2. After repetitive runs at the same temperature using identical starting mixtures, it became clear that Al, K, and Cs concentrate in the SiO_2-rich melt whereas P is most strongly partitioned into the Fe-rich melt (by a factor of 10) followed by REE, Ta, Ca, Cr, Ti, Mn, Zr, and Mg. Both Ba and Sr showed no preference.

Ryerson and Hess (1978), dealing with a more complicated natural system, observed similarly that cations of high charge density, specifically Ti, Fe, Mn, P, Zr, Cr, Ta, Lu, Yb, Dy, Sm, and La, concentrated in an immiscible ferropyroxenitic liquid characterized by a relatively low Si/O ratio and consequent depolymerization. The highly polymerized, network-structured granitic melt attracted cations of lower charge density, such as the alkalies and Cs.

Aluminum is thought to largely occupy tetrahedral sites in copolymerization with silica. The charge imbalance produced by such a substitution is satisfied by a coupled substitution of alkalies. Wood and Hess (1977) dealt in depth with the role of Al_2O_3 in immiscible silicate melts. Molar K_2O/Al_2O_3 is nearly unity in the SiO-rich fraction whereas the FeO-rich liquid is peraluminous (in this system, $K_2O/Al_2O_3 < 1$). Ryerson and Hess (1978) determined that increased P_2O_5 results in higher ferropyroxenite-granite liquid distribution coefficients for the REE due to an expanded solvus for the major elements, and complexing of REE with phosphorus. Studies must be done on the partitioning behavior of elements in natural examples of silicate immiscibility. Cawthorn and McCarthy (1977), for example, found an enrichment of Ni in the mafic fraction of what they interpreted as rocks resultant from immiscibility in picritic liquids.

As put forth in the discussion above concerning differentiation by volatile movement, so-called pneumatolytic elements (Na, Fe, Mn, Ti, P, Rb, La, Ce, Y, Zr, Nb, U) concentrate in the gas phase and eventually find their way back into the melt at a later stage of crystallization. Presumably, then, these elements would appear within late-stage differentiates, or normally within a felsic phase relative to its coexisting mafic fraction.

A similar generalization may be stated for differentiation by means of fractional crystallization. In this case, the so-called incompatible elements, which cannot normally fit in the crystal

structures of common igneous silicate minerals, commonly fractionate into the felsic derivatives. The incompatible nature of these elements is dictated by the mineralogy which fractionates at an early stage in the crystallization of a magma. Researchers have noted that elemental trends within the classic, crystal-fractionated Skaergaard body (Wager and Mitchell, 1951; 1940) agree with trends noticed in many other "differentiated," generally basaltic rock series (Ringwood, 1955). These include both calc-alkaline examples (Nockolds and Allen, 1953) and those of alkalic affinity (Nockolds and Allen, 1954). These studies indicated that ultramafic and mafic rocks are enriched in Mg, Ca, Fe, Cr, Ni, V, Co, and probably Zn and Sc relative to their felsic differentiates. The differentiates, on the other hand, show relative enrichment in Na, K, Rb, Ba, Zr, Li, Cu, and probably REE, Be, Ga, Pb, B, U, and Th. Phosphorus and Ti appear to be most abundant in intermediate and acid varieties. Common pegmatites serve as a good illustration, generally developing unusual mineral suites to accommodate a bizarre elemental composition which reflects their late-stage differentiated (or early partial melt) character.

Firm adherence to, and reliance on, the data given above concerning elemental behavior may be dangerous, as such behavior may change with a change in rock composition or magmatic conditions. However the data serve as a useful generality. The generalized partitioning data for the processes of fractional crystallization, liquid immiscibility, and movement of volatiles are summarized in Table 5. Liquid-liquid partitioning studies may be applicable to studies of mineral-liquid

Table 5. Generalized Elemental Partitioning with Various Differentiation Processes

Element	Liquid Immiscibility	Fractional Crystallization	Volatile Movement
Ca	M	M	--
Mg	M	M	--
Fe	M	M	F
Cr	M	M	--
Ni	M	M	--
V	--	M	--
Co	--	M	--
Zn	--	M	--
Sc	--	M	--
K	F	F	--
Al	F	F	--
Na	--	F	F
Rb	--	F	F
Ba	--	F	--
Li	--	F	--
Zr	M	F	F
REE	M	F	--
Be	--	F	--
Cu	--	F	--
Pb	--	F	--
Ga	--	F	--
B	--	F	--
U	--	F	--
Th	--	F	--
Cs	F	--	--
Mn	M	--	F
Sr	--	F(?)	--
P	M	F-I	F
Ti	M	F-I	F
Ta	M	--	--

M = mafic fraction partitioning F - felsic fraction
I = intermediate fraction.

partitioning which are again becoming popular (eg. Banno and Matsui, 1973; Leeman and Sheideggar, 1977; Takahashi, 1978).

Differentiation through the process of liquid immiscibility results in two coexisting liquids of highly divergent composition exhibiting pronounced elemental partitioning. Although experimental work concerning liquid-liquid elemental partitioning is in an embryonic state, and although partitioning will certainly depend upon composition of the system involved (illustrated by Ryerson and Hess's (1978) work with phosphorus), it appears that partitioning trends resulting from liquid immiscibility differ drastically from typical patterns resulting from other differentiation means such as fractional crystallization or movement of volatiles. Although partitioning data in rocks must be evaluated critically and continuously, such data may serve as useful permissive evidence for identifying rocks which were involved in liquid immiscibility, especially plutonic rocks which experienced long cooling periods. Specifically, enrichment of the ultramafic or mafic fraction in P, Ti, Zr, and REE may be suggestive of liquid immiscibility. Whereas enrichment of these elements in the felsic or intermediate phases might indicate fractional crystallization.

Thermodynamically, a homogeneous liquid will unmix if the total Gibbs Free Energy of the fractions is lower than that of the original mixture. Put another way, silicate liquid immiscibility will occur when the free energy of mixing is positive and kinetics are favorable. Currie (1972), utilizing a thermodynamic model designed to predict whether a silicate liquid of a specific composition would be

immiscible, correctly delineated the immiscibility field first discovered by Roedder (1951). The model, which also correctly denies the existence of immiscibility in other related systems, was applied to certain terrestrial examples. Interestingly, the model favored immiscibility in rocks believed on other grounds to have resulted from immiscible processes and rejected immiscibility in "control" examples of rocks showing no evidence for unmixing. Other, more complicated methods may also be used to predict immiscibility, such as the determination of spinodal surfaces from the geometry of the isothermal isobaric free-energy function of a solution (Barron, 1978).

Mechanics of immiscible separation. After globules of another liquid have separated by immiscibility, the two liquids will change composition by means of diffusion. The growth process of these globules is crudely comparable to growth of a crystal in a solid-solution series. The major difference will be the greater rate of diffusion associated with two coexisting liquids than with crystals and liquid. Differentiation comes about by gravitational action, the rate of vertical movement dependent upon the size of the globules, the effective density difference between the globules and the host liquid, and the effective viscosity of the continuous host phase. Crystals affect both density and viscosity and may inhibit or stall gravitational settling. True fractionation will be obtained if globules settle or rise sufficiently to preclude future equilibration with the host; subsequent mixing of initially immiscible liquids may, in effect, become a mechanical problem.

Philpotts (1972) found that the density contrast between immiscible phases may reach 0.87 g/cm^3 which is comparable to that between many crystals and melts known to indulge in crystal settling. Segregation of immisclble melts should occur just as crystal settling occurs; in fact, globules of melt should separate more rapidly and effectively than crystals would (Roedder, 1978), in part because of the tendency to maintain a spherical form. It thus appears that complete separation of two immiscible silicate melts and their subsequent inability to remix is very likely. Such systems may very well behave as the oil and water of salad dressings.

Lunar Examples

Although Roedder's (1951) discovery of prominent low-temperature silicate liquid immiscibility in the system K_2O-FeO-Al_2O_3-SiO_2 suggested that this process might be widespread in rock genesis, such a view did not become popular and research on immiscibility was uncommon until Roedder and Weiblen (1970a; 1970b) showed that liquid immiscibility was prevalent during late-stage crystallization of lunar basalt.

Various unusual textures in these basalts could be explained very easily by silicate liquid immiscibility. Many of these features involved globules of two distinct glasses within each other, glasses within and isolated near the rims of growing late-stage minerals, immiscible globules nucleating on such minerals, and globules disformed against and coalescing with each other (Weiblen and Roedder,

1973; 1970a). The two individual glasses, which must have coexisted since they are now in some cases separated by a sharp meniscus, each vary slightly in composition but chemically are essentially equivalent to titaniferous ferropyroxenite and potassic granite (see Table 6). The dark-brown, high-index glass, since it contains about 80 percent normative pyroxene (Roedder, 1978), crystallizes readily wherever a pyroxene nucleus is available such as adjacent to pyroxene crystals. Thus, the glass nowhere occurs near pyroxene. This process eliminates evidence of liquid immiscibility and could be relevant in the search for immiscibility in terrestrial, particularly slow-cooled, rocks.

Table 6. Weighted Averages of 37 Analyses of Coexisting Residual Lunar Glasses

	SiO_2	Al_2O_3	FeO	MgO	CaO	Na_2O	K_2O	TiO_2
felsic glass	76.1	11.7	2.5	0.3	1.9	0.4	6.6	0.5
mafic glass	47.8	3.2	21.4	2.3	11.2	0.1	0.3	3.7

It appears that magma generally splits after about 90-95 percent crystallization, although this split occurred in one Apollo 14 rock when at least 12 percent by volume liquid remained (Roedder and Weiblen, 1972). To verify that these glasses indeed resulted from immiscibility, Roedder (1978) produced a 50-50 mixture of the two compositions. A

homogeneous green glass at 1400°C, the mixture formed fayalite plus two glasses at 1045°C.

Although sampling of the two glasses makes trace-element analysis difficult, phosphorus was definitely partitioned strongly into the FeO-rich melt whereas potassium suffered extreme enrichment in the SiO_2-rich fraction. Perhaps not surprisingly, when the glass analyses are plotted on an "immiscibility diagram," the two melts fall very near the outskirts of the immiscible field (Fig. 15).

Terrestrial Examples

Basaltic late-stage immiscibility. After recognition of late-stage immiscibility in lunar basalts, efforts commenced to locate similar features in terrestrial rocks. Roedder (1978) found such evidence in examples of several Hawaiian basalts, in basalts from the North Shore Volcanic Group of Minnesota, and in basaltic rocks near Disko, Greenland. Dé (1974) reports widespread glass globules resultant from late-stage immiscibility within the expansive tholeiites of the Deccan traps. Besides the presence of glasses, Philpotts (1978) notes textures within these tholeiites which are indicative of liquid immiscibility: relict globules; immiscible globular inclusions in plagioclase; the present of a fine-grained mesostasis; and lobate crystal faces of pyroxenes. He also records the percent of liquid present during initiation of magma splitting as 20 percent in the Deccan Traps, 32 percent in basalt from Connecticut, and 44 percent from tholeiites of the North Shore Volcanic

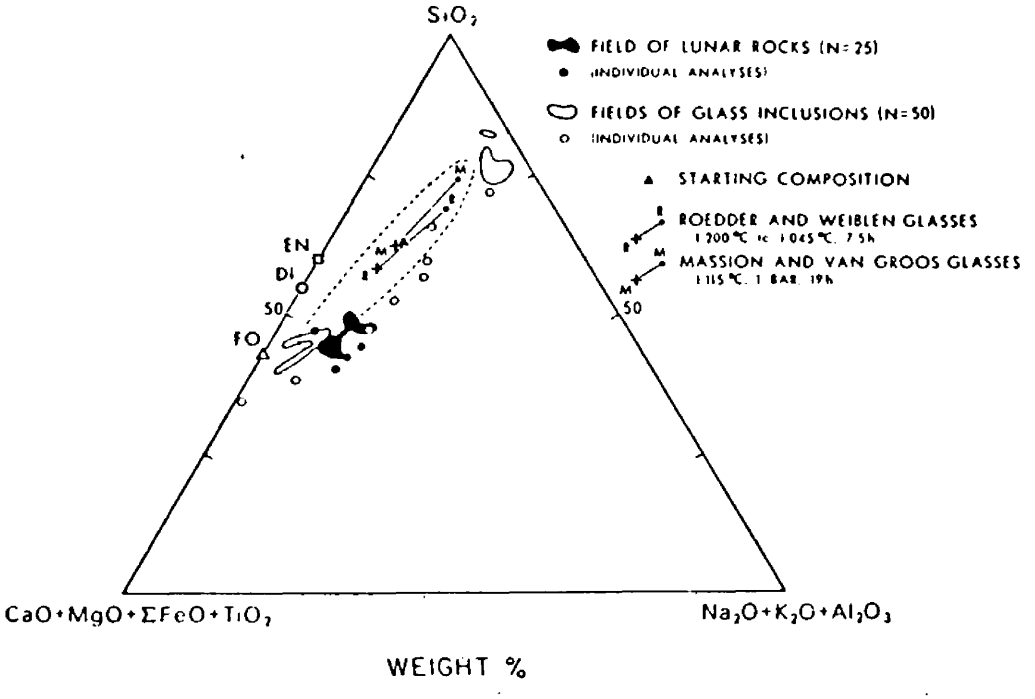

Figure 15. The relation of lunar rocks and glasses and certain experimentally derived coexisting glasses to the immiscibility field of Roedder (1951). En=enstatite; Di=diopside; Fo=forsterite. (From Gelinas and others, 1976)

Group. Wright and Okamura (1977) sampled magma from a Hawaiian lava lake and found that glasses representing two immiscible liquids existed between plagioclase crystals.

A similar type of late-stage immiscibility split was proposed for the Skaergaard mafic layered intrusive complex by McBirney and Nakamura (1974). The liquids of Upper Zone C of the complex have a liquidus temperature about 1000°C, nearly identical to a typical granophyre. A sample of intermediate composition consisting of two parts Upper Zone C and one part granophyre experimentally split into two liquids which plot, as do Upper Zone C and granophyre compositions, to suggest an immiscible relationship. These compositions are plotted in Figure 16 along with the two immiscibility fields of Roedder (1951). The experimentally derived low-SiO_2 glass is enriched in FeO and P_2O_5 and depleted in K_2O. Density differences between granophyric liquids and liquids representing Upper Zone C range from 2.4-2.8. This, coupled with a probable viscosity of about 10^3 poises (McBirney and Nakamura, 1974) for the Fe-rich liquid, is probably sufficient to allow complete separation of two immiscible liquids.

Basaltic early immiscibility. Some occurrences attributed to liquid immiscibility are evidently not late-stage, but rather suggest splitting before significant crystallization. Prokoptsev (1977) noted solidified emulsions of immiscible solicate liquids within alkalic basalt deep-water lavas. The evidence for immiscibility seemed to be obliterated within some basalts during the cooling process, yet some lavas showed immiscible globules coalescing into streamlets.

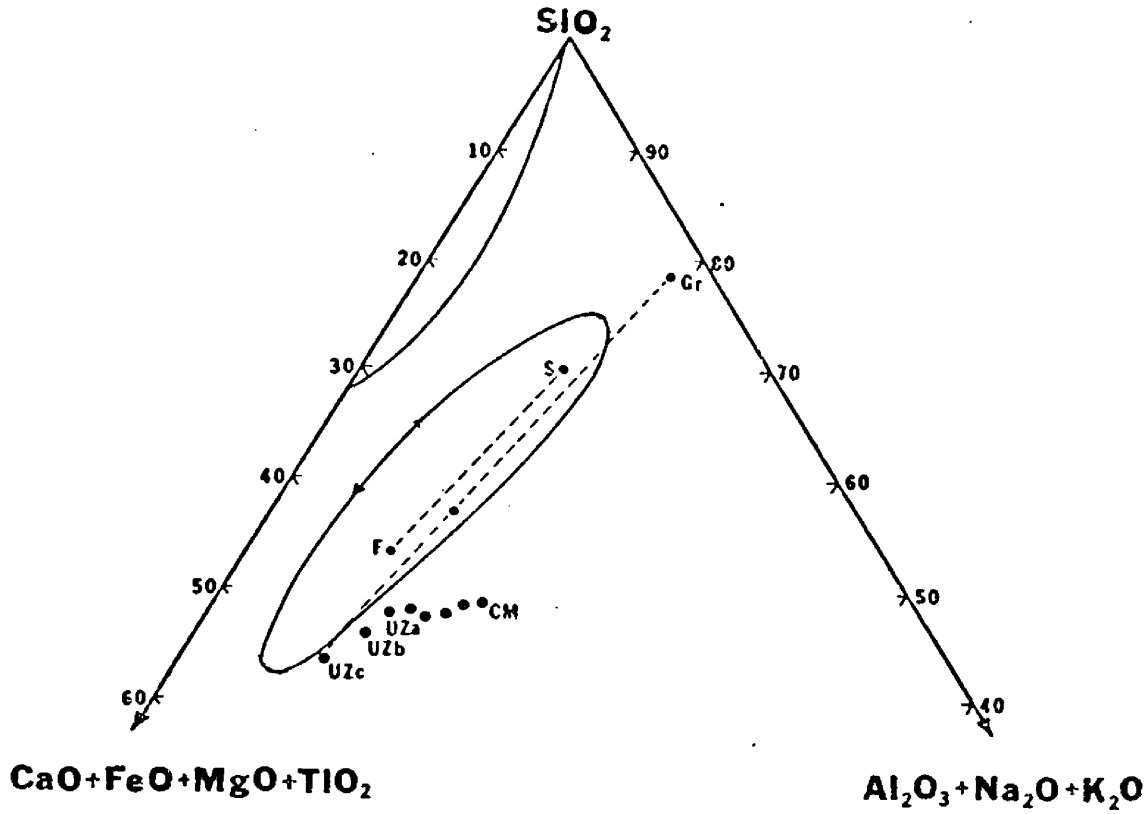

Figure 16. Relations of Skaergaard liquid compositions to the immiscibility fields of Roedder (1951). Liquids corresponding to Upper Zones a,b,and c have an immiscible relationship to granophyric liquids (Gr). An intermediate composition consisting of two parts Upper Zone c and one part granophyre split into two liquids, one iron-rich (F) and the other rich in SiO_2 (S). CM=chilled margin composition. Differentiates are shown to approach Upper Zone compositions and the two-liquid field. (From McBirney and Nakamura, 1974)

Archean tholeiitic lavas in the Abitibi volcanic belt of Canada contain varioles of quartz kerotophyre 5-50 mm in diameter within a highly ferruginous matrix (Gelinas and others, 1976; Gelinas, 1974). These lavas show flow differentiation with coalescing of varioles to form a rhyolitic layer. Besides satisfying Bowen's three criteria for immiscibility--evidence of two glasses of contrasting composition, occurrence of identical crystals in both fractions, and coalescence of globules--these variolitic lavas exhibit the following features suggestive of liquid immiscibility: sharp contacts confirmed by microprobe traverses, unique devitrification textures occurring simultaneously in both; and relics of skeletal quench crystals of mafic minerals in both and sometimes cutting across the interface (implying chemical equilibrium between immiscible liquids and quench crystals). When plotted on an immiscibility diagram, the tielines between variole and matrix materials are nearly parallel to those in the system K_2O-FeO-Al_2O_3-SiO_2, but as these lavas are extremely low in K, an exact "fit" is not expected.

Similar light-colored felsic spheres given the non-genetic name "ocelli" occur in basaltic komateiites of the Onverwacht Group, Barberton Mountain Land, Transvaal (Ferguson and Currie, 1972). The ocelli are particularly common in pillowed units where they decrease in size from about 30 mm in diameter near the pillow centers to 1-2 mm near the outer parts. They can reach diameters of 100 mm in massive flows and commonly merge or show cuspate intersections. Cherty

amygdules clearly cross-cut the ocelli which in some cases constitute 30 percent, by volume, of pillow lava. The ocelli are chemically enriched in SiO_2 (near 60%), Al_2O_3, K_2O, and Na_2O. The darker matrix, with 40-54 percent SiO_2, is greatly enriched in FeO and MgO along with TiO_2, MnO, and CaO. Experimental work on bulk compositions of Barberton komateiite verified the occurrence of liquid immiscibility between 1100°C and 1200°C.

Similar features occur in Proterozoic high-magnesian basaltic lavas of the Ventersdorp Supergroup of South Africa (Cawthorn and McCarthy, 1977). Sharply-bordered ocelli here reaching 150 mm in diameter merge to form layers with a cuspate contact with the matrix. Vesicles now infilled cut across the ocelli matrix boundary, proving the ocelli are not merely filled vesicles. Chemically, the strongly quartz-normative ocelli are enriched in SiO_2 and Na_2O whereas the matrix, whose composition lies close to the plane of silica saturation, shows enrichment of MgO, FeO, and TiO_2. Although divergence on an immiscibility diagram is smaller than that represented by the experimentally-determined immiscibility field, tie lines connecting FeO-rich matrix to more felsic ocelli parallel those expected of conjugate immiscible liquids. Cawthorn and McCarthy also report that nickel, which is enriched in these lavas (400-900 ppm), partitions into the matrix which may have up to 1.45 times the amount relative to adjacent ocelli.

Composite dikes near Winnsboro, South Carolina (Vogel and Wilband, 1978) consist of cuspate pillow-like masses of basic rock surrounded by

granite with no chilled margins or gradational boundaries. Although such a dike may form by several methods, a study of REE partitioning precludes the operation of fractional crystallization or partial melting as a means of differentiation. Liquid immiscibility appears indicated.

Alkaline systems. Felsic ocelli similar to those described above have been noticed in a number of alkalic dikes (eg. Ramsay, 1955; Phillips, 1968; Philpotts and Philpotts, 1969; Philpotts, 1971). In fact, liquid immiscibility has long been invoked to explain many of the chemical and textural oddities common to the alkaline undersaturated rocks (Kogarko and others, 1974).

At Callander Bay and Seabrook Lake, Ontario (Cullers and Medaris, 1977; Currie, 1976) alkalic ocellar dikes are associated with pyroxenite, biotite pyroxenite, ijolite, quartz monzonite, and carbonatite. Based on textures, composition, and elemental partitioning, an immiscibility origin for the ocelli structures is probable. Currie's (1972) thermodynamic model yielded the largest free-energy favorability for liquid splitting for the Callander Bay dikes.

Philpotts has worked extensively with ocellar dikes within the Monteregian Hills of Quebec. Textural as well as chemical relations between felsic ocelli and their basic matrices point strongly to immiscibility relations (Philpotts, 1976), with the divergent compositions defining an interpreted immiscibility field on an FMA diagram (Fig. 17). These compositions lie close to, yet outside the boundary of Freestone's (1978) stable two-liquid field (Fig. 18). However the

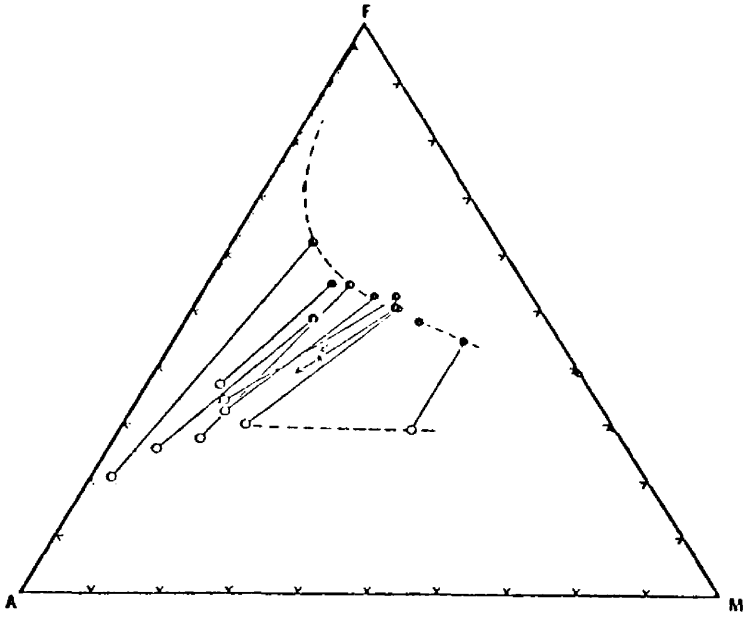

Figure 17. FMA diagram of ocelli (open circles) and matrix (solid circles) from Monteregian dikes and sills. The dashed lines outline approximately the interpreted field of immiscibility. (After Philpotts, 1976)

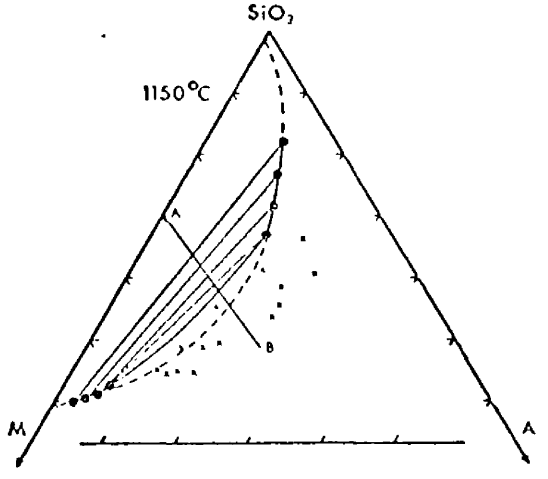

Figure 18. Ocelli and matrix compositions (X's) plotted on an immiscibility diagram. Dashed line outlines the extrapolated immiscibility field. A=mole % Al_2O_3 + K_2O + Na_2O; M=mole % MgO + CaO + FeO + TiO_2 + P_2O_5. (From Freestone, 1978)

complexity of the natural system, together with fluid pressures, may depress the liquidus enough to cut the metastable immiscibility dome which lies just beneath it. Elemental partitioning supports this view of an origin through immiscibility, since silica, alumina, and alkalies concentrate in the ocellar syenites while FeO, CaO, MgO, TiO_2, and P_2O_5 are enriched in the host gabbroic rocks (Philpotts, 1976).

Most of the major Monteregian intrusions form two groups of rocks, the darker-colored pyroxenites and peridotites, and the lighter-colored ones ranging from monzodiorite to syenite (Philpotts, 1976). Bimodal intrusions are not uncommon (eg. Woussen, 1970; Currie, 1976) and it is very tempting indeed to correlate the ocellar syenite and basic fractions of the matrix with their plutonic equivalents. The areal relationship between ocellar dikes and bimodal complexes is at least permissive evidence for a liquid immiscibility origin for the Monteregian intrusive complexes. Furthermore, Currie's (1972) thermodynamic model shows a Gibbs Free Energy which favors magma splitting for some plutonic complexes, Mount Saint Hilaire in particular. There, a circular pluton about three kilometers across is composed of about 50 percent mildly alkalic gabbro intruded by agpaitic syenite. The intermediate compositional gap between gabbro and monzonite, or their equivalent non-ocellar dike rocks, within the Monteregian province, corresponds to the compositional range of the ocellar rocks (Fig. 19). This gap surely resulted from either stable immiscibility fractionating original magmas or from crystallization trends reflecting a liquidus topography severely

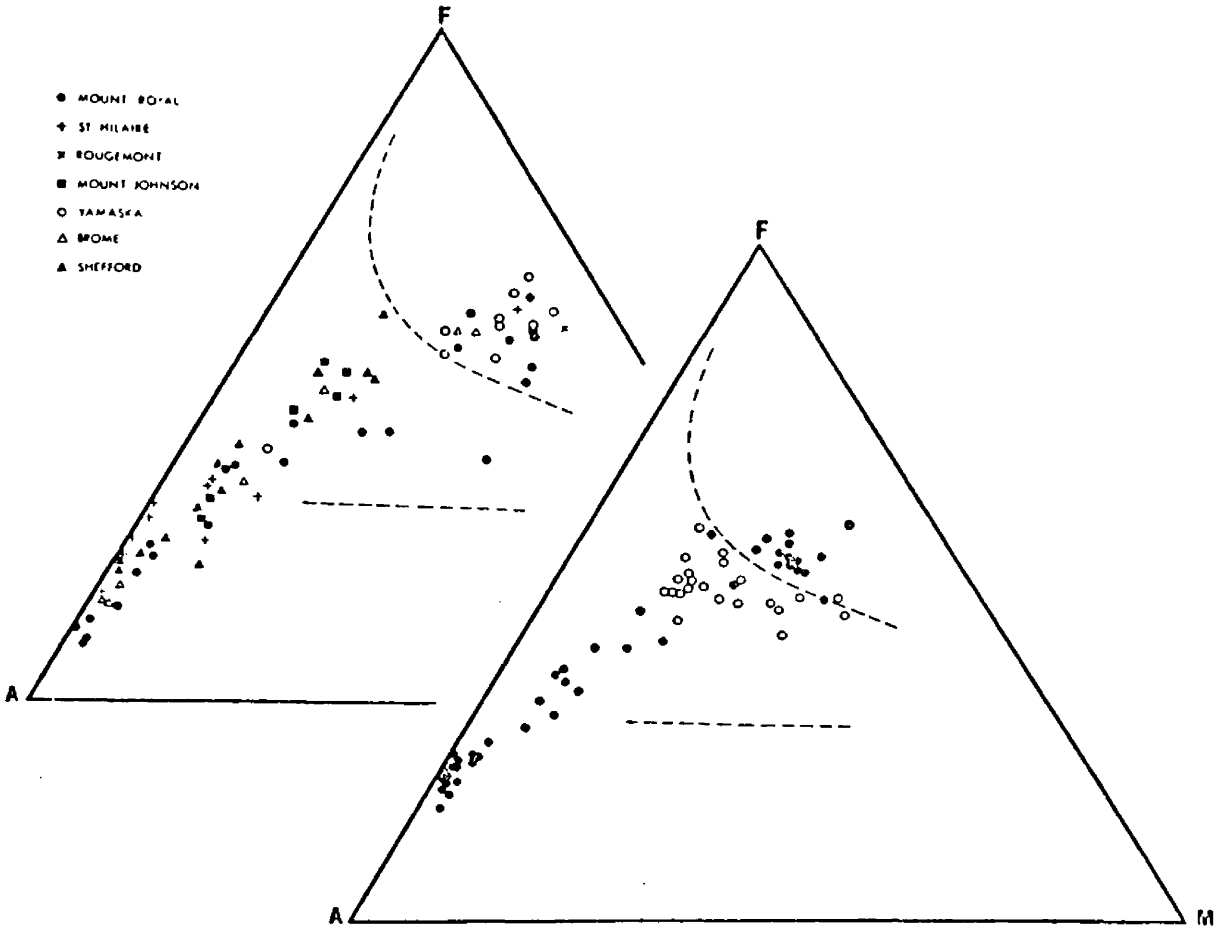

Figure 19. above: FMA diagram of plutonic rocks within the Monteregian Province.
below: FMA diagram of fine-grained dike rocks in the Monteregian Province. Solid circles, corresponding to non-ocellar dikes, show a compositional gap equivalent to the gap in plutonic rocks of the province. Open circles, representing analyses of gross, unseparated ocellar rocks, fills this compositional gap. The dashed lines are the approximate boundaries of the interpreted immiscibility field. (From Philpotts, 1976)

distorted by a subliquidus field of metastable immiscibility. The coincidence of the gap with the bulk compositions of ocellar dikes suggests the former. If immiscibility was operative on a grand scale, plutonic compositional variety within the two major categories may reflect post-immiscibility differentiation by more conventional means such as fractional crystallization.

Bimodal rock associations are not uncommon and may owe their existence to processes of liquid immiscibility. The Ice River alkaline complex of Canada (Currie, 1975) presents a good case for immiscibility. Feldspar-free pyroxenites and ijolites were emplaced contemporaneously with feldspar-rich syenites at about 1000° C and 2.5 kb with P_{CO_2} = 0.3 - 0.5 x P_T and f_{O_2} near the QFM buffer. The basic rocks are rich in titanaugite, sodic hedenbergite, magnetite, sphene, apatite, and biotite or phlogopite. Crystal fractionation has been ruled out as a differentiation mechanism (Currie, 1975). Philpotts (1976) suggests other associations which may have arisen through processes of immiscibility such as the volcanic rocks of the Auvergne district of France, and rocks of Tahiti and Clarion Island, Mexico. Other localities worthy of examination include the Rainy Creek pyroxenite-syenite stock near Libby, Montana (Pardee and Larson, 1929; Boettcher, 1967), the Gem Park igneous complex of Colorado (Parker and Sharp, 1970) and the alkalic complex near Powderhorn, Colorado (Temple and Grogan, 1965). Based on chemical grounds, it appears, however, that the basalt-rhyolite assemblage common in extensional terranes (Yoder, 1973) may not represent separation by immiscibility.

Liquid Immiscibility at Skalkaho Mountain

Chemical suitability. The Skalkaho igneous complex certainly exhibits a bimodal character similar to complexes some have attributed to processes of liquid immiscibility. The discussion concerning differentiation methods interrupted above is continued here, where the Skalkaho complex is evaluated in terms of liquid immiscibility. Lacking direct textural evidence even in the form of associated ocellar dikes (perhaps because of the dominance of plutonic textures), other criteria are considered.

The igneous rocks at Skalkaho are alkalic, and thus fall into a general igneous rock grouping almost negligible in volumetric occurrence, yet extremely important in terms of terrestrial examples of magmatic silicate liquid immiscibility. Although no modal quartz or feldspathoids were noted, it appears that the pyroxenitic fraction is normative undersaturated whereas the syenitic fraction is normative oversaturated. Such a relationship between comagmatic rocks is unusual and difficult to rationalize when considering the thermal divide separating such compositions. This divide may be seen in "Petrogeny's residua system" as the albite-orthoclase join or may be illustrated by the albite-olivine join in a ternary diagram plotting molecular proportions of normative quartz, nepheline, and olivine. The difficulty of the comagmatic juxtaposition is involved with the apparent inability to jump the hump during fractional crystallization. Philpotts (1976), however, has shown via the Monteregian alkalic dikes

that differentiation through liquid immiscibility may result in oversaturated syenitic ocelli occurring within an undersaturated mafic matrix. Liquid immiscibility, then, may serve as a good explanation for comagmatic rocks which apparently ignored the thermal divide during their differentiation history. The Skalkaho complex may be an example.

Considering only rocks exposed at the surface, a very crude estimate may be arrived at for the composition of the body by considering the chemistry of a certain rock and its exposed area. This calculated ideal composition agrees well (Table 7) with a rock composed of 2/3 microcline microperthite (data from Deer and others, 1976, p. 300, analysis No. 6) and 1/3 pyroxene (analysis of anhydrous pyroxenite, sample no. 27B). Such an alkaline intermediate rock might fall into the immiscibility field, depending on just where the field is located in this system.

The compositional make-up of a silicate system has been shown to profoundly affect the existence and dimensions of the stable liquid immiscibility field. At Skalkaho, the igneous rocks exhibit high K_2O/total alkalies values, ranging from 0.522 to 0.780 in the rocks chemically analyzed. The high K_2O content is reflected in abundant biotite and potassium feldspar. High K_2O/total alkalies, while not necessary for the existence of liquid immiscibility, generally favors a pronounced divergence between coexisting liquids.

Table 7. Idealized Chemistry of Entire Complex

	Calculated composition of complex using chemical anlyses and relative percentage of corresponding rock exposed on surface	Pyroxene analysis (analysis of anhydrous pyroxenite, sample #27B)	Microcline analysis (from Deer and others, 1976, p. 300, analysis #6)	Idealized composition of complex assuming 2 parts microcline and 1 part pyroxene
SiO_2	61.53	54.64	64.2	61.01
TiO_2	0.57	0.87	--	0.29
Al_2O_3	13.64	3.24	19.1	13.81
FeO	3.13	6.68	0.4	2.49
CaO	6.48	19.00	0.34	6.56
MgO	6.37	13.97	--	4.66
MnO	0.10	0.32	--	0.11
Na_2O	2.18	0.62	2.60	1.94
K_2O	6.00	0.67	12.70	8.69

Apatite abounds, constituting over one-third the volume of some rocks. The amphibole pyroxenites, for example, average about 1.2 to 1.5 percent P_2O_5 as estimated from modal apatite values. Phosphorus was seen to greatly expand experimental immiscibility field dimensions. Moreover, many rocks thought to represent immiscible systems are anomalously high in phosphorus.

Titanium also widened the miscibility gap in experimental systems. In the Skalkaho complex, the widespread abundance of sphene alone indicates enrichment of TiO_2, with some rocks containing well over

6 percent estimated TiO_2. More titanium may be locked up in magnetite, garnet, or some pyroxene.

In contrast, increased Ca, Mg, and Al have been shown to slightly inhibit immiscibility and shrink the two-liquid field. The rocks at Skalkaho are peraluminous with K_2O+Na_2O/Al_2O_3 ranging from 0.37 to 0.66 in the rocks analyzed. They are not, however, highly enriched in Al_2O_3, with values between 2.33 percent and 19.37 percent in the same rocks. As in some of the experimental work on silicate immiscibility, the mafic fraction tends to be more peraluminous than the felsic fraction. For the complex as a whole, MgO and CaO values are not extreme, both estimated near 6.5 percent.

Increased volatile content in general increases the dimensions of the immiscibility field. The abundance of biotite and amphibole indicate that water was plentiful, probably in the later stages of magmatism. The abundant miarolitic cavities in the pegmatite are attributed to high CO_2 content. The somewhat violent intrusive nature of the complex, mirrored in the intricate intrusion patterns together with the fenite and some pyroxenite varieties attributable to metasomatism, also suggest moderate to high volatile content.

It is unclear exactly what the effect of the high percentage of volatiles, P, Ti, and K together with the somewhat abundant Al, Ca, and Mg was on the magmatic system. However, from experimental work related above and from localities cited as representative products of liquid immiscibility, it is believed that the chemistry of the igneous

complex at Skalkaho could have been extremely conducive to liquid immiscibility. The dimensions of the immiscibility field of course may not be determined.

The analyzed pyroxenites and syenites of the Skalkaho complex are represented on an immiscibility diagram in Figure 20. The bimodal character is evident, and the two groups lie generally at the extremes of the immiscibility field determined in the system K_2O-Al_2O_3-FeO-SiO_2. Moreover, the general trend of the tie lines which could run between the two groups parallels that seen between experimental coexisting melts, lunar residual glasses, ocelli and dike matrices, and other immiscible pairs. Although the fit with the experimental field is somewhat coarse, it must be remembered that this field changes drastically with minor alterations in magmatic constituents and conditions. The fit, though coarse, is remarkable and certainly serves as strong permissive evidence for liquid immiscibility. The FMA diagram utilized for the Monteregian ocellar dikes could not be used here since the distinction between oxidation states of iron crucial to that method is unavailable.

Elemental partitioning, specifically of P, Ti, Zr, and REE may help to differentiate those bimodal rocks formed through fractional crystallization from those formed by liquid immiscibility. Phosphorus, the element most noticeable partitioned in liquid immiscibility work, is greatly enriched in the pyroxenite fraction at Skalkaho. Although

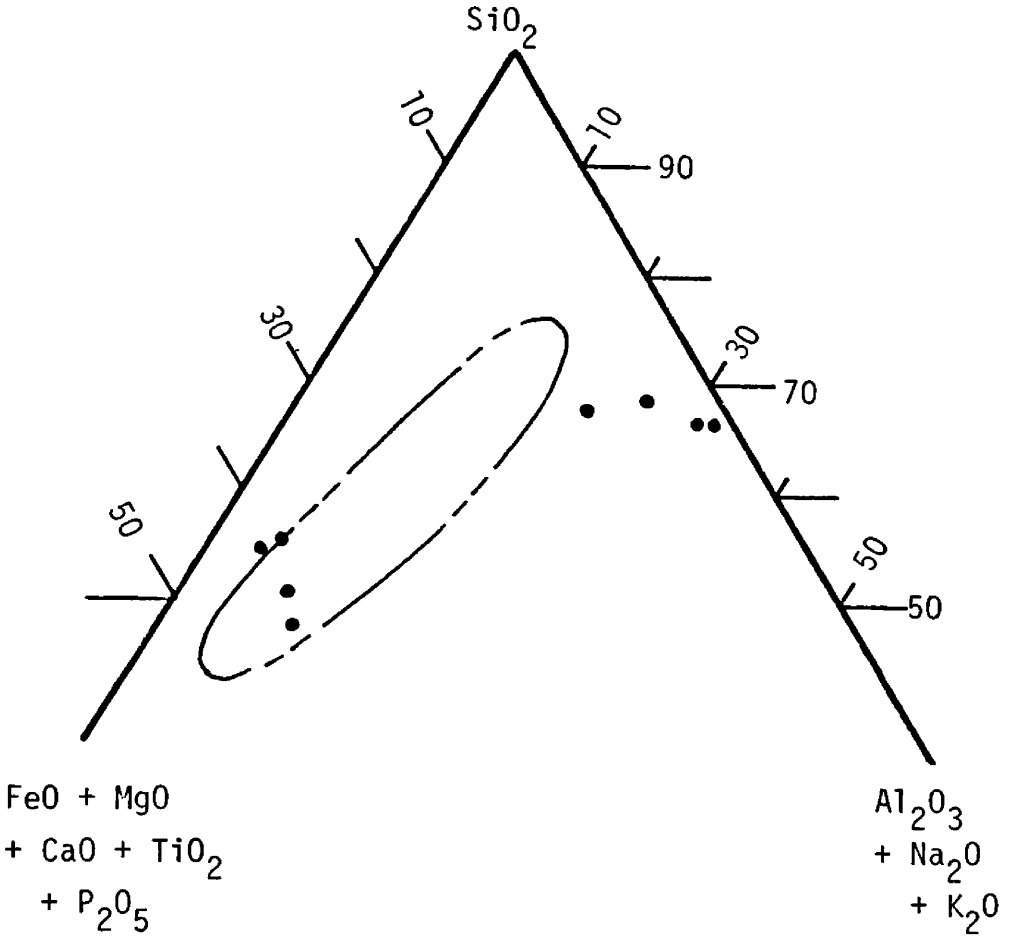

Figure 20. Skalkaho complex pyroxenites and syenites plotted on an immiscibility diagram. (immiscibility field from Roedder, 1978)

chemical analyses for P are lacking, this trend may be seen in the modal apatite analyses (see Table 1). Titanium partitioning in the mafic fraction may similarly be illustrated by the modal analyses of sphene. This trend is also illustrated by means of a variation diagram plotting Ti against Ca using data from the available chemical analyses (Fig. 21a). Figures 21b through 21i are similar plots for the REE and Th which show slight but definite preference for the mafic fraction. These trends strongly imply the previous operation of liquid immiscibility as opposed to fractional crystallization or movement of volatiles. Figures 21j and 21k, showing pyroxenitic association of Cu and Li, also adds credence to the likelihood of immiscibility. No assessment of Zr partitioning may be made.

Intermediate rocks. The bimodal character of the complex is the feature which initially suggests the possibility of liquid immiscibility processes. Two small outcrops were found, however, of a rock apparently intermediate in composition between the syenitic rocks and the pyroxenite. These hybrid rocks may represent one of two things.

First, if stable liquid immiscibility operated at Skalkaho these hybrids, located essentially between masses of syenite and pyroxenite, may represent something akin to an original two-liquid melt which has not yet physically unmixed. "Force of crystallization" of pyroxene may have overcome liquid-liquid surface forces, with early-formed pyroxene crystals obliterating any trace of the spheroidal shapes indicative of

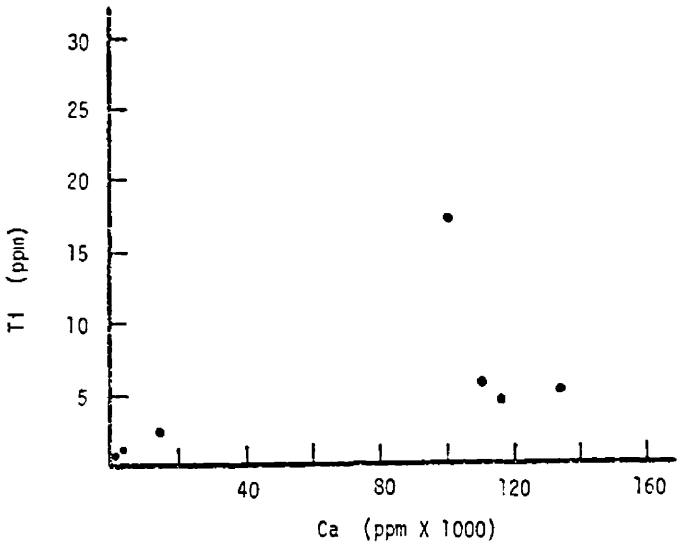

Figure 21a

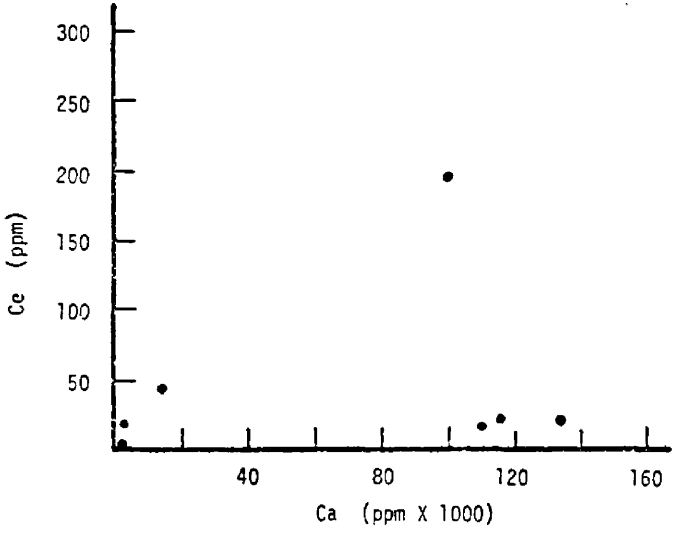

Figure 21b

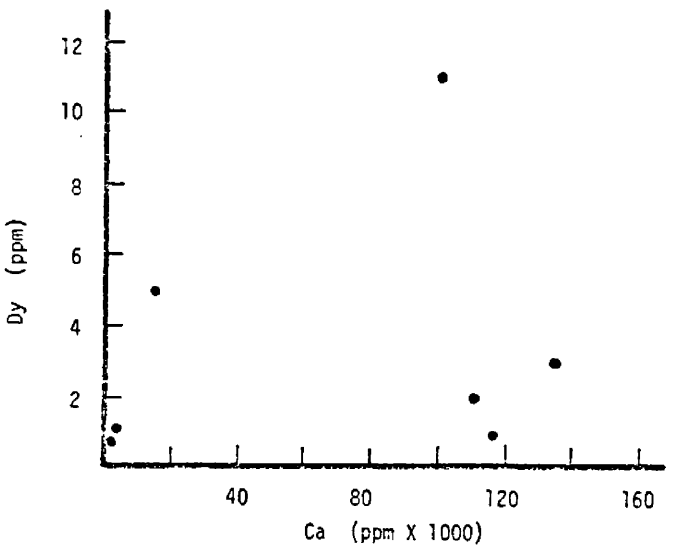

Figure 21c

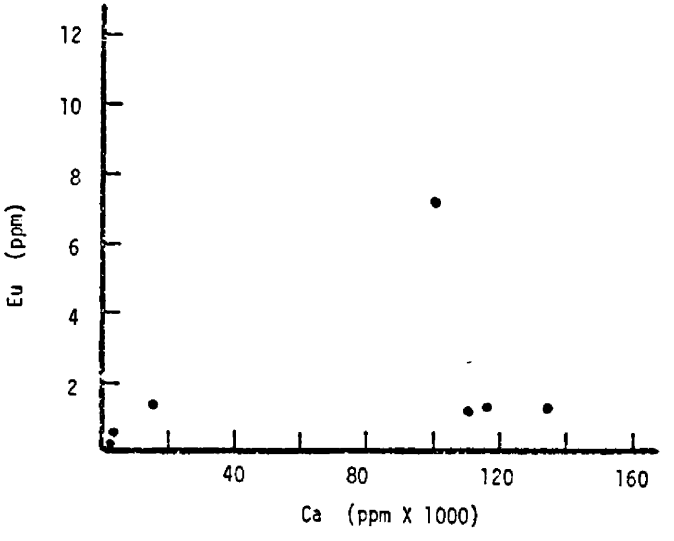

Figure 21d

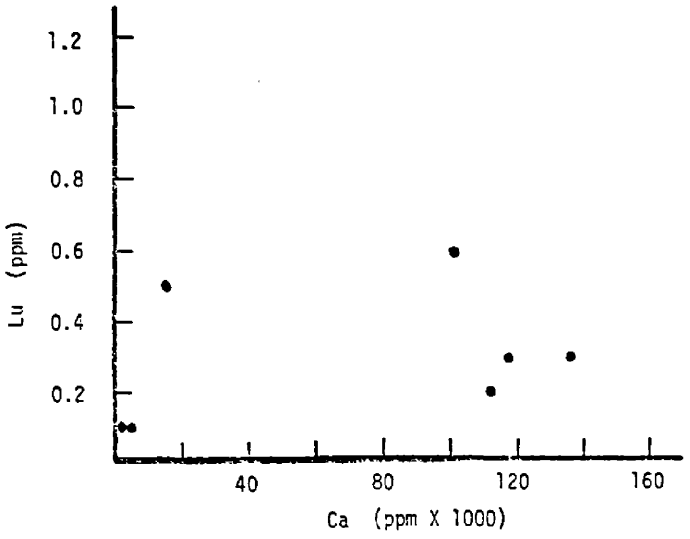

Figure 21e

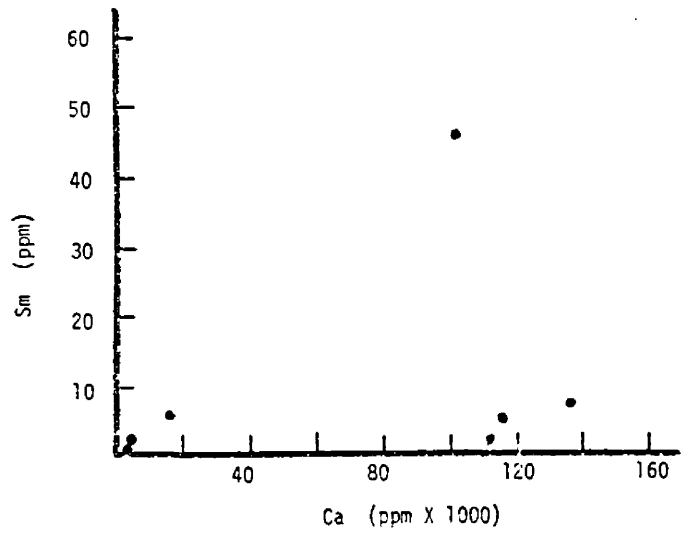

Figure 21f

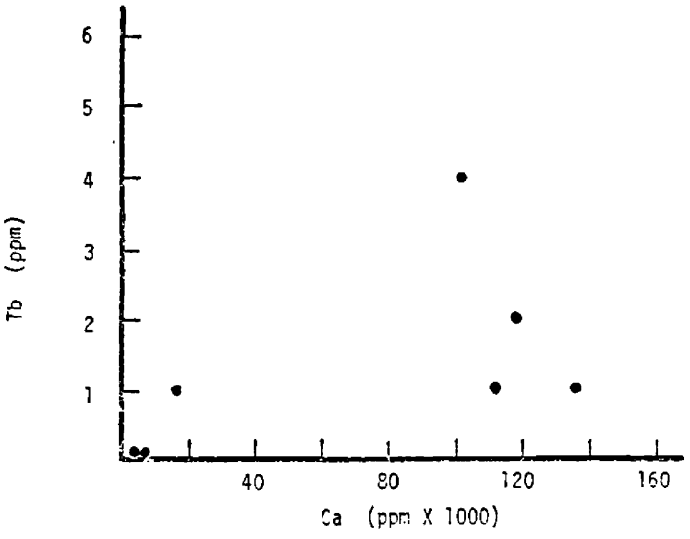

Figure 21g

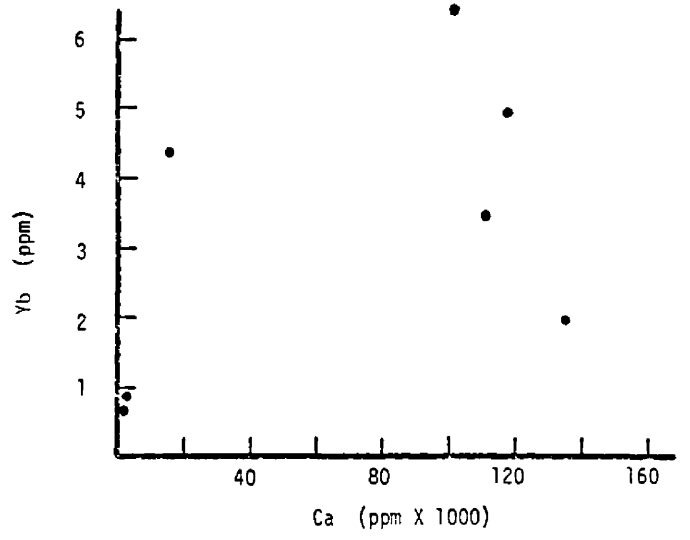

Figure 21h

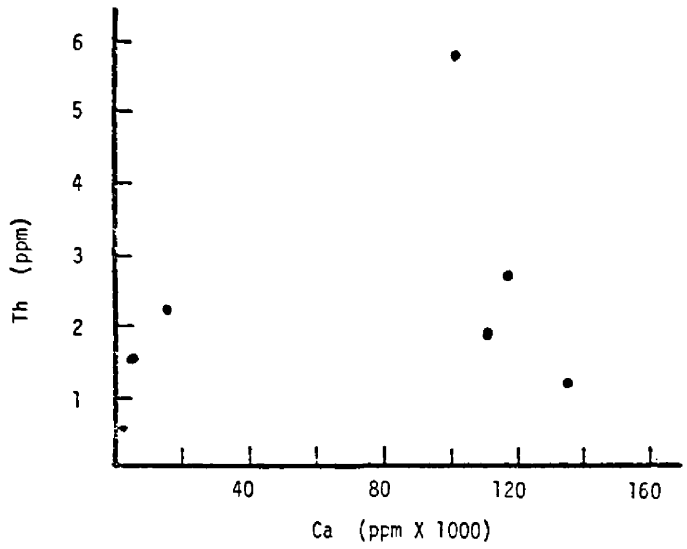

Figure 21i

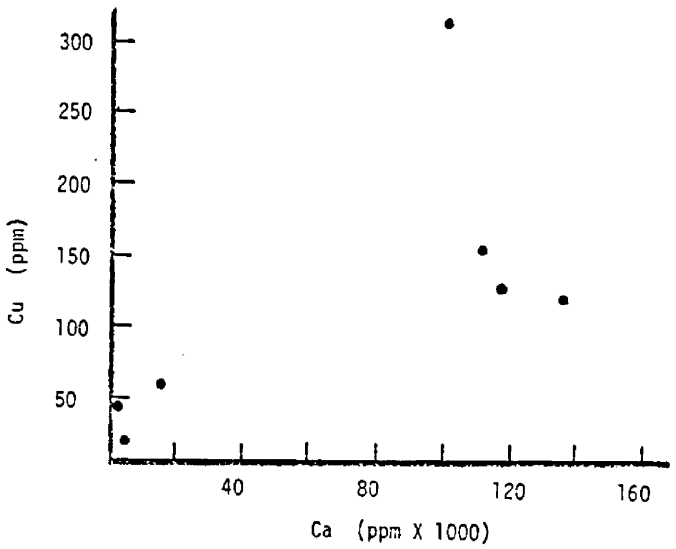

Figure 21k

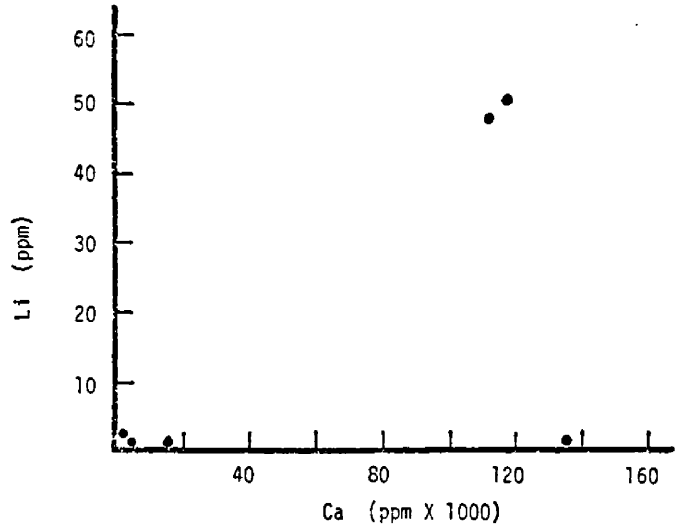

Figure 21j

immiscible globules. The presence of lobate pyroxene crystal faces in some terrestrial tholeiites make this alternative questionable. More likely, after stable immiscibility had resulted in coalescence and total separation of liquid fractions, changing conditions allowed some remixing which was mechanically limited to border zone areas. Changing temperature or pressure, or a change in composition brought about by volatile release or by fractional crystallization within the separate fractions themselves, might move the remaining liquids towards a miscible relationship. The hybrid rocks and mafic-rich border syenitic rocks may then represent zones of remixing. They would be expected to exhibit gradational boundaries which they do.

Secondly, if stable liquid immiscibility conditions did not exist at Skalkaho, the intermediate compositional gap must reflect a sigmoidal or flattened liquidus. A subliquidus metastable immiscibility dome has been shown to cause such a liquidus deflection. This topology might result in rapid transition during fractional crystallization from crystallization of ultramafic rocks to felsic rocks with a very small drop in temperature. The hybrid and mafic-rich syenitic rocks may represent those rocks formed over this short span of time. It is unlikely, however, that differentiation by this process would result in the elemental partitioning pattern seen.

Shallow nature. Virtually all igneous silicate rocks showing features suggestive of an original through liquid immiscibility appear

to have crystallized at relatively shallow depths within the crust (Hyndman and Alt, verbal comm., Feb. 1979). Noted examples include the Monteregian ocellar dikes and bimodal plutons, the Abitibi tholeiitic variolitic lavas, the ocellar komateiites of the Barberton Mountain Land, and the Ice River Alkaline complex. This feature is compatible with the view that silicate liquid immiscibility fields stabilize and expand at relatively low pressures (<5-10 kb) and shrink at higher pressures to become fields of subliquidus metastable immiscibility.

The Skalkaho complex shows several features which indicate its shallow nature. The pegmatite contains abundant large miarolitic cavities attributed to high CO_2 content. Such cavities are limited to epizonal intrusives such as those granitic plutons which crystallized at depths less than two kilometers. Also associated with the complex are trachyte dikes interpreted to represent venting of the syenite. These shallow dikes, containing numerous flattened vesicles, provide more direct evidence to the shallowness of the syenitic body itself. Moreover, most of the water locked up in the micas and amphibole of the pyroxenites is believed to have been derived from shallow country rock. Syenitic contacts with the country rocks are very sharp. The low-pressure, near-surface character of the Skalkaho complex is compatible with the observed similar character inherent to virtually all suspected examples of silicate immiscibility.

Similar plutons. Plutons displaying a bimodal character similar to the Skalkaho complex are not uncommon, existing in varied tectonic settings and in some cases associated with ocellar dikes. Several well-documented examples exist in the Monteregian province of Quebec. Mount Saint Hilaire (Currie, 1976, p. 50-52) is a strikingly bimodal complex consisting of about half mafic to ultramafic rocks including pyroxenite, yamaskite, and gabbro, lying adjacent to a body of agpaitic nepheline syenite. The complex is enriched in TiO_2, and apatite and magnetite are ubiquitous. Currie notes that the development of Mount Saint Hilaire is poorly understood even though the pluton is generally considered a petrologic key to the whole province. Its bimodal rocks reflect the general petrology of the region. Several complex paragenetic schemes proposed to explain Mount Sain Hilaire have not met with great acceptance.

Mount Bruno consists chiefly of peridotite and hornblende peridotite with younger cross-cutting bodies of quartz-bearing alkali syenites (Currie, 1976, p. 48-50). Olivine and titanaugite comprise most of the ultramafic rocks with small amounts of labradorite always present. Cumulate textures are common in the center of the ultramafic intrusion.

Mount Megantic, which is the easternmost representative of the Monteregian province, consists of a granitic body bordered by a ring dike of quartz-bearing alkali syenite containing areas of alkalic

gabbro (Philpotts, 1976). The three major rock types, associated with lamprophyric dikes, are believed to be genetically related, although a plausible petrogenetic hypotheses is missing.

Farther north, the Aillik complex (Currie, 1976, p. 112-115) consists of dikes occurring as flatly dipping cone sheets that suggest a plutonic center beneath Aillik Bay. Most of the dikes are unusually iron-rich ultramafic rocks composed of phlogopite, augite, and rare olivine phenocrysts in a carbonatized fine-grained matrix. Also present are syenitic dikes containing nepheline, albite, augite, and hornblende. These dikes, as well as the Monteregian rocks mentioned above, are believed to be very shallow features.

Russian literature on alkaline bimodal igneous complexes is confusing since nearly all associated syenitic rocks are referred to as fenites and attributed to metasomatism of country rock. Furthermore, many of the ultramafic to mafic rocks are also thought to be metasomatic. However, the Maimecha-Kotui region of northern Siberia (Egorov, 1970) contains alkalic rocks associated with the Baikal lineament which chearly exhibit an igneous bimodal character similar to that evidenced at Skalkaho. Dikes, eruptives, and plutons in the area are either ultramafics (olivinite, jacupirangite, melteigite), nepheline and alkalic syenites, or magnetite-apatite-rich carbonatites. Tomkeieff (1961) provides a somewhat confusing review of alkaline ultramafic rocks in the USSR which indicates that ultramafic-syenitic complexes may be quite common.

LeBas (1977) described the geology around the Rangwa complex of western Kenya which includes the Kisingiri, Sagurume, Homa Mountain, Usaki, Ruri, and Ragwa igneous centers. Bimodal volcanic and intrusive rocks are common, with the majority of intrusives being either broadly pyroxenitic (biotite varieties are widespread) or syenitic (including so-called "fenites"). Carbonatite eruptives and intrusives are also common, and apatite and magnetite are abundant and widespread in the invariably shallow-seated rocks. Some pyroxenites of the area are nearly identical to those at Skalkaho. Although some pyroxenites are assigned a cumulate origin and many syenitic rocks are called fenites, a plausible comprehensive petrogenesis for the igneous rocks is not proposed.

It appears that compositionally divergent glassy inclusions in apatite crystals from an ijolite of the Usaki complex imply that two silicate liquids coexisted at the time of apatite formation (LeBas and others, 1977). These glass inclusions were of two general compositions: one rich in K_2O (about 6 weight percent), poor in Na_2O (about 0.3%), and oversaturated; the other rich in Na_2O (6-14%), poor in K_2O (about 0.2%), and undersaturated. The potassium-rich ocelli at Callander Bay, Ontario are similar in composition to the potassium-rich inclusions. The host ijolite contains about 4 percent apatite. Numerous similar bimodal complexes exist in the abundant alkaline rocks of Africa (Heinrich, 1966).

The carbonatite-alkalic rock complex of Ipanema, Sao Paulo, Brazil (Heinrich, 1966, p. 407-409) consists of peridotite, jacupirangite, pyroxenite, and some ijolite surrounded by nepheline syenite and fenite. Masses of titaniferous magnetite rock and dikes of various apatite-bearing rocks containing aegerine, hastingsite, biotite, magnetite, and orthoclase are common. One variety consists almost entirely of aegerine and apatite. Vermiculite is developed from biotite as it is at the nearby similar complexes of Jacupiranga and Registro. The bodies are all highly enriched in phosphorus and titanium.

Similar, more subtly bimodal rocks occur in Colorado. The Gem Park complex (Parker and Sharp, 1970) consists mostly of pyroxenite locally grading to gabbro with subordinate amounts of syenite, nepheline syenite, and carbonatite. The Iron Mountain intrusive (Shawe and Parker, 1967) is very similar. The pyroxenes are salite-augite commonly showing a Schiller effect due to exsolution of magnetite rods. Other minerals include poikilitic amphiboles, minor olivine and plagioclase, and accessory magnetite, apatite, sphene, and rare sulfides. In addition to the syenites, some fenite is reported. Vermiculite was mined from the Iron Mountain complex. The nearby Powderhorn complex (Nash, 1972; Temple and Grogan, 1960), consisting mostly of pyroxenite with some ijolite, magnetite-perovskite rock, and fenite, is thought to expose two structural levels, illustrative of a more eroded version of the Gem Park complex.

The Ice River complex in the Canadian Cordillera, composed of pyroxenites, ijolites, and syenites, was discussed above. Other Canadian alkalic plutonic rocks of bimodal character include the Hematite Lake sills, the Lackner Lake and Nemegosenda Lake ring complexes, the partially layered Kamiak Lake complex, and the Big Spruce Lake complex (Currie, 1976).

The rock occurrence most similar to the Skalkaho complex, however, is the Rainy Creek stock (Pardee and Larsen, 1929; Boettcher, 1966, 1967) just 275 km to the north. The initial intrusion of coarse-grained biotite pyroxenite with a core of pegmatitic biotite invaded Wallace Formation metasediments, probably in middle Cretaceous time. The biotite core, rich in alkaline pegmatites, is considered by Boettcher to have resulted from the accumulation of volatiles and alkalies near the roof of the pluton. He attributes the feldspar-pyroxene pegmatites to latest crystallization from a highly H_2O-charged fluid. Following the initial intrusion, magnetite pyroxenite intruded a zone of weakness between the igneous complex and country rocks, forming a ring dike. All the ultramafic rocks are considered to be differentiates of a common magma crystallized under high P_{H_2O}, P_{O_2}, and temperature conditions.

A syenitic body believed to be altered nepheline syenite intruded adjacent to the southwestern portion of the ring complex. Phonolite and trachyte dikes, fenitized country rock, late alkaline

granite dikes, and quartz and quartz-carbonate veins complete the list of rocks related to the complex. Boettcher concluded that groundwater leaching transformed biotite to vermiculite, whereas hydrobiotite alteration may represent a hydrothermal process. Boettcher states that "the alkaline rocks at the surface may be mobilized fenites" (Boettcher, 1966, p. 144). The fenitizing ions were abbributed to a deep-seated ijolite or carbonatite.

Bimodal intrusive complexes, especially of alkalic affinity, are fairly common and widespread, existing throughout the world in varied geologic and tectonic settings. Such complexes are commonly assigned somewhat specific and restricted petrogenetic hypotheses not applicable to many similar complexes in differing locales. In many studies, a genesis for the rocks remains unproposed. For some of these complexes similar to the Skalkaho complex, liquid immiscibility origins have recently been put forth (Currie, 1972; Philpotts, 1976; Philpotts and Hodgson, 1968). Certainly, to satisfy the law of simplicity a petrogenetic framework should be sought which could be successfully applied to most if not all of these bimodal intrusions. Fractional crystallization seems untenable and mechanisms such as filter-pressing lack universality and require specialized situations.

CHAPTER VI

SUMMARY AND CONCLUSIONS

The Skalkaho hypabyssal plutonic complex, intruded into Wallace Formation calc-silicate metasediments near the western edge of the Sapphire tectonic block, exhibits a bimodal character whereby pyroxenites lie adjacent to syenitic rocks. The silica-undersaturated pyroxenites range from anhydrous pyroxenites, through biotite pyroxenites, to amphibole pyroxenites rich in apatite, magnetite, and sphene. A pegmatite of anhydrous mineralogy rich in miarolitic cavities is associated with this centrally-located pyroxenite mass. The over-saturated syenitic rocks include nearly pure potassium feldspar rocks but grade to alkalic syenites. These two main intrusive rock masses arose largely through magmatic crystallization, but replacement textures and field relations indicate some metasomatic overprint. Minor fenitized country rock adjacent to the pyroxenite resembles the sort of metasomatic product common around alkalic carbonatite complexes. Linear calcite-magnesiohastingsite forms may represent an intrusive stage of this implied carbonatite. Vesicular trachyte to alkali trachyte dikes cutting the pyroxenites represent surface breaching of the syenite.

The syenitic and pyroxenitic masses comprising most of the complex appear to be both comagmatic and contemporaneously emplaced.

Differentiation of the syenite from a parent magma by fractional crystallization does not seem plausible. While movement of volatiles may have played a minor role in the development of the volatile-laden complex, it can not be responsible for the gross bimodal quality.

Chemical composition, elemental partitioning, the nearly complete lack of intermediate rock types and cumulate textures, and the parameters of emplacement suggest an origin through liquid immiscibility. Compositions of the divergent bodies fall near opposite sides of the immiscibility field on an experimental liquid immiscibility diagram and show good correlation to naturally occurring pairs of immiscible silicate liquids. These include coexisting glasses found in late-stage crystallization pockets in lunar and terrestrial basalts, variolites and matrices of mafic and ultramafic lava flows, and ocelli and matrices in alkalic dikes.

Bimodal igneous complexes similar to the Skalkaho complex are not uncommon, particularly in alkaline terranes. Many of these intrusions have unclear overall petrogeneses. It is concluded from this study that the process of liquid immiscibility, evidently operable in certain silicate systems under certain conditions, is responsible for the development of the compositionally divergent rocks of the Skalkaho complex. Silicate liquid immiscibility as a major means of differentiation must be researched more fully, and other bimodal rock packages should be reexamined in light of the most-recent developments concerning this separation-differentiation process.

REFERENCES

Alling, H. L., 1938, Plutonic perthites, Jour. Geol., v. 46, p. 142.

Armstrong, R. L., 1974, Magmatism, orogenic timing, and orogenic diachronism in the Cordillera from Mexico to Canada, Nature, v. 247, p. 348-351.

Badley, R. H., 1977, Petrology and chemistry of the East Fork dike swarm, Ravalli County, MT., unpublished M.S. Thesis, Univ. of Montana.

Banno S., and Matsui, Y., 1973, On the formation of partition coefficients for trace elements distribution between minerals and magma, Chem. Geol., 11, p. 1-15.

Barron, L. M., 1978, The geometry of multicomponent exsolution, Am. Jour. Sci., v. 278, p. 1269-1306.

Berg, R. B., 1962, Petrology of anorthosite bodies, Bitterroot Range, Ravalli County, Montana, Unpublished M.S. thesis, Univ. of Montana.

Bhattacharji, S., and Smith, C. H., 1964, Flowage differentation, Science, 145, p. 150-153.

Boettcher, A. L., 1967, The Rainy Creek alkaline-ultramafic igneous complex near Libby Montana I: Ultramafic rocks and fenite, Jour. Geol., v. 75, p. 526-553.

_____, 1966, The Rainy Creek igneous complex near Libby, Montana, Ph.D., thesis, Pennsylvania State University.

Bowen, N. L., 1928, The Evolution of the Igneous Rocks, Princeton University Press, Princeton, N.J., 332 p.

Burchfiel, B. C., and Davis, G. A., 1975, Nature and controls of Cordilleran orogenesis, western U.S.: Extensions of an earlier synthesis, Am. J. Sci., v. 275-A, p. 363-396.

Cawthorn, R. G. and McCarthy, T. S., 1977, Partitioning of nickel between immiscible picritic liquids. Earth Planet Sci. Letter, vol. 37, No. 2, p. 339-346.

Cheney, J. T., 1975, Kyanite, sillimanite, phlogopite, cordierite layers in the Bass Creek anorthosites, Bitterroot Range, Montana, Northwest Geology, v. 4, p. 77-82.

Crowley, F. A., 1960, Columbium-rare-earth deposits, southern Ravalli County, Montana, Montana Bur. Mines and Geol. Bull. 18.

Cullers, R. L. and Medaris, G. Jr., 1977, Rare earth elements in carbonatite and cogenetic alkaline rocks; examples from Seabrook Lake and Callander Bay, Ontario, Contrib. Min. Petr., v. 65, no. 2, p. 143-153.

Currie, K. L., 1976, The alkaline rocks of Canada, Geol. Surv. Canada Bull. 239.

_____, 1975, The geology and petrology of the Ice River alkaline complex, Geol. Surv. Canada Bull. 245.

_____, 1972, A criterion for predicting immiscibility in silicate liquids, Nature, 240, p. 66.

Dé, A., 1974, Silicate liquid immiscibility in the Deccan traps and its petrogenetic significance, Geol. Soc. America Bull. 85, pp. 471-474.

Deer, W. A., Howie, R. A., and Zussman, J., 1976, An introduction to the rock-forming minerals, Longman, London, 528 p.

Donaldson, C. H. and Dawson, J.B., 1978, Skeletal crystallization and residual glass compositions in a cellular alkalic pyroxenite nodule from Oldoinyo Lengai, Contr. Miner. Petr. 67, p. 139-149.

Egorov, L. S., 1970, Carbonatites and ultrabasic-alkaline rocks of the Maimecha-Kotui Region, N. Siberia, Lithos 3, pp. 341-359.

Ferguson, J. and Currie, K. L., 1972, Silicate immiscibility in the ancient "basalts" of the Barberton Mountainland, Transvaal, Nature 235, p. 86.

Ferguson, J. and Currie, K. L., 1971, Evidence of liquid immiscibility in alkaline ultrabasic dikes at Callander Bay, Ontario, Jour. Petrol. 12, p. 561-580.

_____, McIver, J. and Danchin, R., 1975, Fenitization associated with the alkaline-carbonatite complex of Epembe, South West Africa, Trans. Geol. Soc. S. Africa 78, p. 111-122.

Freestone, I. C., 1978, Liquid immiscibility in alkali-rich magmas, Chem. Geol (Amsterdam) 23/2, p. 115-123.

Gelinas, L., 1974, Textural and chemical evidences of liquid immiscibility in variolitic lavas, EOS 55/4, p. 486-487.

Gelinas, J. Brooks, C., and Trzcienski, W. E., 1976, Archean variolites-quenched immiscible liquids, Can. Jour. Ear. Sci. 13, p. 210-230.

Greig, J. W., 1927, Immiscibility in silicate melts, Am. J. Sci. 15th Series 13, p. 1-44.

Heinrich, E. Wm., 1967, Carbonatites-Nil silicate igneous rocks, Earth Sci. Review 3, p. 203-210.

_____, 1966, The Geology of Carbonatites, Rand McNally, 555 p.

_____, 1965, Microscopic Identification of Minerals, McGraw-Hill Book Co., 414 p.

_____, and Levinson, A. A., 1961, Carbonatite niobium-rare earth deposits, Ravalli County, Montana, Amer. Miner. 46, p. 1424-1447.

Holgate, N., 1954, The role of liquid immiscibility in igneous petrogenesis, Jour. Geol. v. 62, p. 439-480.

Hyndman, D. W., (in prep), Petrology of Igneous and Metamorphic Rocks, 2nd Edition, McGraw-Hill Book Co.

_____, 1979, Bitterroot dome - Sapphire tectonic block, an example of a plutonic-core gneiss-dome complex with its detached suprastructure, in Cordilleran Metamorphic Core Complexes: P. J. Coney, Max Crittenden, Jr., and Gilt Davis, editors, Geol. Soc. Amer. Memoir, (in press).

_____, 1972, Petrology of Igneous and Metamorphic Rocks, McGraw-Hill, 533 p.

_____, Talbot, J. L. and Chase, R. B., 1975, Boulder batholith: A result of emplacement of a block detached from the Idaho batholith infrastructure?, Geology, v. 3, p. 401-405.

Irvine, T. N., 1976, Metastable liquid immiscibility and MgO-FeO-SiO_2 fractionation patterns in the system Mg_2SiO_4 - Fe_2SiO_4 - $CaAl_2Si_2O_8$ - $KAlSi_3O_8$ - SiO_2, Carnegie Inst. Yearbook 75, p. 597-611.

_____, 1975, The silica immiscibility effect in magmas, Carnegie Inst. Wash. Yearbook 74, p. 484-492.

Jens, J. C., 1974, A layered ultramafic intrusion near Lolo Pass, Idaho, Northwest Geology, v. 3, p. 38-47.

Johannsen, A., 1939, A Descriptive Petrography of the Igneous Rocks, The Univ. of Chicago Press, Chicago, Ill., 318 p.

Joplin, G.A., 1968, A Petrography of Australian Igneous Rocks, Amer. Elsevier Publ. Co. Inc., N. Y., 482 p.

Kogarko, L. N., Ryabchikov, I. D., and Sørensen, H., 1974, Liquid fractionation, in Sørensen, H. (ed.), The Alkaline Rocks, John Wiley & Sons, p. 488-500.

Koster van Gross, A. F., 1975a, The effect of high CO_2 pressures on alkalic rocks and its bearing on the formation of alkalic ultrabasic rocks and the associated carbonatites, Am. J. Sci. 275, p. 163-185.

_____, 1975b, The distribution of strontium between co-existing silicate and carbonate liquids at elevated pressures and temperatures, Geochim et Cosmochim Acta, 39, p. 27-34.

_____, and Wyllie, P. J., 1973, Liquid immiscibility in the join $NaAlSi_3O_8$-$CaAl_2Si_2O_8$-Na_2CO_3-H_2O, Am. J. Sci. 273, p. 465-487.

_____, _____, 1969, Melting relationships in the system $NaAlSi_3O_8$-NaCl-H_2O at one Kb pressure, with petrological applications, Jour. Geol., v. 77, p. 581-605.

_____, _____, 1968, Liquid immiscibility in the join $NaAlSi_3O_8$-Na_2CO_3-H_2O and its bearing on the genesis of carbonatites, Am. J. Sci. 266, p. 932-967.

_____, _____, 1966, Liquid immiscibility in the system Na_2O-Al_2O_3-SiO_2-CO_2 at pressures to 1 kb, Am. J. Sci. 264, p. 234-255.

Kushiro, I., 1975, On the nature of silicate melt and its significance in magma genesis: regularities in the shift of the liquidus boundaries involving olivine, pyroxene, and silica minerals, Am. J. Sci. 275, p. 411-431.

_____, 1975, Liquidus boundaries in silicate systems applied to partial melting of rocks, Geol. Soc. Amer. Abstr. with Prog. 6/6, p. 527.

LaTour, T. E., 1974, An examination of metamorphism and scapolite in the Skalkaho region, southern Sapphire Range, Montana, Unpublished M.S. thesis, Univ. of Montana, 95 p.

LeBas, M. J., 1977, Carbonatite-Nephelinite Volcanism: An African Case History, Wiley Publ., New York, 347 p.

_____, Aspden, J., and Woolley, A. R., 1977, Contrasting sodic and potassic glassy inclusions in apatite crystals from an ijolite, Jour. Petrol., v. 18, No. 2, p. 247-262.

Leeman, W. P., and Sheideggar, K. F., 1977, Olivine/liquid distribution coefficients and a test for crystal-liquid equilibrium, Earth Planetary Sci. Letters 35, p. 247-257.

Karkov, V. K., Nasedkin, V. V., and Ryabinin, Y. N., 1974, Liquation in ultramafic alkalic magma at high pressures, Dokl Acad. Sci. USSR, Ear. Sci. Sect. 256, No. 1-6, p. 154-155.

Nassion, P. J., and Koster van Gross, A. F., 1973, Liquid immiscibility in silicates, Nature, v. 245, p. 60-62.

McBirney, A. R., and Nakamura, Y., 1974, Immiscibility in late-stage magmas of the Skaergaard intrusion, (Ann. Rep. Geophys. Lab), 73, Carnegie Inst. Yearbook, p. 348-352.

Metz, M. C., 1971, The geology of the Snowbird deposit, Mineral County, Montana, Unpubl. M. S. Thesis, Washington State University, 69 p.

Moore, J. G., and Calk, L., 1971, Sulfide spherules in vesicles of dredged pillow basalt, Am. Miner. 56, p. 476-488.

Mudge, M. R., 1970, Origin of the disturbed belt in northwest Montana, Geol. Soc. Amer. Bull., v. 81, p. 377-392.

Nakamura, Y., 1974, The system Fe_2SiO_4-$KalSi_2O_6$-SiO_2 at 15 kb, Carnegie Inst. Yearbook 73, p. 352-354.

Nash, W. P., 1972, Mineralogy and petrology of the Iron Hill carbonatite complex, Co, Geol. Soc. Amer. Bull. 83, p. 1361-1382.

Naslund, H. R., 1977, An investigation of liquid immiscibility in the system K_2O-CaO-FeO-Fe_2O_3-Al_2O_3-SiO_2, Carnegie Inst. Yearbook 76, p. 407-410.

_____, 1976, Liquid immiscibility in the system $KalSi_3O_8$-$NaAlSi_3O_8$-FeO-SiO_2 and its application to natural magmas, Carnegie Inst. Yearbook 75, p. 592-597.

Nockolds, S. R., and Allen, R., 1954, The geochemistry of some igneous rock series, Part 2, Geochim et Cosmochim Acta, v. 5, p. 245-285.

_____, _____, 1953, The geochemistry of some igneous rock series, Geochim et Cosmochim Acta, v. 4, p. 105-142.

Pardee, J. T. and Larsen, E. S., 1929, Deposits of vermiculite and other minerals in the Rainy Creek district near Libby, MT., U. S. G. S. Bull. 805, pp. 22-28.

Parker, R. L. and Sharp, W. N., 1970, Mafic-ultramafic igneous rocks and associated carbonatites of the Gem Park Complex, Custer and Fremont Counties, CO, U. S. G. S. Prof. Paper 649.

Perry, E. S., 1948, Talc, graphite, vermiculite, and asbestos in Montana, Mont. Bur. Mines Geol. Mem. No. 27, p. 28-30.

Phillips, W. J., 1968, The crystallization of the teschenite from Lugar sill, Ayrshire, Geol. Mag., v. 105, p. 23-34.

Philpotts, A. R., 1978, Textural evidence for liquid immiscibility in tholeiites, Miner. Mag., v. 42, p. 417-425.

_____, 1976, Silicate liquid immiscibility: its probable extent and petrogenetic significance, Am. J. Sci., v. 276, p. 1147-1177.

_____, 1972, Density, surface tension, and viscosity of the immiscible phase in a basic, alkaline magma, Lithos, 5, p. 1-18.

_____, 1971, Immiscibility between feldspathic and gabbroic magmas, Nat. Phys. Sci., v. 229, p. 107-109.

_____, 1967, Origin of certain iron-titanium oxide and apatite rocks, Econ. Geol., v. 62, p. 303-315.

_____, and Hodgson, C. J., 1968, Role of liquid immiscibility in alkaline rock genesis, Int. Geol. Cong. 23rd, Czech Rept. Sess. Sec. 2, p. 175-188.

_____, and Philpotts, J. A., 1969, Liquid immiscibility between syenitic and gabbroic magmas, Geol. Soc. Amer. Abstr. with Prog. 1, pt. 7, p. 1176.

Presley, M. W., 1973, Metamorphism in the Sapphire Mountains, Montana, Northwest Geology, v. 2, p. 36-41.

_____, 1970, Geology of the Willow Creek drainage basin, southern Sapphire Mountains, Montana, Unpublished M.S. Thesis, Univ. of Montana, 56 p.

Price, R. A., 1971, Gravitational slipping and the foreland thrust and fold belt of the North American Cordilleran: Discussion, Geol. Soc. Amer. Bull., v. 82, p. 1138.

Prokoptsev, N. G., 1977, The early magmatic liquational-dynamic differentiation of alkalic basalt deep-water lavas, Acad. Sci. USSR Dokl, Earth Sci., Sec. V228, No. 1-6, p. 186-188.

Ramsay, J. G., 1955, A camptonite dyke suite at Mona, Ross-shire and Iverness-shire, Geol. Mag., v. 92, p. 297-309.

Rankin, A. H. and LeBas, M. J., 1974, Liquid immiscibility between silicate and carbonatite melts in naturally occurring ijolite magma, Nature, v. 250, p. 206-209.

Ringwood, A. E., 1955, The principles governing trace element distribution during magmatic crystallization, Geochimica et Cosmochimica Acta, v. 7, p. 189-202; 242-254.

Roedder, E., 1978, Silicate liquid immiscibility in magmas and in the system K_2O-FeO-Al_2O_3-SiO_2: an example of serendipity, Geochimica et Cosmochimica Acta, v. 42, p. 1597-1617.

_____, 1951, Low-temperature liquid immiscibility in the system K_2O-FeO-Al_2O_3-SiO_2, Amer. Miner., v. 36, p. 282-286.

_____, and Coombs, D. S., 1967, Immiscibility in granitic melts as indicated by fluid inclusions in ejected granitic blocks from Ascension Island, Jour. Petrol., v. 8, p. 417-452.

_____, and Weiblen, P. W., 1972, Petrographic features and petrologic significance of melt inclusions in Apollo 14 and 15 rocks, Proc. 3rd Lunar Sci. Conf., p. 251-279.

_____, _____, 1970a, Lunar petrology of silicate melt inclusions, Apollo 11 rocks, Proc. of Apollo II Lunar Sci. Conf., p. 801-837.

_____, _____, 1970b, Silicate liquid immiscibility in lunar magma evidenced by fluid inclusions in lunar rocks, Science, v. 167, p. 641-644.

Ryerson, F. J., and Hess, P. C., 1978, Implications of liquid-liquid distribution coefficients to mineral-liquid partitioning, Geochim et Comsochim Acta, v. 42, p. 921-932.

Shawe, D. R., and Parker, R. L., 1967, Mafic-ultramafic layered intrusion at Iron Mountain, Foremont County, Co., U. S. G. S. Bull 1251-A, p. A1-A28 [1968].

Skinner, B. J., and Peck, D. L., 1969, An immiscible sulfide melt from Hawaii, Econ. Geol. Mono., No. 4, p. 310-322.

Sørensen, H. (ed.), 1974, The Alkaline Rocks, John Wiley & Sons, New York, 622 p.

Stanton, R., 1972, Ore Petrology, McGraw-Hill.

Streckeisen, A., 1976, To each plutonic rock its proper name, Earth-Science Reviews, v. 12, p. 1-33.

Takahaski, E., 1978, Partitioning of Ni^{2+}, Co^{2+}, Fe^{2+}, Mn^{2+}, and Mg^{2+} between olivine and silicate melts: compositional dependence of partition coefficients, Geochim Cosmochim Acta, v. 42, p. 1829-1844.

Temple, A. K. and Grogan, R. M., 1965, Carbonatite and related alkalic rocks at Powderhorn, CO., Econ. Geol., v. 60, p. 674-692.

Tomkeieff, S. I., 1961, Alkalic ultrabasic rock and carbonatites in the USSR, Intern. Geol. Rev., v. 3, p. 739-758.

Tröger, W. E., 1979, Optical Determination of Rock-Forming Minerals, E. Schweizerbart'sche Verlagsbuchhandlung, Stuttgart,

Visser, W. and Koster van Groos, A. F., 1979, Phase relations in the system K_2O-FeO-Al_2O_3-SiO_2 at 1 atmosphere with special emphasis on low temperature liquid immiscibility, Amer. J. Sci., v. 279, p. 70-91.

_____, _____, 1976, Liquid immiscibility in K_2O-FeO-Al_2O_3-SiO_2, Nature, v. 264, p. 420-427.

Vogel, T. A., and Wilband, J. T., 1978, Coexisting acidic and basic melts: Geochemistry of a composite dike, Jour. Geol., v. 86, p. 353-371.

Wager, L. R., and Brown, G. M., 1968, Layered Igneous Rocks, Oliver and Boyd, London, 588 p.

_____, and Mitchell, R. L., 1951, The distribution of trace elements during strong fractionation of basic magma -- a further study of the Skaergaard intrusion, East Greenland, Geochim et Cosmochim Acta, v. 1, p. 129-208.

_____, _____, 1950, The distribution of Cr, V, Ni, Co, and Cu during the fractional crystallization of the basic melt, Int. Geol. Congr. 18th, London, 1948, Rept. Pt. 2, p. 140-150.

Watkinson, D. H., 1970, Experimental studies bearing on the origin of the alkalic rocks -- carbonatite complex and niobium mineralization at Oka, Quebec, Can. Mineralogist, 10, p. 350-361.

Watson, E. B., 1976, Two-liquid partition coefficients: Experimental data and geochemical implications, Contr. Miner Petr., v. 56, No. 1, p. 119-134.

_____ and Naslund , H. R., 1977, The effect of pressure on liquid immiscibility in the system K_2O-FeO-Al_2O_3-SiO_2-CO_2, Carnegie Inst. Yearbook 76, p. 410-414.

Weiblen, P. W., and Roedder, E., 1973, Petrology of melt inclusions in Apollo samples 15598 and 62295, and of clasts in 67915 and several lunar soils, Proceedings of the 4th Lunar Sci. Conf., 4:681.

Wiswall, G., 1976, Structural styles of the southern boundary of the Sapphire Tectonic Block Anaconda-Pintlar Wilderness area, Montana, Unpublished M. S. Thesis, Univ. of Montana, 62 p.

Wood, M. I., and Hess, P. C., 1977, The role of Al_2O_3 in immiscible silicate melts, EOS, 58, p. 520.

Woussen, G., 1970, La géologie du complex igné du Mont. Royal, Can. Miner, v. 10, p. 432-451.

Wright, T. L., and Okamura, R. T., 1977, Cooling and crystallization of tholeiitic basalt, 1965 Makaopuhi lava lake, Hawaii, U. S. G. S. Prof. Pap. 1004.

Wyllie, P. J., 1966, Experimental studies of carbonatite problems: the origin and differentiation of carbonatite magmas, in Tuttle, O. F. and Gittens, J. (eds.), Carbonatites, Interscience Publ.

_____, Cox, K. G., and Biggar, G. M., 1962, The habit of apatite in synthetic and igneous systems, Jour. Petr. 3, p. 238-243.

Yoder, H. S., Jr., 1973, Contemporaneous basaltic and rhyolitic magmas, Amer. Mineral., v. 58, p. 153-171.